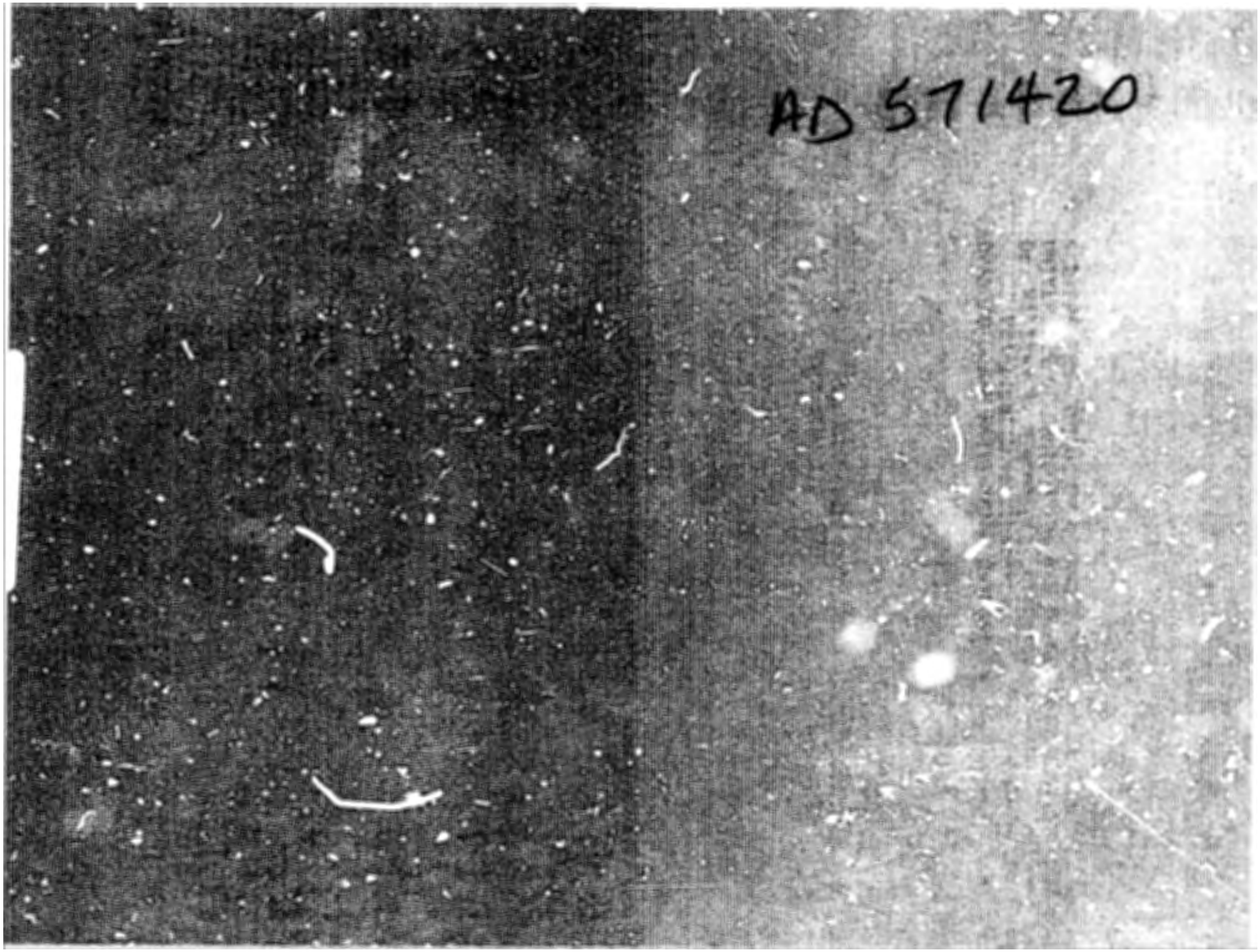
AD 571420

DISCLAIMER NOTICE

THIS DOCUMENT IS THE BEST QUALITY AVAILABLE.

COPY FURNISHED CONTAINED A SIGNIFICANT NUMBER OF PAGES WHICH DO NOT REPRODUCE LEGIBLY.

Unclassified

Security Classification

DOCUMENT CONTROL DATA - R & D

(Security classification of title, body of abstract and indexing annotation must be entered when the overall report is classified)

1 ORIGINATING ACTIVITY (Corporate author) The Regents of the University of California University of California, San Diego La Jolla, California 92037	2a. REPORT SECURITY CLASSIFICATION Unclassified 2b GROUP Not Applicable

3 REPORT TITLE
Annual Report
Advanced Ocean Engineering Laboratory

4 DESCRIPTIVE NOTES (Type of report and inclusive dates)
December 15, 1969 to December 31, 1970

5 AUTHOR(S) (First name, middle initial, last name)
Dr. William A. Nierenberg
Dr. Fred N. Spiess
Dr. Walter H. Munk
Dr. Robert D. Moore
Dr. Hugh Bradner
Dr. John D. Isaacs
Dr. Douglas L. Inman
Dr. William G. Van Dorn

6 REPORT DATE December 31, 1970	7a. TOTAL NO. OF PAGES 133	7b. NO OF REFS 19
8a CONTRACT OR GRANT NO N00014-69-A-0200-6012 b. PROJECT NO c. d.	9a. ORIGINATOR'S REPORT NUMBER(S) SIO Reference No. 71-4 9b. OTHER REPORT NO(S) (Any other numbers that may be assigned this report) AOEL Report #16	

10 DISTRIBUTION STATEMENT
Distribution of this document is unlimited

11 SUPPLEMENTARY NOTES	12. SPONSORING MILITARY ACTIVITY Advanced Research Projects Agency c/o Office of Naval Research Arlington, Virginia 22217

13 ABSTRACT

This annual report reflects the technical status of projects conducted within the Advanced Ocean Engineering Laboratory at the Scripps Institution of Oceanography. These projects are: (1) Stable Floating Platform - to conceive, design, build and demonstrate the feasibility of large stable floating platforms in the open sea. (2) Benthic Array - a program to develop and construct a quartz vertical accelerometer appropriately packaged and adapted for long term ocean bottom use. (3) Overpressures Due to Earthquakes - a study of earthquakes and resultant overpressures as they may effect oceangoing vehicles and subsurface structures. (4) Advanced Studies in Nearshore Engineering - field studies of the water-sediment interface under wave action in and near the breaker zone; and laboratory investigation of the velocity field of breaking waves. (5) Electromagnetic Roughness of the Ocean Surface - concerns utilization of radio signals scattered from the sea surface to determine the directional spectrum of ocean waves.

DD FORM 1473 (PAGE 1)
0102-014-6600

Unclassified
Security Classification

Unclassified
Security Classification

KEY WORDS	LINK A		LINK B		LINK C	
	ROLE	WT	ROLE	WT	ROLE	WT
Advanced Ocean Engineering						
Stable Floating Platform						
Seismic Array						
Overpressures Due to Earthquakes						
Nearshore Engineering						
Electromagnetic Roughness of the Ocean Surface						
Quartz Vertical Accelerometer						
Gravimeter						
Two-Axis Tiltmeter						
Pendulous Gimbal Structure						
Digital Data Logging System						
Incremental Tape Recorder						
Analog Multiplexer						
Low Powered Analog-to-Digital Converter						
Crater-Sink Sand Transfer System						
Tombolo (Sand Spit)						
Seaquakes						
Oceanbottom Seismometer						
Radar Cross Section						
Ocean Wave Spectrum						
Water-Sediment Interface						
Breaking Waves						

Disclaimer

The views and conclusions contained in this document are those of the authors and should not be interpreted as necessarily representing the official policies, either expressed or implied, of the Advanced Research Projects Agency or the U. S. Government.

Advanced Ocean Engineering Laboratory

Annual Report

Table of Contents

Part I

STABLE FLOATING PLATFORM

Principal Investigator
Dr. Fred N. Spiess
Phone (714) 453-2000, Extension 2476

ADVANCED OCEAN ENGINEERING LABORATORY
Sponsored by
ADVANCED RESEARCH PROJECTS AGENCY
ADVANCED ENGINEERING DIVISION

ONR Contract N00014-69-A-0200-6012

Part I

Stable Floating Platform

Table of Contents

List of Figures

STABLE FLOATING PLATFORM

I Early Program History

The Stable Floating Platform project was one of the initial elements in the Scripps-ARPA program. In its first year it was concerned with procurement of facilities (computer and wind-wave channel--viewed as useful beyond direct application to this problem) and with a broad look at possible platform types. The program was rather diffuse since it lacked any ground rules about specific goals and constraints and did not address any particular mission. During the summer and fall of 1969, this situation was reviewed by ARPA and Scripps. The result was a decision that ARPA would arrange for studies of maritime military applications and that Scripps would focus on platforms to support ocean R & D, with emphasis on bringing in technology which had not previously been applied in this context. The basic philosophy at Scripps was to proceed toward full scale construction at modest cost since the only real way of advancing technology in this field at this time seems to be through actual application.

II Review of 1970

The calendar 1970 program was carried out with this in mind. Hydraulic laboratory facility procurement was completed, studies of research mission types were made, consideration was given to requirements and possible platform concepts, a design study was made to compare the two most promising platform types, model tests at 1/100 scale were initiated and a 1/8 scale model of a three-legged platform was built and operated in San Diego Bay. Each of these topics will be discussed further below. The most important step was taken in November when the decision was made to focus on a single particularly promising design--a four-legged platform to be made by assembling (at sea, on site) a pair of two-legged modules utilizing concrete as the material for all legs (figure 1). It appears that a platform having a 500 ton payload and with 200 ft. length and 100 ft. beam is feasible at roughly a four million dollar cost. Size and payload could be increased by building additional modules.

III Wave Channel

The wave channel test facility started operations in March and has been in use since that time. Primary work has been concerned with validating its performance (by direct measurement and through observation of a 1/100 scale FLIP model (figure 2) - in this latter case we have full scale data for comparison). Two related reports have been produced. One of these (by Robert Oversmith, AOEL Report 11, SIO Reference Number 70-29) describes the facility as it existed in October of this year. At that time, the wave aspects were fully operational as was the computer and

the data acquisition system. The other report describes the measured [illegible] characteristics of the wave fields (by Donald Bellows, WHOI Report [illegible], also Reference Number 70-37). Since that time, the blower system for wind generation has been installed and checked out. The pumps and piping to produce longshore diurnal currents have yet to be completed; however, work using that portion of the system has rather low priority at this time.

IV. Research Mission Analysis

Studies of the types of research missions requiring stable platforms were made primarily through discussions with Scripps scientific staff and with individuals at the two principal Navy laboratories (NUC and NOSC) involved in ocean system development. From these, it emerged that a wide number of activities could be involved. The most clearly focussed and immediately important is underwater acoustic research related to long range detection systems. At the present time, this work very much needs the capability of supporting hydrophone arrays of appreciable horizontal extent (over 100 ft.) at various depths in the water. The platform which we are working toward could easily fill this need, doing it in a way which would allow the collateral recording and analysis equipment to be located at the sea surface close to the arrays (thus easing telemetry problems from the hundreds of hydrophones) and also allowing the entire assembly to be moved to any of a variety of geographic locations.

Two other classes of research activity also seem important and supportable from this type craft: sea floor work (fine scale sampling, installation and inspection of equipment, benthic ecology) and work in the upper part of the water column (internal and surface waves, deep scattering layer, optical properties, fish behavior). These would require the ability of the vehicle to deploy and support a wide variety of equipment (submersibles, sea floor tractors, optical systems, high resolution sonars). Beyond these three research areas, the platform would naturally be involved in engineering studies to validate design processes and to look at such matters as open ocean breakwaters and extraction of energy from surface waves.

V. Preliminary Platform Study

With these programs in mind, a preliminary analysis was made of a wide variety of configurations. The gross constraints agreed on at that time were: 200 tons payload, cost in the 3 to 5 million dollar range, flippable spar type legs, non-flipping lab and living spaces, heave response comparable to FLIP, scientific party of 10 to 15. After some consideration, two configurations were chosen for a preliminary comparative study--a three-legged platform following Closten's sea-legs concept and a two-leg catamaran style chosen because of its probable low cost.

This study was completed in October and the results (L. R. Glosten reference 70-28) forwarded to ARPA.

The paper study was paralleled with construction of a 1/8 scale model of the three leg unit. This was built during October and operated in San Diego Bay during November. The model was large enough to dramatize problems associated with universal joints at the leg tops and difficulties with bringing legs into contact with the platform in the horizontal (figure 3). In the vertical (figure 4) it showed, qualitatively, the expected stability. Taken together the model and paper studies showed that a combination of factors (very favorable cost for the two-leg, concrete units; difficulties in mating legs to platform in the horizontal for the three-leg platform) pointed to a preference for the two leg unit and led to the decision, referred to above, to pursue a four-leg platform composed of a pair of two-leg modules to be joined after independent transition of each to the vertical (stable) leg position.

VI Future Planning

Final action for the year (and a prelude to the coming year's activities) was initiation of a design study of the four-leg platform, including motion analysis, 1/100 and 1/8 scale models and a naval architectural study of costs and important design points (platform hull design, modules connection techniques and related problems). Motion and force analysis is being made by P. Rudnick, 1/100 scale model work by R. Oversmith, 1/8 scale model by C. S. Mundy and naval architecture by L. R. Glosten. Results of these steps should be available in March and April with the possibility of moving toward preparation of specifications for the full scale platform starting in May.

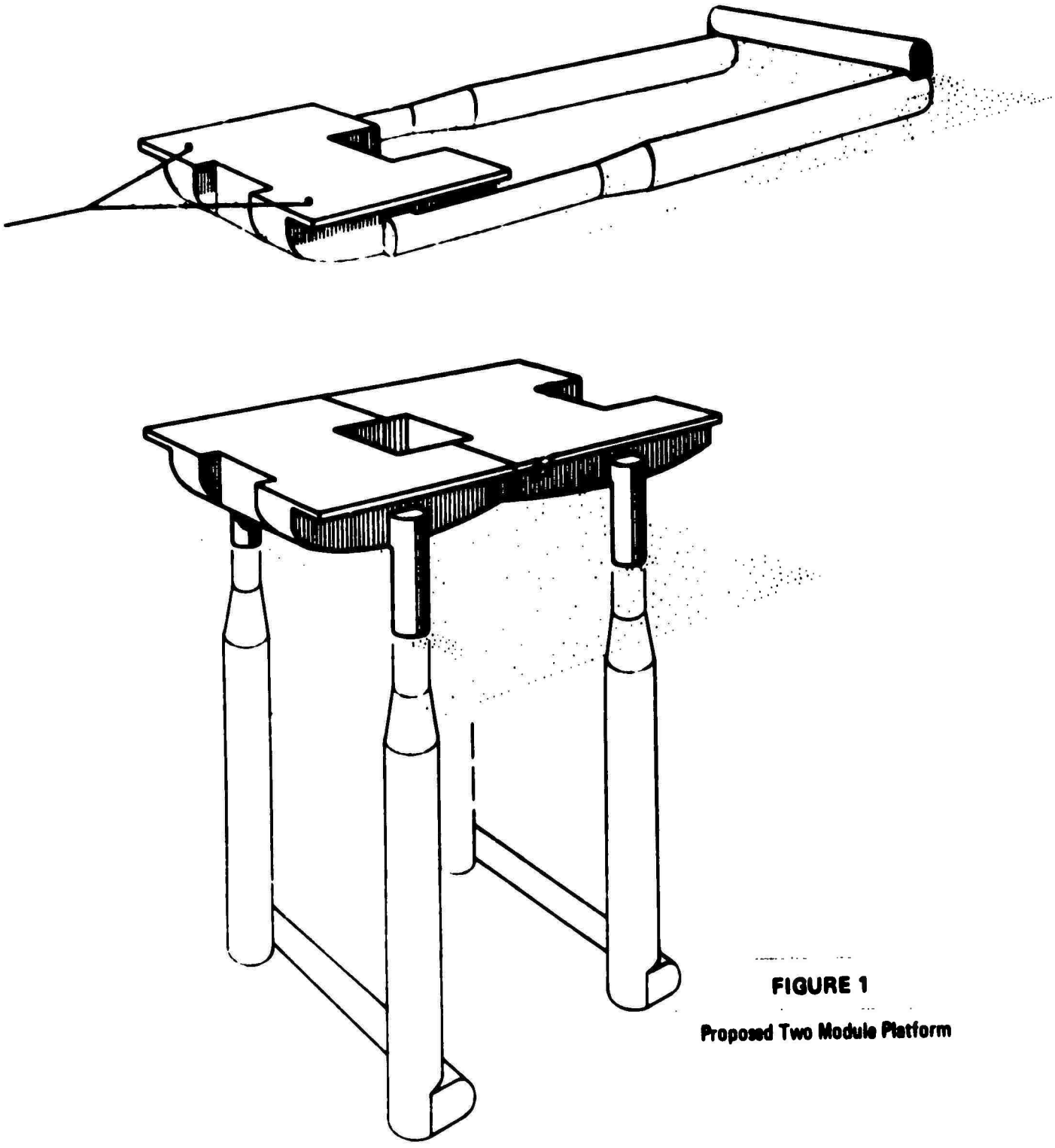

FIGURE 1

Proposed Two Module Platform

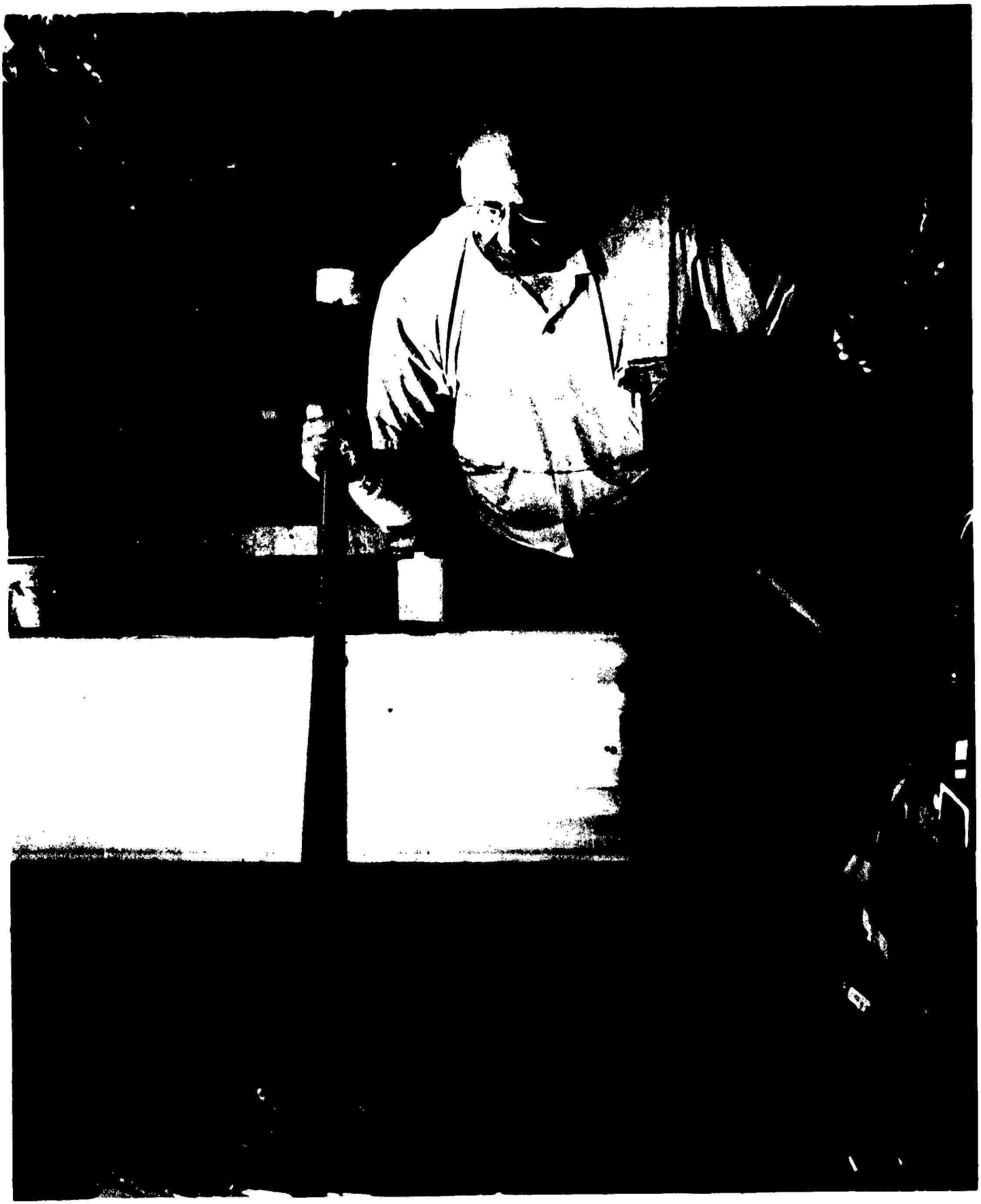

Figure 2 - 1/100 Scale Model of FLIP

Figure 3 - 1/8 Scale Model prior to flipping

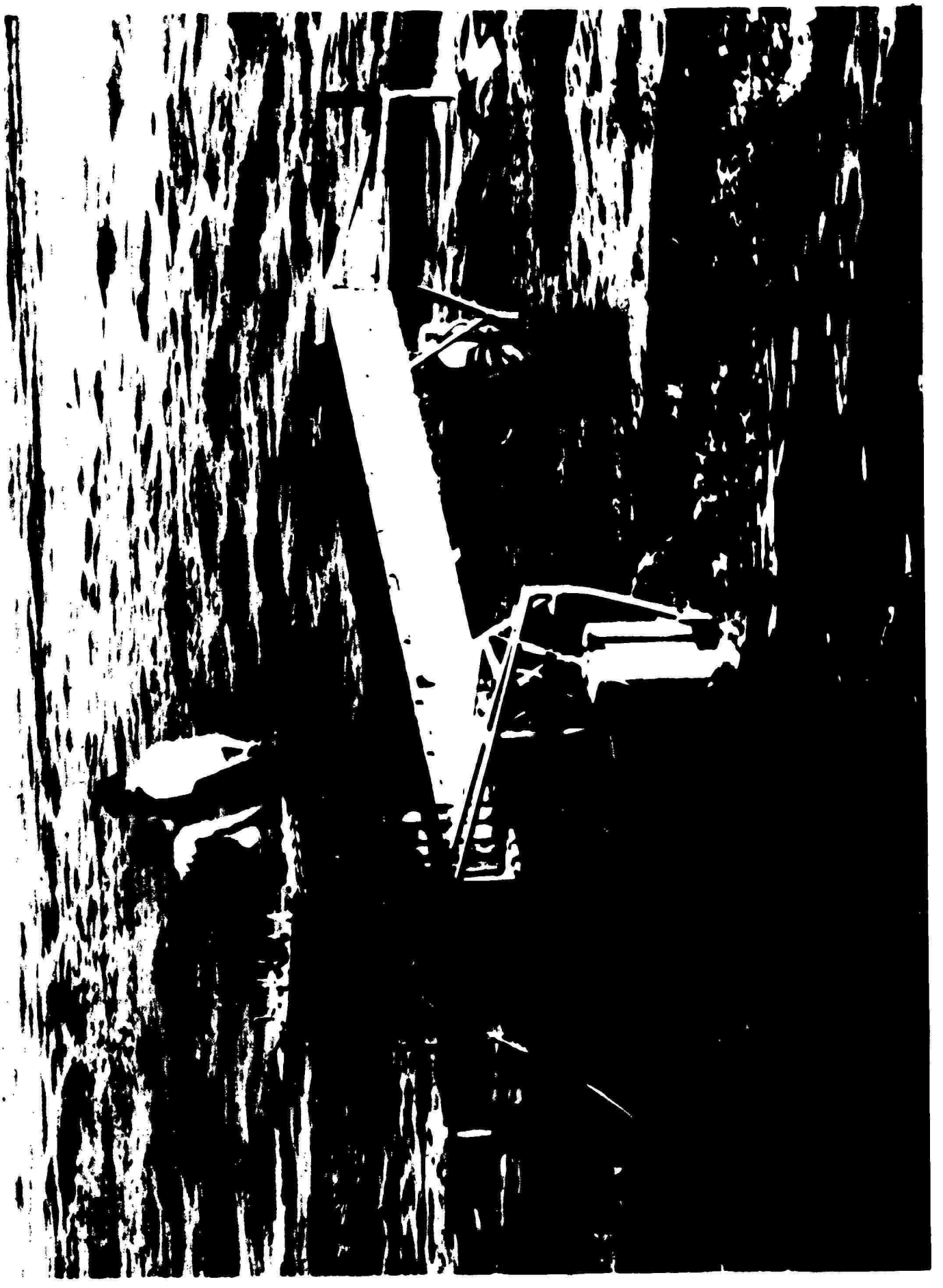

Figure 4 - 1/8 Scale Model in stable condition

BLANK PAGE

Part II

BENTHIC ARRAY

Co-Principal Investigators

Dr. Walter H. Munk
Phone (714) 453-2000, Extension 1741

Dr. Robert D. Moore
Phone (714) 453-2000, Extension 1759

ADVANCED OCEAN ENGINEERING LABORATORY
Sponsored by
ADVANCED RESEARCH PROJECTS AGENCY
ADVANCED ENGINEERING DIVISION

ONR Contract N00014-69-A-0200-6012

Part II

Benthic Array

Table of Contents

SUMMARY

The goal of this project is to adapt the high performance quartz vertical accelerometer developed by Block & Moore at IGPP for use on the ocean bottom. Specifically an instrument package is being constructed which will enable the quartz accelerometer to be operated on the ocean bottom to depths of 20,000 feet. The package will be completely self-contained, including all necessary power supply, electronics, data recording, acoustical control and telemetry systems. The package will be capable of operation without surface support for periods of 7 to 30 days. Work on the project was first started about November 1, 1969. During the first year of work, the problems to be solved were:

1. The basic configuration of the underwater package.
2. Redesign of instrumentation and data logging electronics in a low power form suitable for operation from storage batteries.
3. Reconfiguration of the mechanical structure of the accelerometer to enable its use within the constraints imposed by operation on the ocean bottom inside a 22" ID pressure sphere.

The broad-problem areas listed above included several specific problems most of them in the area of low power electronics which were both difficult and crucial to the project. These have all been solved as is discussed in the attached report and at present we see no fundamental obstacles to the completion of a working instrument package. Our present hope is to have a complete package ready for preliminary ocean bottom tests by January 1, 1972.

Work on this project was first started about November 1, 1969. At that time the problem could only be stated in very general terms, namely, to construct a version of the present IGPP quartz vertical accelerometer appropriately packaged for ocean bottom use. By January 1, 1970 the system configuration indicated in the block diagram (Figure 1) had been decided upon.

In order to operate with the sensitivity desired for this work, certain stringent environmental requirements with respect to the quartz accelerometer must be satisfied. The most difficult of these being the control of the instrument temperature which must be held to better than 10^{-5}°C. In addition, once the capsule is in place on the ocean bottom, the gravimeter must be leveled to better than 1/2° error on any axis. After considerable thought it was decided that the leveling problem could be handled adequately with a completely passive pendulous gimbal arrangement. The temperature problem remained a thorny one however.

In the land-based version of the instrument, the active part of the accelerometer is enclosed within three coaxial cylindrical metal enclosures. The first of these, having an outside diameter of about 8 inches and a length of about 8 inches, is the instrument's stainless steel high-vacuum enclosure. This is essentially part of the instrument and will be retained in the ocean bottom version. The vacuum can is suspended within a second cylindrical can approximately 9 inches outside diameter and 11 inches long. This is referred to as the thermostat can and in the land-based instrument, the temperature control heater, monitoring and sensing thermistors are mounted on this can. The thermostat can is placed within a third outer can which is simply a light-weight aluminum can used to constrain the polystyrene foam

balls used as thermal insulation in the land-based instrument. The dimensions of this final can are approximately 25 inches long by about 16 inches OD. Since the pressure spheres which are to be used to house the underwater instrument have an inside diameter of 22 inches it is clear that a structure of this size is precluded. As a matter of fact, allowing adequate space for the pendulous gimbal assembly, an object of the dimensions of the normal thermostat can is a fairly tight fit in the spheres.

In the land-based instrument it has been found that an average heater power input of about three watts is sufficient to maintain the temperature of the thermostat can about 15°C above ambient. For the ocean bottom version, it was decided that the only hope would be to use the normal thermostat can as the outer can, put the heater winding and temperature sensing thermistors on the surface of the vacuum can and try and insulate between the vacuum can and the thermostat can as well as possible. It was decided early in the game that the maximum number of storage batteries it would be practical to handle in the instrument's battery package would be about 16 twelve volt, 100 ampere-hour batteries. Experience in underwater work here has shown that a 100 ampere-hour battery can be depended on to deliver an average current of 100 milliamperes for 30 days with high reliability. Allowing for the fact that other equipment had to be operated it seemed unlikely that we would be able to assign any more than four of these batteries to the temperature controller. This means our maximum average heater power would be limited to an average current of 100 milliamperes from a 48 volt source or approximately 5 watts. One advantage of the ocean bottom environment is that the ocean bottom temperature is sufficiently stable that it is not necessary to maintain the gravimeter as much as 15°C above ambient. In

fact a rise of 5°C is adequate. The question then was could an average power of 5 watts maintain the gravimeter 5°C above ambient temperature with the sort of insulation we obtain within the constraints discussed above.

This question can only be answered experimentally and the experiment could not be conducted until the gimbal assembly had been completed and installed in the instrument's support plate and until the mounting hardware and final outer instrument can had been constructed. As soon as this point was reached, a dummy vacuum can was mounted in the thermostat can in the way it which it will be done in the final instrument. Insulation was put in place and the resulting assembly was installed in the gimbal. The pressure spheres were put over this portion of the instrument support frame thus putting the system in exactly the same environment it would see when in use on the ocean bottom. An experiment was then conducted to find a relationship between total power input to the heater and rise in temperature above ambient. The results obtained are shown in the graph in Figure 2. These data indicate a temperature rise of about 2.4°C per watt of heater power. This is well within the margin we can handle and means the temperature control problem, at least in principle, can be dealt with. It should be pointed out that this was a considerable milestone in the project because had the experiment come out badly, we would have been in a very sticky position indeed.

Another decision coming out of the preliminary work on the project was the actual configuration of the capsule. After some thought, it was decided that the amount of gear required to make the system operative would occupy at least three 22 inch ID pressure spheres. The most reasonable arrangement of three spheres and the one that we finally adopted places the

three spheres in a horizontal plane at the points of a equilateral triangle. The package consisting of the three pressure spheres and the triangular aluminum support plate tying them together will be supported by the battery pack which will rest on the ocean bottom. This arrangement is shown in Figure 3. The bottom spheres would be supported by three mating pads on the top of the battery pack and the instrument capsule will be held down to it by a cable in tension. The package will be recovered by severing this cable, the instrument capsule being positively buoyant. The distribution of the various system components among the three spheres will be as follows:

One sphere will contain the gravimeter, two-axis tiltmeter and pendulous gimbal structure. A second sphere will contain two electronic packages consisting of the analog electronics, that is the electronics associated with the quartz accelerometer, the tiltmeter, the temperature recording circuitry and accelerometer temperature control circuitry; along with another package consisting of the electronics associated with the digital data logging system. The third sphere will be occupied one-half by the incremental tape recorder and one-half by electronics associated with communications between the capsule and the surface. These will consist both of transmitting and receiving facilities. The transmitting facility will be used to telemeter status information from the capsule to the surface in order that it can be determined from the surface whether the system is functioning or not. The receiving facility will be used to receive commands to perform various operations such as release, start-up, telemeter data, etc., sent from the surface to the capsule.

The main triangular aluminum support plate which essentially ties the

three capsule system together was then designed and fabricated. Card cages to hold the electronics and the electronic capsule were also designed and fabricated. The aluminum support plate with those parts of its ultimate contents that have been completed up until the present time is shown in Figure 4.

Having got these general considerations out of the way, it was then possible to survey the block diagram given for the next most important problem areas. It was decided early in the game that since very little is known about the stability of the ocean bottom when supporting a load of this kind that the question of possible secular tilting of the system would become an important one when trying to interpret underwater data. The only solution seemed to be to include in the package a two-axis tiltmeter of sufficient sensitivity to enable a decision to be made as to whether anomolous data could be explained by tilt or not. Because of the uncertainty in the leveling of the pendulous gimbal assembly, the tiltmeter would have to have a dynamic range sufficient to take care of this uncertainty, namely, about ± 1/2° or ± 0.1 radian. Since the digitizer has a resolution of 12 bits for a ± 10 volt input, this means a least count on the tiltmeter output would represent about 5×10^{-5} radians. This is sufficient sensitivity to identify anomalies in the gravity data due to tilt.

Since no commercially made tiltmeter of small enough size having the stability and resolution required for this application exists to the best of our knowledge, we have constructed a two-axis tiltmeter. The principle of the tiltmeter is very simple and is shown in the schematic drawing in Figure 5. Basically it consists of a short pendulum with a length of about

6 inches. The pendulum consists of a stiff piece of stainless steel tubing which supports a copper mass. The pendulum is hinged by a short piece of fine tungsten wire which connects the stainless steel tubing to a fixed support. Two pair of fixed capacitor plates are distributed around the pendulum bob arranged so as to detect motion of the bob in two orthogonal directions. The capacitor plates are used in exactly the same way as the capacitor plates in the quartz accelerometer are used to determine its mass position. In the case of the tiltmeter, the signal appearing on the moving plate is a mixture of signals representing angular deflection about two orthogonal axes. The signals can be separated by using a different AC frequency to excite one pair of capacitor plates than to excite the other. One reason the capacitor plate system was chosen was that the two instrumentation channels for the tiltmeter then become essentially identical to the instrumentation channel of the gravimeter as can be seen from the block diagram. This tiltmeter has an outside diameter of about 3 inches and an overall length of about 9 inches and lab tests indicate that it is capable of resolving tilt signals between 10^{-5} and 10^{-6} radians in an environment considerably less stable than it will be present on the ocean bottom. Figure 6 is an assembly drawing of the actual tiltmeter which shows some refinements that were not discussed with respect to the system, namely, two systems of damping magnets, one at each end of the stainless steel tube that supports the mass, the outer seal can that supports the tiltmeter and the mechanism necessary to clamp and unclamp the tiltmeter on command.

The next problem area identified was that of the phase-sensitive detector. As can be seen from the block diagram, three of these are required for the system. Although printed circuit board phase detectors of high performance are available commercially, unfortunately they are

characterized by high power consumption, typically ± 24 volts at ± 75 milliamps. After some effort, a phase sensitive detector has been developed which consumes less than 3 milliamps from ± 12 volts and meets or exceeds the performance of the best commercially available versions. This unit was discussed in a previous progress report and will not be discussed further here. A schematic diagram of the phase-sensitive detector and a summary of its operating specifications are appended to this report.

The components of the data logging system consist of an analog to digital converter for converting the DC input voltages into 12 bit words, an analog multiplexer and the logic associated with timing, formating, bit shuffling etc. The strictly logic part of the system presents no problem because of the advent of very low power digital logic manufactured by RCA in their COS/MOS series. Simply fabricating the system from this logic solves the power problem. However, two problems remain; that of the A to D converter and the multiplexer.

After examining commercially available 12-bit A to D's it was learned that typical power consumption figures for these units are of the order of 300 milliamperes at 5 volts to power the logic and ± 40 milliamperes at ± 15 volts to power the analog portion. Power consumption at this level is completely out of the question. Some time was spent considering possible ways of attacking this problem and several manufacturers were approached to see if they might be interested in building a low power unit around COS/MOS logic. During this investigation, contact was made with Mr. James Pastoriza of the Pastoriza Division of Analog Devices, Inc. and after some discussion, he agreed that he had sufficient interest in the project of

developing a low power A to D converter that he would be happy to participate with me in this as a joint development. We decided to go this route and the result is a low power 12 bit A to D converter of rather spectacular performance. Even at very high rates to the order of 10,000 conversions a second the total power demand is only 40 milliamps from a single 12 volt supply. At a conversion rate of one per second, which is what will be used in our system, the average power requirement is 50 microamps from 12 volts. The final draft of a paper which has been submitted for publication to Electronics describing the design and performance of the low power A to D converter is appended to this report.

The analog multiplexer presented a similar situation to that caused by the A to D converter, namely, that no commercial multiplexer of anything like low enough power consumption were available. Fortunately, the multiplexer is somewhat less complicated development than the A to D converter and approximately one week was taken in developing an eight input analog multiplexer. The operation of the multiplexer is straightforward. MOSFET transistors are used for switches both for the eight input lines and for a hold arrangement which is incorporated into the multiplexer. When the hold input is activated all eight inputs of the multiplexer are cut off and the operational amplifier holds the value that it was receiving from the active input at the time that the hold was executed. This means that the multiplexing and sample-and-hold function are combined in one unit. A circuit diagram of the multiplexer and a summary of its operating specifications is appended to this report.

A final difficult problem related to the logging system was that of a magnetic tape recorder. The tape recording format and sampling rates we

plan to use have been discussed in a previous report and will not be gone over again here. However, they require that for operation for a period of thirty days, a total of 2400 feet of tape would be required at a recording density of 200 bits per inch. After considerable investigation of commercially available recorders, it was found that none existed which could handle 2400 foot reels of tape. The Kennedy Company makes a low power recorder but it is restricted to a special Kennedy tape cassette which can hold only 300 feet of tape. Precision Instrument Company also has a low power recorder (although not as low power as the Kennedy) available, but it can handle only 7 inch reels. Since the tape recorder was crucial to the ultimate existence of the system, it was decided to attempt to build one here. The approach taken was to use the mechanical portion of an old Digi-Data recorder which happened to be available and build completely new electronics and make some modification to the mechanical portion in order to achieve low power operation. The final result of this effort was a working recorder which, at a stepping rate of two steps per second, consumes an average current of 10 milliamps from a single 12 volt supply. A complete set of schematic diagrams for the electronic portion of the tape recorder, along with a functional description of the electronics is appended to this report.

As an example of the sort of unforeseen and thorny problem one can run into in a project like this, I present our experience with finding a satisfactory solution to providing some sort of braking device for the gimbal. When the instrument is being handled on shipboard and during the time it is descending in the ocean, it is desirable to have the gimbal rigidly clamped to protect the equipment mounted on it. Once the package

is on the ocean bottom it is then necessary to free the gimbal allowing it to level itself pendulously and then to relock it once it has come to its level position. This requires a braking mechanism which can be locked and unlocked on command. Furthermore, since this mechanism will have to be operated by the available capsule power supply, it must consume negligible power when in either the clamped or unclamped position, consuming measurable power only when making transitions between the two states. Over a period of about six months, something like six attempts at various structures involving solenoids and such like were made. None of these worked satisfactorily.

The final solution is proving in tests to be very satisfactory and involves the mechanical arrangement shown in Figure 7. The operation of the brake is essentially the same as that of the familiar disc brake now used on many automobiles. The upper portion of Figure 7 shows sectional view of the operating parts of the brake. The brake operates by a caliper action between a fixed shoe and a moving shoe as shown in the figure. The moving shoe is moved vertically in the figure by a wedge which is driven back and forth by a screw which is in turn driven by a small gear-head DC motor. When the motor rotates in one direction, the wedge will advance from left to right as shown in the figure contacting the ball bearing on the back of the moving shoe and slowly lifting the moving shoe towards contact with the fixed one. Anything in between the two shoes will at some point become rigidly clamped between them. If one continues the motor until a preset amount of torque is developed by it, then a braking action with a preset amount of force will be created. If the motor is shut off at this point, the friction of the thread, wedge and gear train easily holds the moving shoe in place thus resulting in a steady braking action without power

being applied to the motor. In order to release the brake, it is simply necessary to reverse the motor and run the wedge back in the opposite direction. The wedge continues to move until it contacts a microswitch which shuts off the motor drive current. The bottom portion of Figure 7 shows a side view of the brake as actually installed on the gimbal. Two brakes are used, one operating between each pair of gimbal rings in order to clamp both axes of the gimbal. The motor and brake shoe part of the brake is mounted on one gimbal ring, the vertical vane being attached to the adjacent gimbal ring. When the brake assemply clamps on the vane, the two gimbal rings are tied rigidly together, when the brake releases the gimbal is allowed to move freely.

The braking force exerted by the brake in the clamped position is determined automatically as follows. Before the moving shoe contacts the fixed shoe via the vane, the amount of torque required to move the wedge along is quite low. The motor current under these conditions is about 5 milliamps. As soon as the moving shoe contacts the vane the force required to move the wedge builds up rapidly and consequently the motor torque builds up rapidly. This is reflected in a rapid increase in motor current as the motor approaches a stall condition. The electronic driving circuit monitors the motor current and is set to shut off the motor drive current when it has reached a value of approximately 30 milliamps. The electronics required to operate this system for both the clamp and unclamp operations and to do so reliably and with a minimum consumption of power turns out to be fairly complicated. The schematic diagram for this electronics along with a functional description of its operation is included at the end of the report.

This description of the development of the braking system is included mainly as an illustration of how some things that might be overlooked at

the beginning of one's assessing a project like this can turn out to be quite complex problems by the time they are solved.

At the present time we are in the process of installing the tiltmeter and a working gravimeter in the gimbal and putting together the necessary electronics to get them going in the lab. In addition work is proceeding in defining the properties we will require of the acoustic surface link in preparation for procuring the components for it. A specification has been written for the data logging system which we're going to have built by an outside contractor. Figure 8 is a flow diagram showing the presently anticipated schedule of progress for the coming year. At the present time we're pretty much conforming to what is on the diagram except that the fabrication of the final accelerometer will be held up for another couple of weeks due to non-availability of essential personnel.

BLANK PAGE

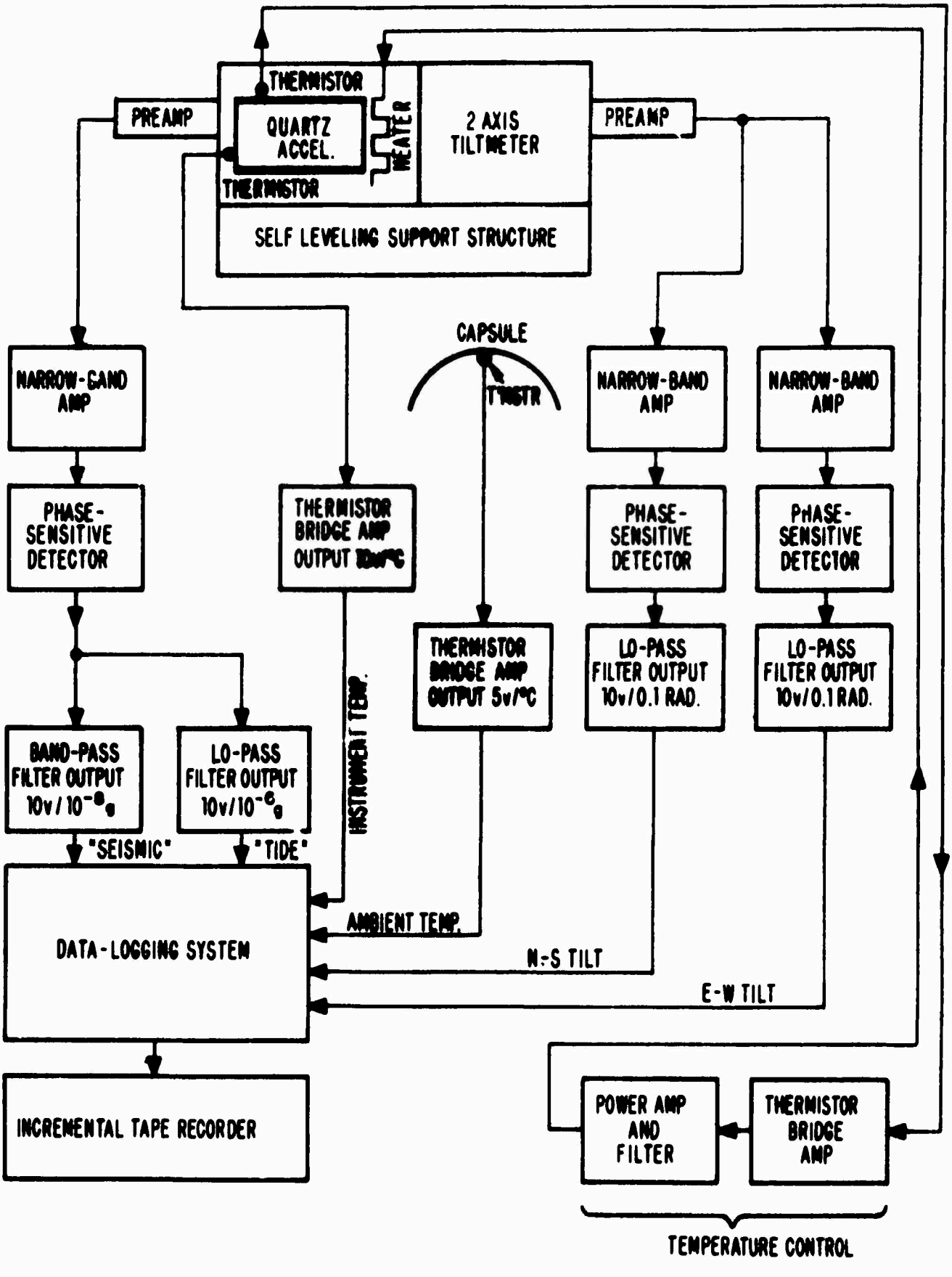

BLOCK DIAGRAM, CAPSULE INSTRUMENTATION

Figure 1

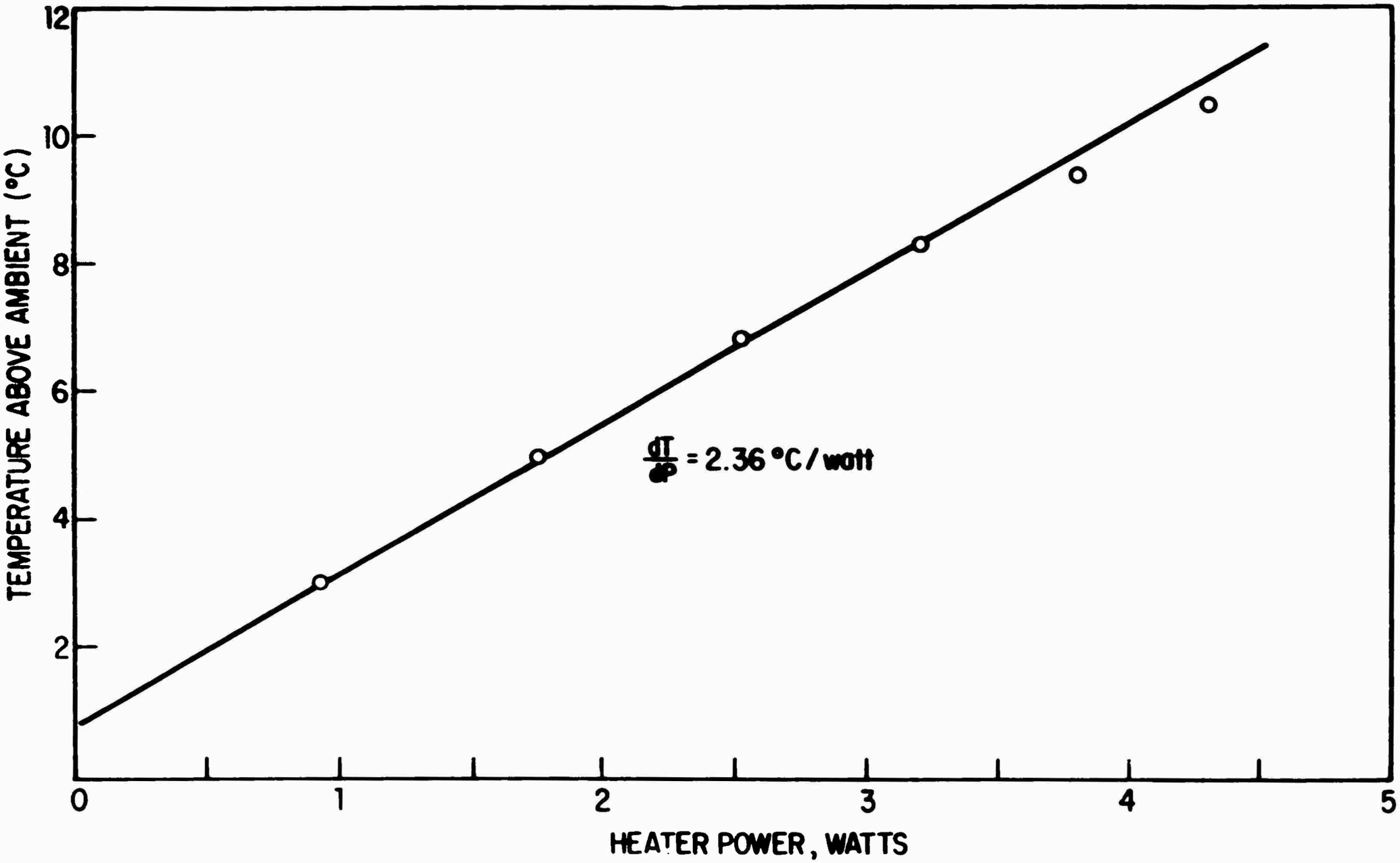

GRAVIMETER TEMPERATURE, RISE ABOVE AMBIENT, VS HEATER POWER

Figure 2

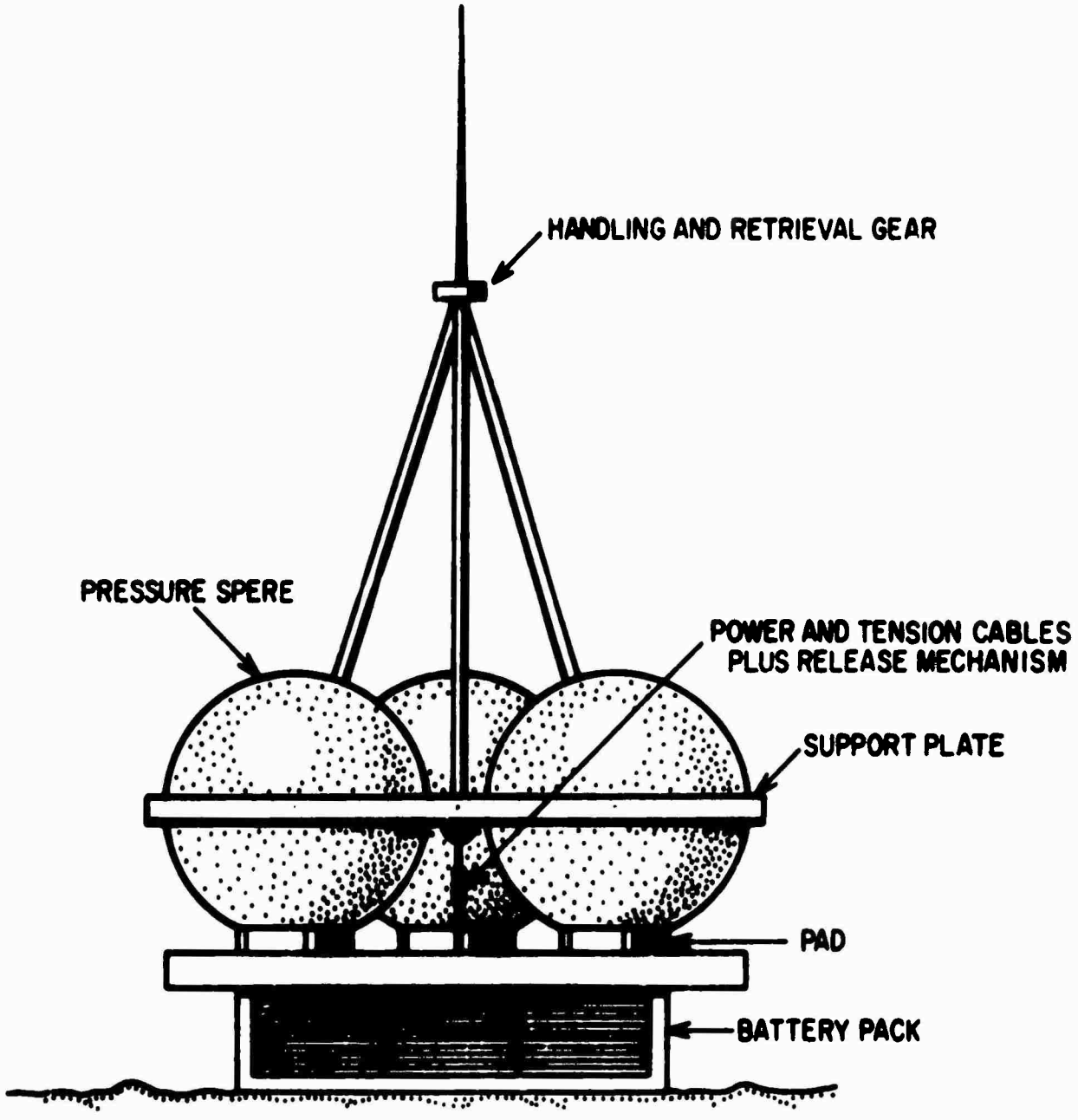

CAPSULE LAYOUT

Figure 3

FIGURE 4 Support plate with some system components installed. In the foreground the large cylindrical housing of the quartz accelerometer can be seen in its gimbal. The smaller cylindrical object to its left is the two-axis tiltmeter. In the lower foreground one of the six aluminum hemispheres that ultimately complete the package can be seen. In the right background the card-cage for the data-logging electronics is visible. The card-cage for the analog electronics which is not visible in the photo is mounted on the underside of the metal plate carrying the upper card-cage. In the left-background the incremental tape recorder can be seen.

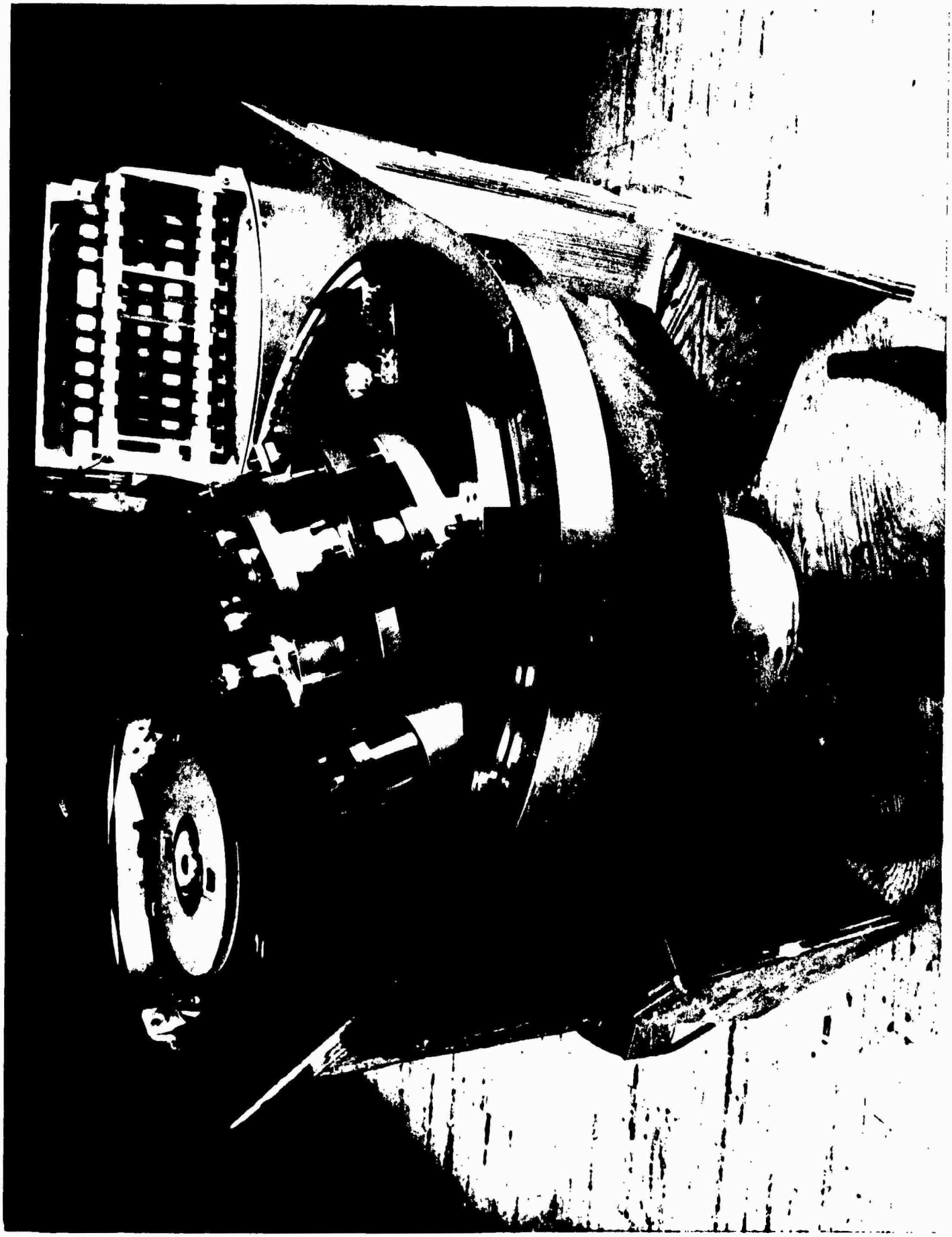

Figure 4 - Support plate with some system components installed.

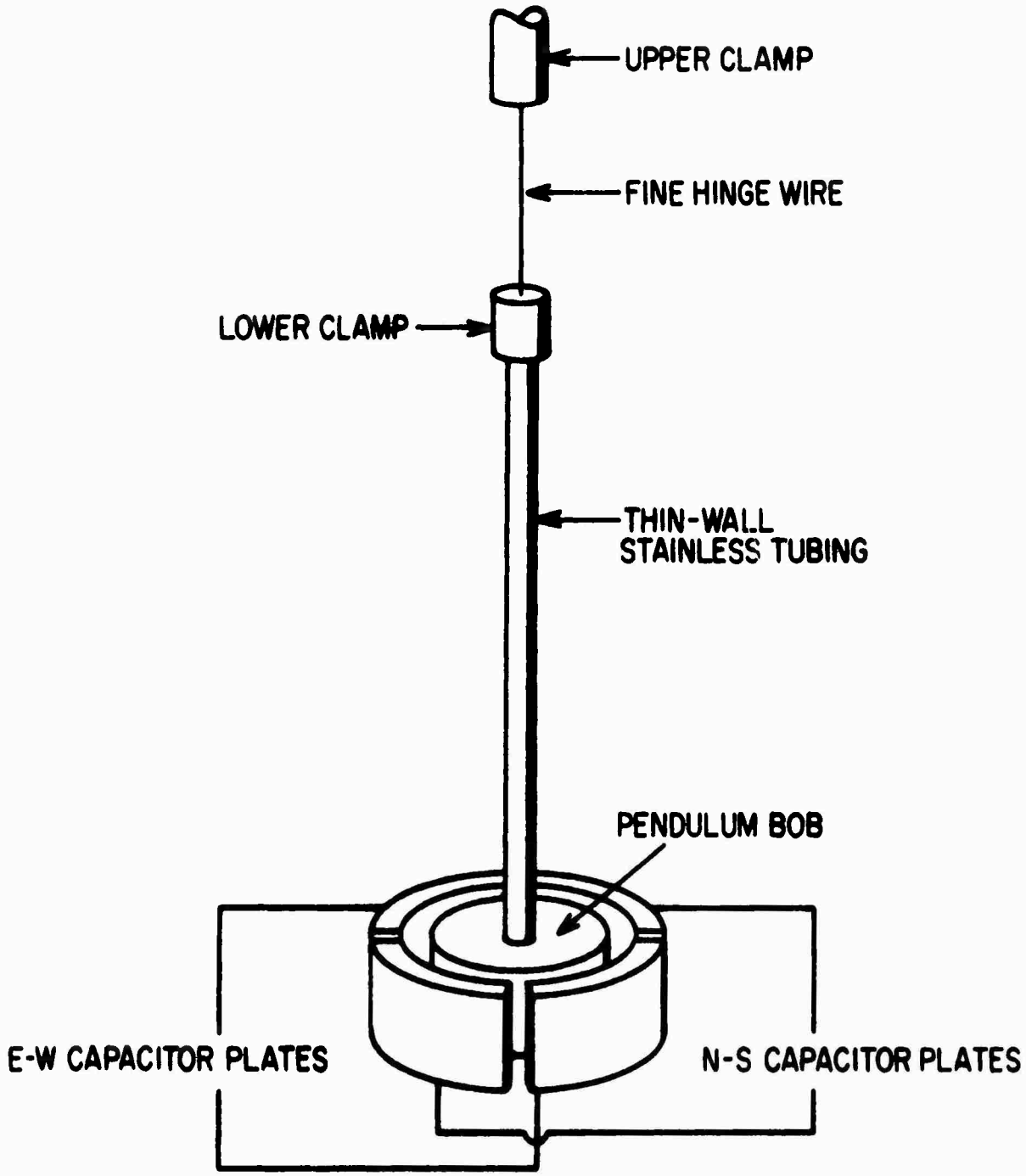

TILTMETER, SIMPLIFIED SCHEMATIC

Figure 5

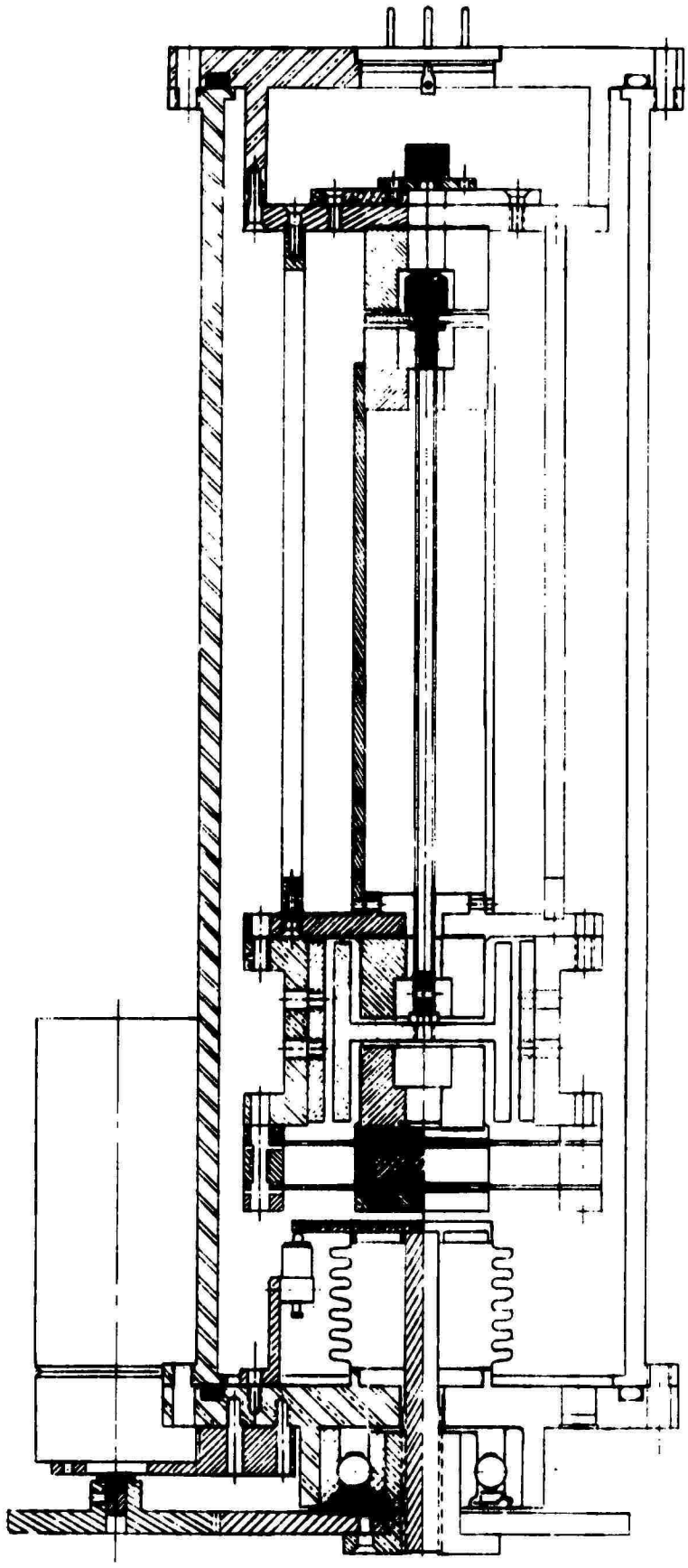

TILT METER

ONE INCH
SCALE

Figure 6

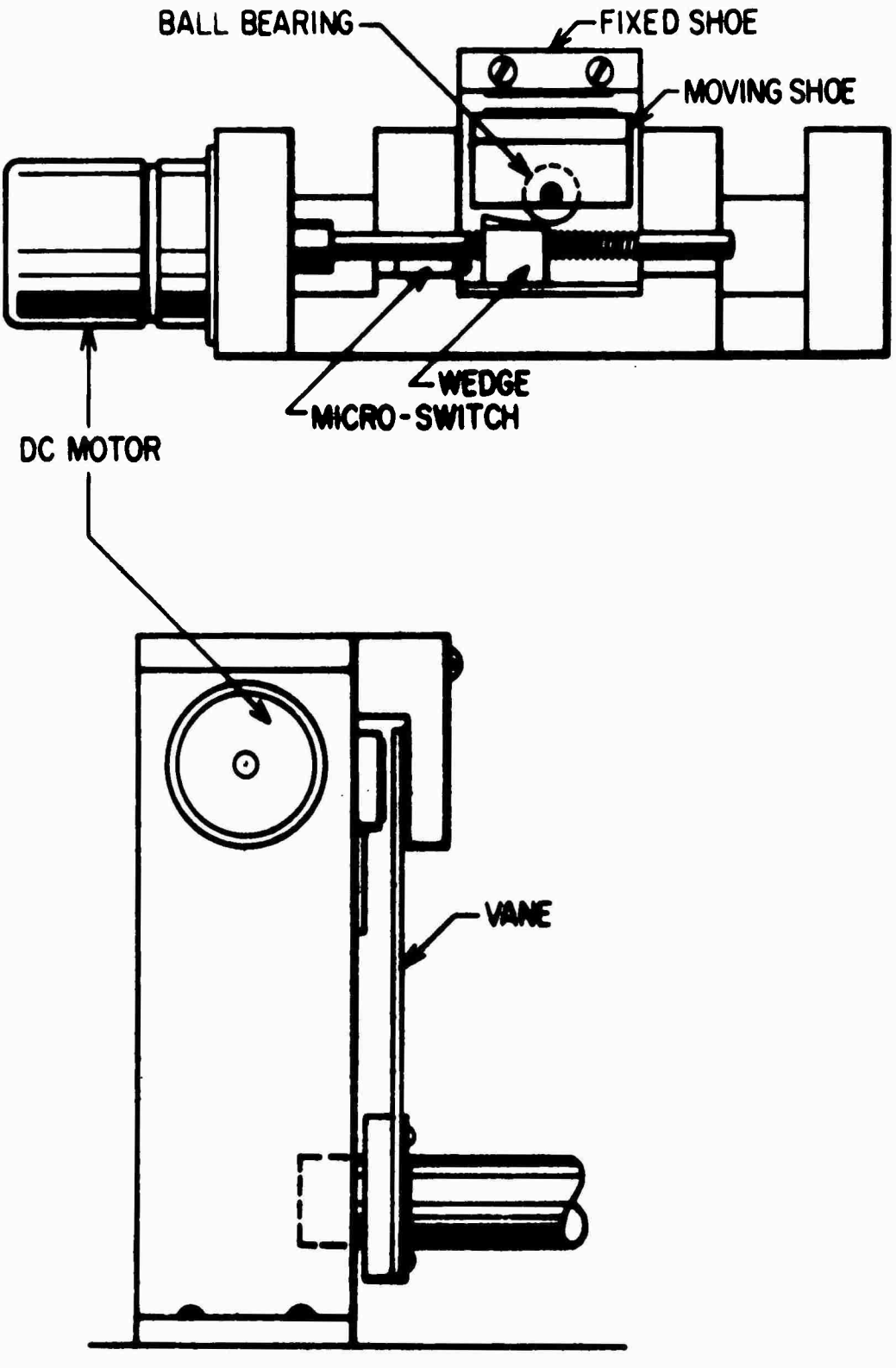

GIMBAL BRAKE

Figure 7

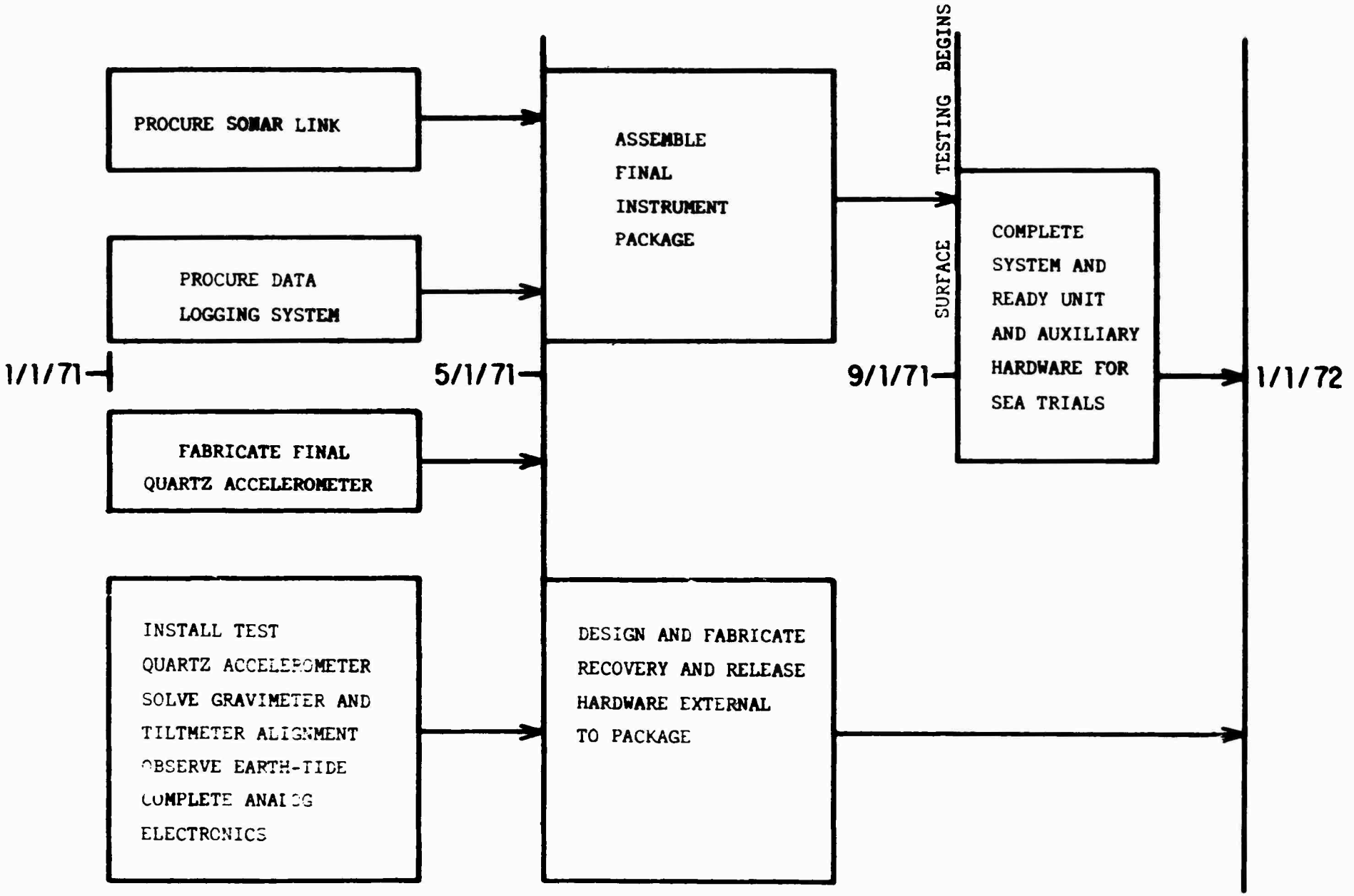

BENTHIC ARRAY, PROGRAM FOR 1971

Figure 8

BLANK PAGE

PHASE SENSITIVE DETECTOR SPECIFICATIONS

Power Consumption:	3.32 mA @ +12v
	1.87 mA @ -12v
Linearity:	0.1%
Dynamic Range:	> 30
Temperature Sensitivity:	100 ppm/°C

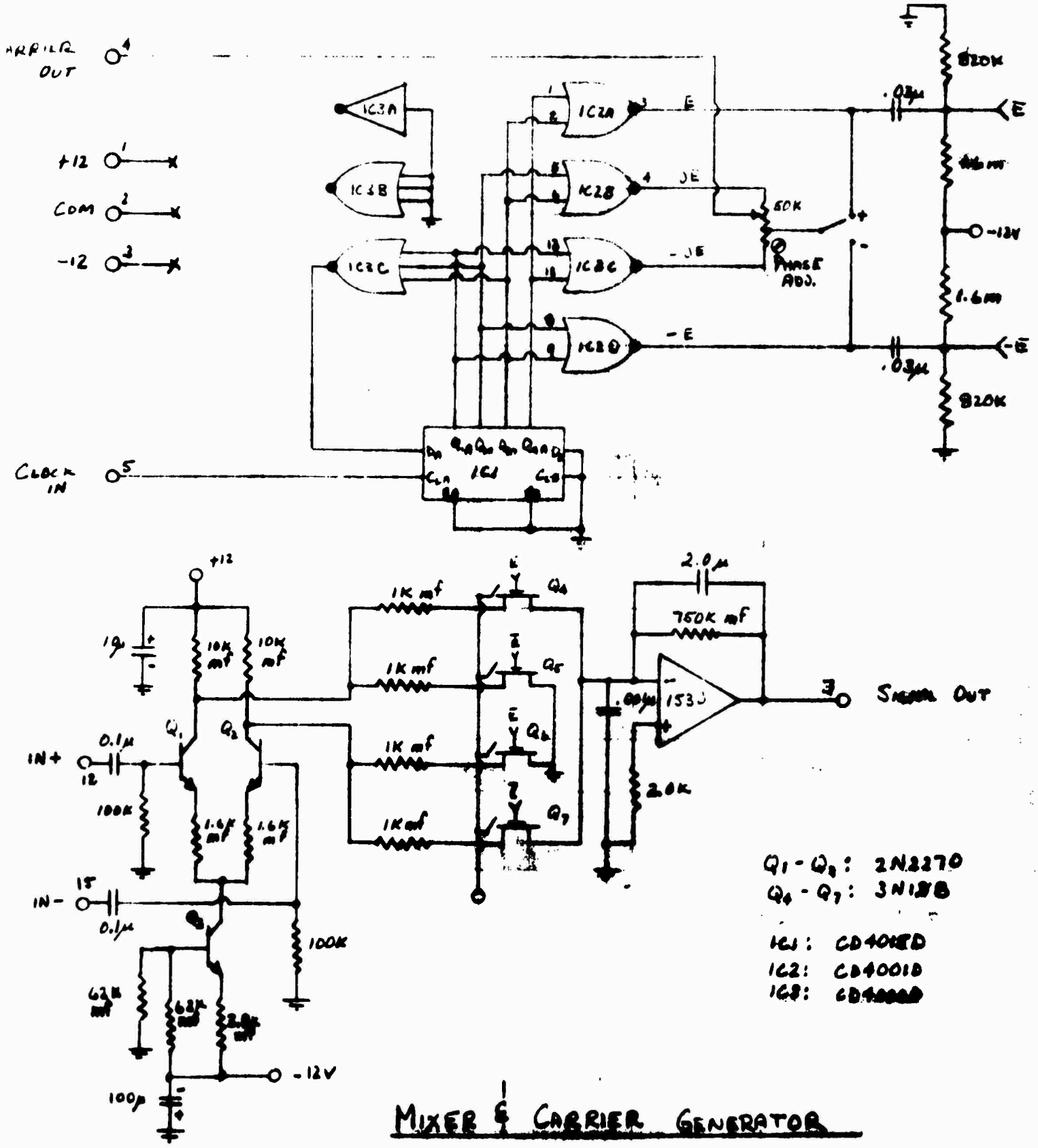

$Q_1 - Q_3$: 2N2270
$Q_4 - Q_7$: 3N187

IC1: CD4047BD
IC2: CD4001B
IC3: CD4011BD

MIXER & CARRIER GENERATOR

1-6-71 SLW

DESIGN OF A LOW POWERED ANALOG-TO-DIGITAL CONVERTER

by

Robert D. Moore
Institute of Geophysics and Planetary Physics
University of California, San Diego

and

James J. Pastoriza
Pastoriza Division, Analog Devices, Inc.
Newton Upper Falls, Massachusetts

BLANK PAGE

DESIGN OF A LOW POWERED ANALOG-TO-DIGITAL CONVERTER

1. Requirements

Growing interest and concern about our physical environment has resulted in a considerable increase in data collecting activities for prolonged periods at remote and inaccessible locations. Typical situations are ocean buoys, earth and space probes, and radiation monitoring devices. The best way to collect and store such data which is inherently low in frequency but still relatively voluminous because of the prolonged periods of monitoring is in digital form. Typically a multiplexer, A/D converter and a magnetic or paper tape recorder are required. Figure 1 shows a typical application for such a data monitoring system. In some of these applications the only power available is from batteries or other limited capacity sources such as solar cells, in others AC mains power is available. In general AC mains power in remote locations tends to be quite unreliable and thus, if long term recording is to be carried out, standby battery operation of equipment is essential. In either case, system components of very low power consumption are desirable.

The fundamental requirement of this type of A/D converter is that it consumes as little power as possible and often as little space as well. While high speed in the converter is not usually required in long-term monitoring applications, resolution is important. For example, consider an application where atmospheric pressure is to be recorded for a week or more with a resolution of one microbar Over periods of a week or more, atmospheric pressure at most sites will vary by at least ± .01 bar. This represents a dynamic range of 10^4:1(80 db) which is, if anything, low for data of this type. This means that in addition to low power consumption the converter should have a resolution of at least 12 bits (1:4096).

[illegible] battery power [illegible] long term variation [illegible] the change in the converter output with [illegible] than 1/2 bit for a supply change of 20% . [illegible] with batteries is the gases sometimes emitted [illegible] types of thin film resistor material. Therefore, [illegible] considered and prudence frequently dictates [illegible] components. Temperature conditions may be either [illegible] variables. To be generally useful, the low power A/D should therefore also have good temperature stability.

.. Techniques for reducing power

The most obvious power consumption in a standard A/D converter occurs in the logic and so it is in this area we first look to for improvement. Fortunately, just at this time COS/MOS type complementary logic is coming into wide use and offers an ideal solution requiring no compromises in speed or accuracy, and actually some simplifications in logic design. The power consumption of this logic is low under any conditions but its quiescent power dissipation is spectacularly low. The complete logic for the converter being discussed here consumes only a few uA under quiescent conditions, i.e. between conversions. The one drawback is the higher price of COS/MOS logic, but this may be a temporary one as competitive manufacturers enter the field. The table in Figure 2 shows the relative merits of different types of logic. COS/MOS logic for a 12 bit A/D including a clock requires about 1 mA maximum current at high conversion rates.

In most conventional A/D designs the supply current taken by the converter depends on whether it is converting or not. Between conversions the converter takes a quiescent current I_Q and during conversions, a larger

current I_C is required. In general the average current is proportional to the conversion rate, the minimum value being I_Q. Clearly then, especially for applications involving low conversion rates, it is desirable to reduce I_Q to as low a value as possible. The simple expedient of using COS/MOS reduces the contribution of the logic to I_Q to a very low value. An additional dramatic reduction of I_Q can be made by switching the analog portion of the converter off between conversions. The switching on and off of the Analog section offers an additional convenience. It eliminates the requirement for two power supplies, since in the act of switching it is possible to simultaneously invert the positive voltage to provide a symmetrical negative voltage. Thus the entire A/D can operate on a single 12 volt battery.

It is easy to write an equation which gives the average supply current taken by the converter as a function of sample rate. Let I_S be the average supply current, I_Q be the standby or quiescent current taken by the converter when not converting, I_C be the current taken while converting, T be the conversion time and R be the conversion rate, then,

$$I_S = I_Q + RT\, I_C \qquad (1)$$

(Since the maximum conversion rate is $R = \frac{1}{T}$, the product RT is always less than 1.) Figure 3 shows data taken on the prototype converter. The points represent measured average current values. The equation of the line is:

$$I_S = 0.005 + 0.004\ RT \qquad (2)$$

where I_Q is [illegible]. The slope of the line was determined from a least-[illegible] fit to these three points, the value of I_Q by direct measurement. A feeling for the extremely low power consumption of this converter can be had from the above supply current values for 1, 10 and 100 conversions per second as given by equation 2, namely ~ 10 μA, ~ 50 μA and ~ 400 μA respectively. At a 100 per conversion rate the current drain of 40 mA from the single 15 V supply is still very low compared to conventional 12 bit converters of this speed.

3. The Final Design

The final circuit divides up naturally into three sections: logic, analog section and switched power supply. A COS/MOS logic section was packaged in one module containing all of the logic for successive approximation A/D conversion. The scheme is illustrated in figure 4. A conversion is started by the application of a positive-going edge to the "convert command" input. This clocks FF1 driving the reset line to logical 1, setting FF3 and resetting FF4 through FF14, these flip-flops, FF3 through FF14, constitute the data register and contain the binary number equivalent to the input voltage at the end of a conversion. The Q outputs of these flip-flops control the AD505 μDAC switches used in the D/A converter. At the beginning of a conversion this register is thus set to 100000000000. The reset line also resets the last twelve bits of the 16 bit shift register. This results in the $\overline{\text{STATUS}}$ line (STATUS is an output pulse which is one during a conversion) going to zero which starts the clock. The first positive going clock transition clocks a one into the first bit of the first shift register. This resets FF1.

STATUS going to one switches on the switched power supply. The MSB flip-flop (FF3) is left set through the first four clock pulses in order to give the analog section time to settle down. By the time the bit in the shift register has reached the 2^{10} position the comparator output will have settled at a level appropriate to the relative magnitude of the MSB-weighted feedback current to the comparator and the current produced by the input voltage. If the MSB is to be kept this level will be logical 0 , otherwise logical 1 . This level controls the state into which FF2 is clocked. The $\bar{Q}$ output of FF2 controls the "keep/reject" line (K/R) which controls the data inputs of all the flip-flops in the data register. When the bit in the shift register is shifted to the 2^{10} position FF4 is set, clocking FF3 which will be reset if the K/R line is low, left set otherwise. One clock period later the bit is shifted to the 2^{9}position. This sets FF5 which clocks FF4 as before. This process continues until one clock period after FF14 is set. The next positive-going clock transition shifts the bit to the last position in the shift register. This clocks FF14, drives STATUS low and stops the clock thus completing the conversion.

The analog section consists of the analog devices model AD550 monolithic µDAC switches, the model AD850 thin film resistor network, the comparator, an emitter-follower regulator to provide a +5V supply for the µDAC's and regulators to provide reference voltage to set the µDAC current levels and to provide offset so that bipolar voltages can be handled. (The converter shown here is set up for an input range of ±10V with an offset binary output code i.e.

-10V = 000000000000, 0V = 100000000000, + 10V = 111111111111.)

The AD505 and AD850 are discussed in detail elsewhere[1]. The µDAC's are operated at 64% of their rated current to accomodate the available 12V supply. (They are designed to operate from a 15V supply.)

The [illegible] power supplies are shown in figure 5. Q_3 [illegible] current source collector current being set by the 6.19K resistor and the voltage across [illegible] (used as a diode). Q_4 is a 6.4 volt reference zener, [illegible] for the μDAC and is normally used, as here, to temperature compensate the base-emmiter drops of the μDAC current switches. (The numbers on the ladder outline represent μDAC DIP pack pin numbers.) The base of Q_4 is connected to the base of all the μDAC current switches and thus a stable 6.4V is established to set the currents in the weighting resistors. The collector current of Q_3 is used to establish a stable voltage drop of about - 3V , relative to +11, across the 3.48K resistor. This, plus the drop across D_2 is used to set the base voltage on Q_1 and Q_2 . D_2 temperature compensates the base-emmiter drops of Q_1 and Q_2 . Q_1 is used as a current source to provide the current through Q_4 and [illegible] . Q_2 is a current source to provide the current for reference zener [illegible] . This zener provides a stable + 6.4V source to provide the offsetting current to the summing junction. The 1M resistor is necessary to insure start-up of the current sources.

This circuit has two important features. Since it is switched on at the beginning of each conversion it is important that the reference voltages settle rapidly after turn-on. This circuit configuration settles very rapidly, the reference voltages being completely stabilized within a few μsec of turn-on. Secondly, any variation of the nominally ±11V lines is absorbed by the current sources. This results in a sensitivity to supply voltage changes of only one bit for a 3.5V (29% of 12V) change. The unit will operate to specifications over a supply voltage range of 10 to 14V.

Figure 6 shows the design of the switched power supply for the analog section. The line marked "+ 12" is energized continuously and powers the logic. Between conversions the logic is quiescent and consumes only the very low power

characteristic of quiescent COS/MOS logic. Upon receiving a conversion command signal the logic executes a conversion cycle. A positive going STATUS pulse is generated by the logic during the conversion cycle. This pulse controls Q_1 in the switched power supply. When the STATUS line goes positive, Q_1 emitter goes high, providing the switched positive supply voltage. During the quiescent period the emitter of Q_1 has been low, holding MOSFET Q_3 on and transistor Q_2 off. C_1 is charged to nearly 12V through Q_3 and D_1 during this time. When the emitter of Q_1 goes high, during a conversion, Q_2 is turned hard on and Q_3 is turned off. Thus, during conversions, the positive end of C_1 is brought near ground providing a switched negative supply line at the point indicated. It should be noted that this scheme has the further advantage that the power supply lines to the analog section are well decoupled from the logic during conversion. The presence of Q_3 is important to efficiency in terms of power consumption. If Q_3 were replaced by a resistor, its resistance would have to be quite low to insure complete charging of C_1 between conversions at high conversion rates. This small resistor would then take a large current from the +12 line during conversions. The high off resistance ($\sim 10^9\Omega$) and low on resistance ($\sim 30\Omega$) of Q_3 provide an efficient solution to this problem.

4. Final Specifications

The unit is operated with a total of 70 μsecs convert time. This means that the clock runs at a rate of about 4.4 μsecs per bit. The first 17.5 μsecs are used for settling time for the regulator and comparator and the rest of the general analog circuitry. The remaining 52.5 μsecs is used for conversion to a resolution of 12 bits. Figure 7 is a tabulation of final specifications achieved on this unit, Figure 8 is a complete schematic diagram.

BLANK PAGE

REFERENCES

1. Analog Devices Technical Bulletin; "μDAC model AD550 monolithic quad current switch for D/A and A/D conversion".

ACKNOWLEDGEMENT

This research was supported in part by the Advanced Research Projects Agency of the Department of Defense and was monitored by the Office of Naval Research under Contract N00014-69-A-0200-6012.

Figure 1 Interior of pressure sphere containing data logging electronics for deep sea tide-gauge. Equipment shown and associated sensors are operated on the ocean bottom at depths from 5,000 feet to 20,000 feet, for periods up to one month. Power source is standard automobile-type 12V lead-acid cells. Data are recorded on low-power digital magnetic tape unit (swung out to right). Application is typical of those requiring low power hardware (data lights are used for surface checking only).

Photo, courtesy Dr. Frank E. Snodgrass.

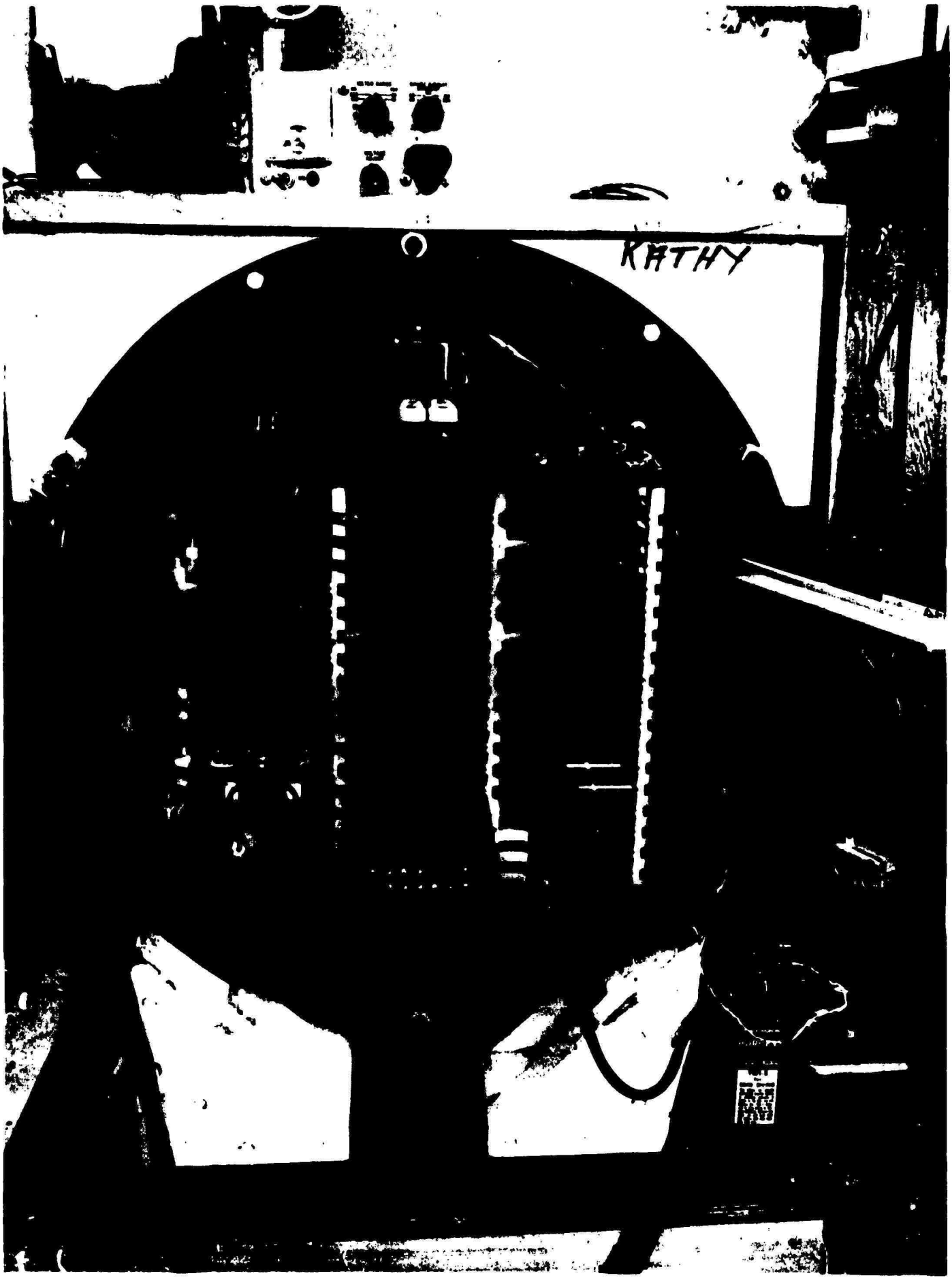

Figure 1 - Interior of Pressure Sphere

COST AND POWER CONSUMPTION COMPARISONS OF COS/MOS
AND OTHER COMMON LOGIC TYPES

Logic Type	Cost	Power (Standby)
TTL	$29.00	350 mA @ 5v
Low Power TTL	$63.00	30 mA @ 5v
COS/MOS (epoxy package)	$52.86	5 µA @ 5v

Figure 2

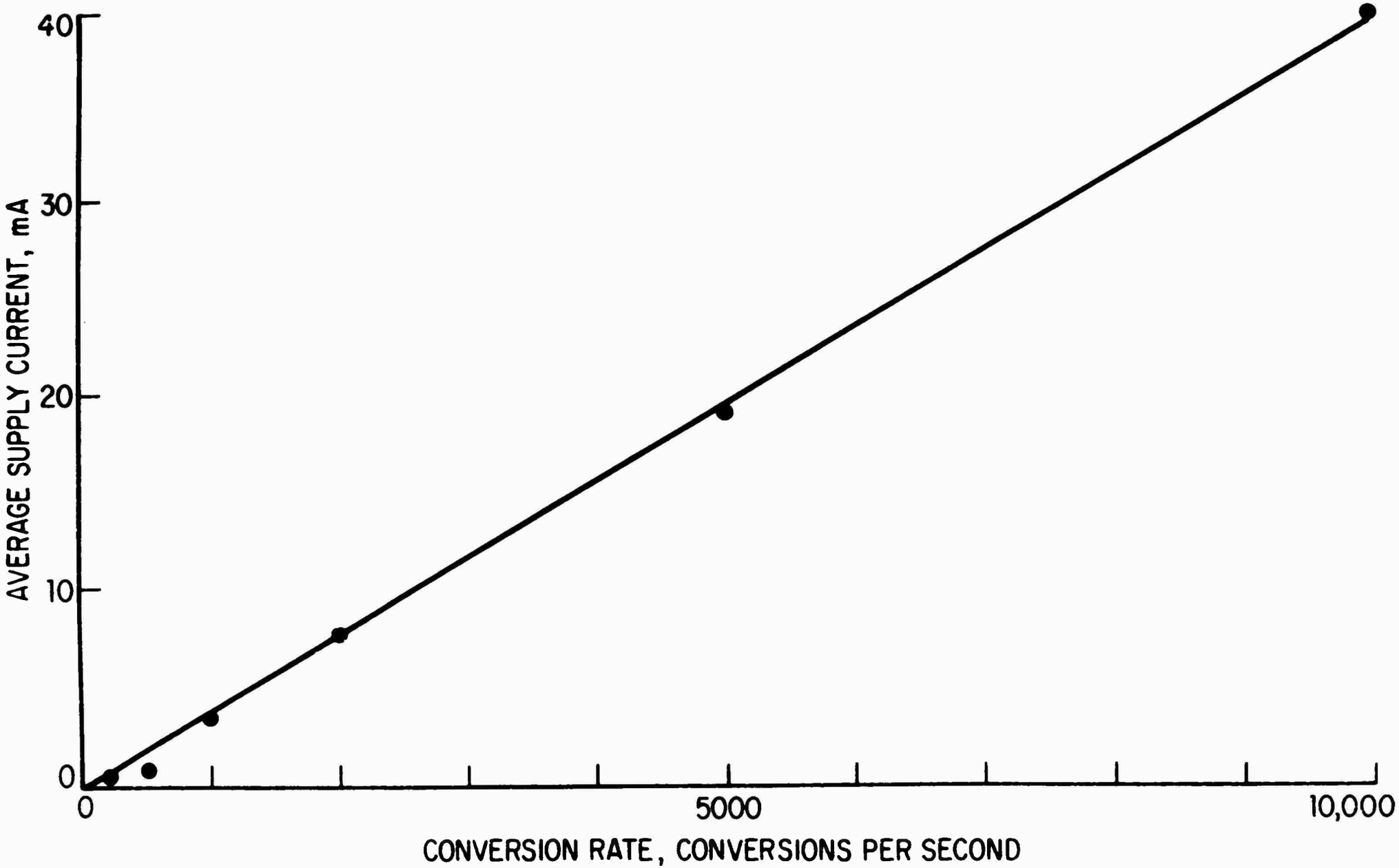

Figure 3 Average supply current V_S conversion rate

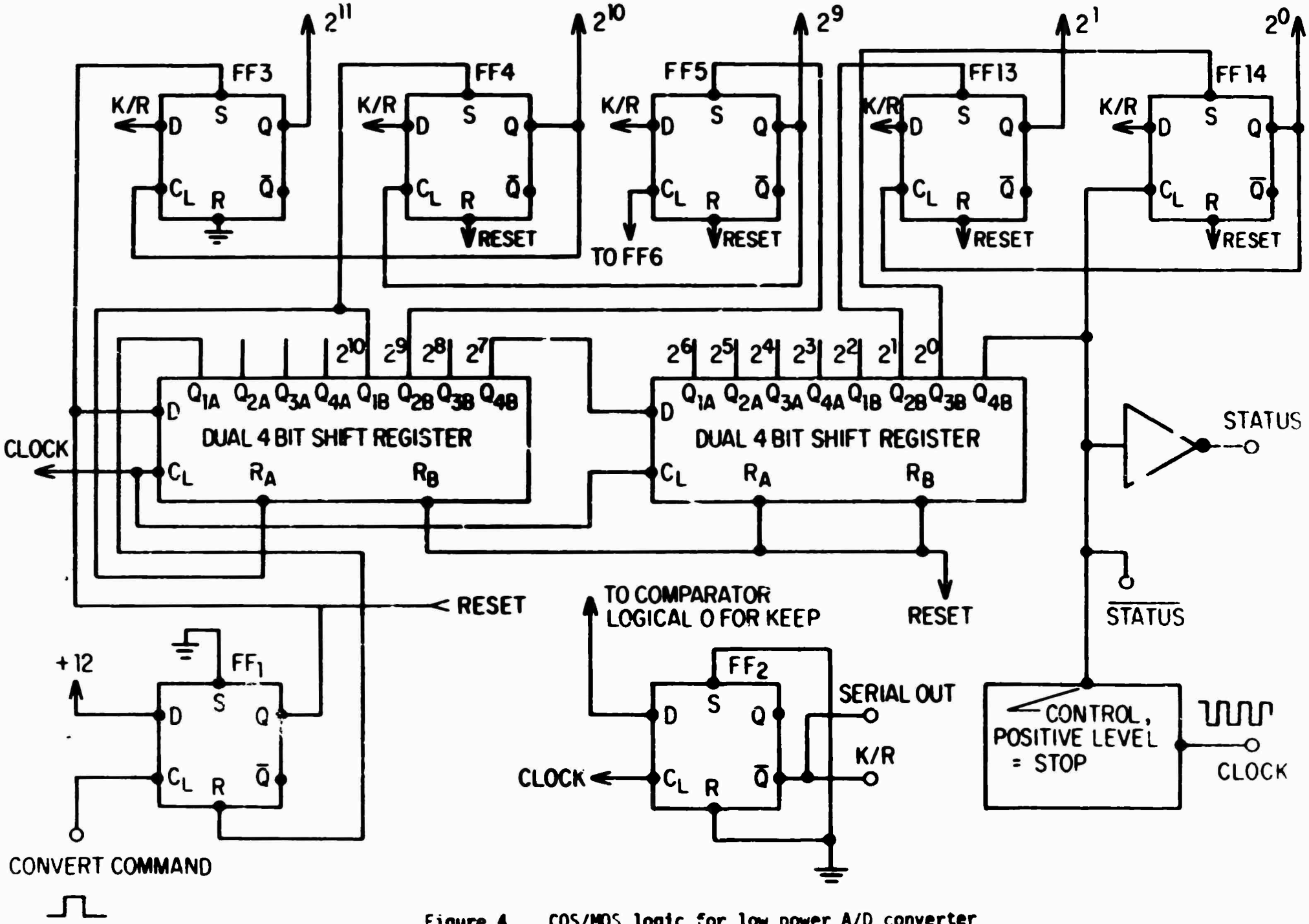

Figure 4 COS/MOS logic for low power A/D converter

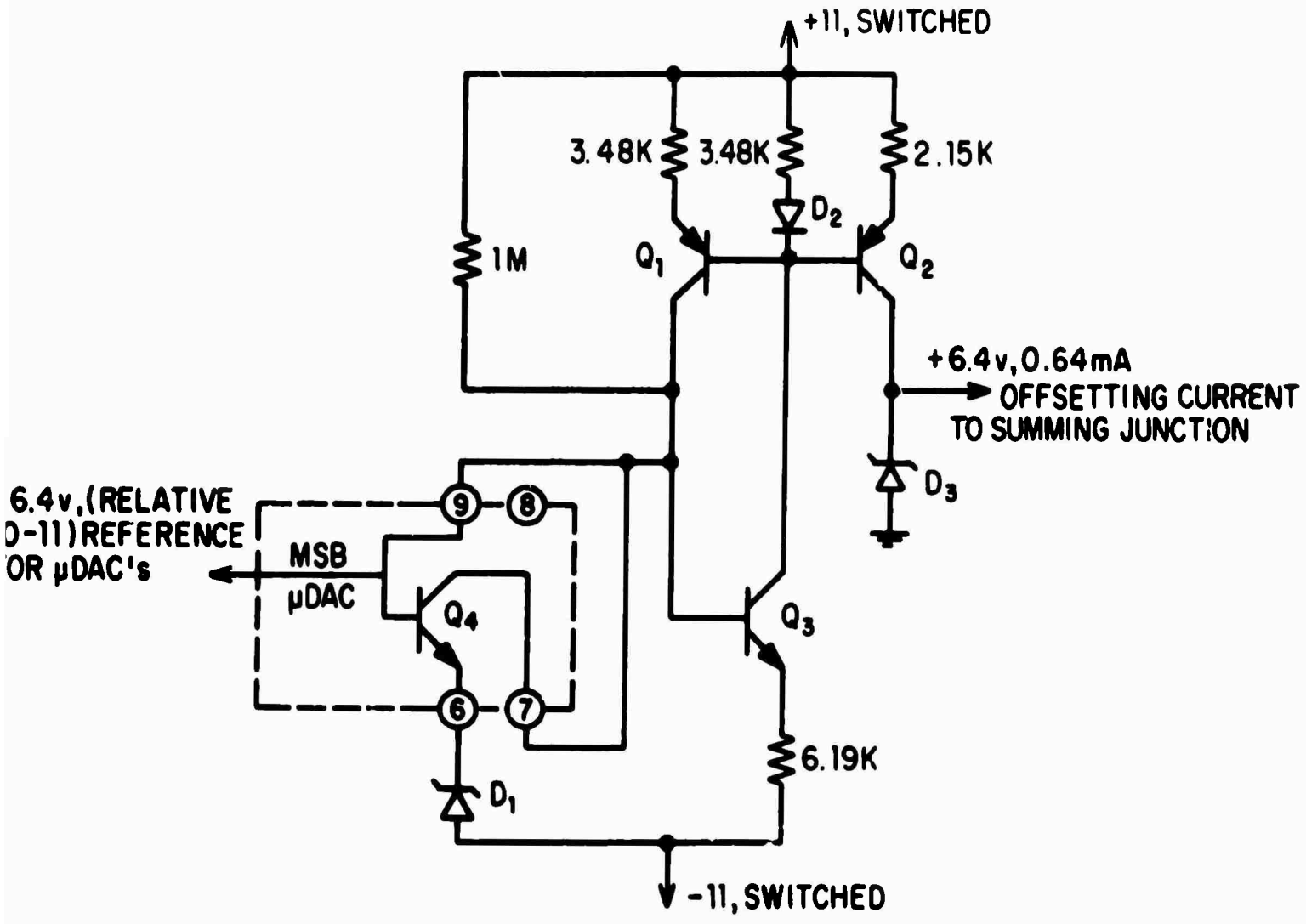

Figure 5 Regulated reference supplies, analog section.

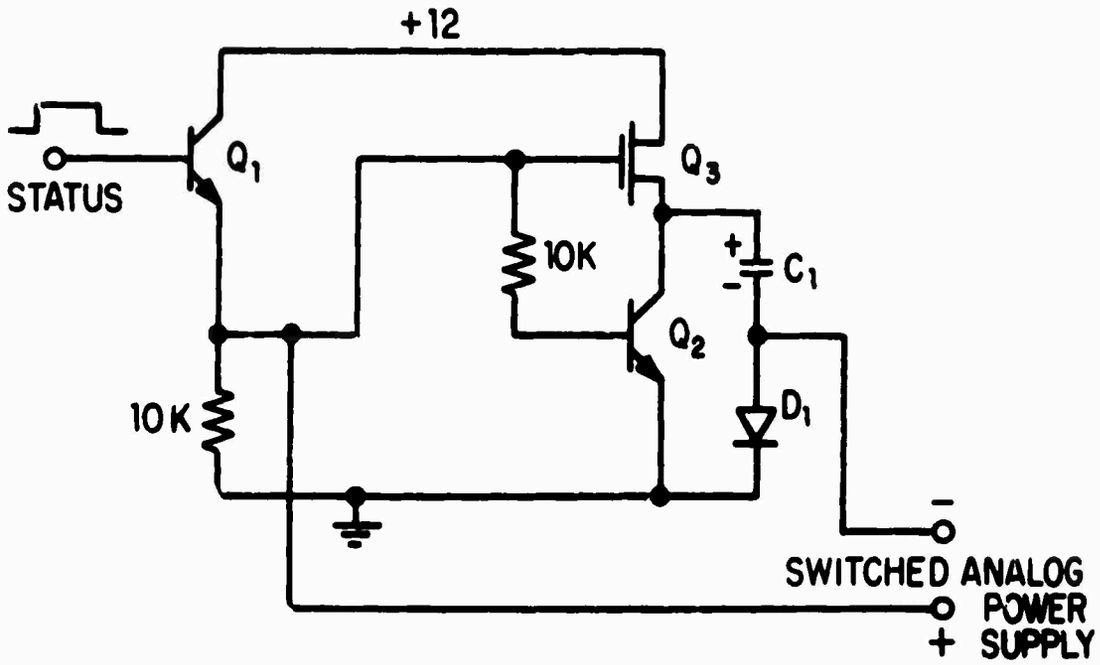

Figure 6 Switched power supply for Analog section

LOW POWER A TO D CONVERTER,
FINAL SPECIFICATIONS

Power Supply:	Logic +6 to +15V Analog +12 to +15V
Current Drain - typical: (Analog and Digital @ +15V)	Conv. Rate — Avge Supply Current 5 KHz — 20 mA 1 KHz — 4 mA 100 Hz — 0.4 mA 1 Hz — 0.01 mA
Conversion Time:	75 µsecs
Input Voltage:	0 to +10 or ± 10V
Input Impedance:	10 K
Accuracy	± ½ LSB
Temperature Coefficient:	± 10 ppm/°C
Resolution:	12 bits
Input Trigger:	1 µsec positive pulse 70% of logic voltage
Output Signal:	MOS compatible
Power Supply Sensitivity:	12 to 15V, ± 1 bit

Figure 7

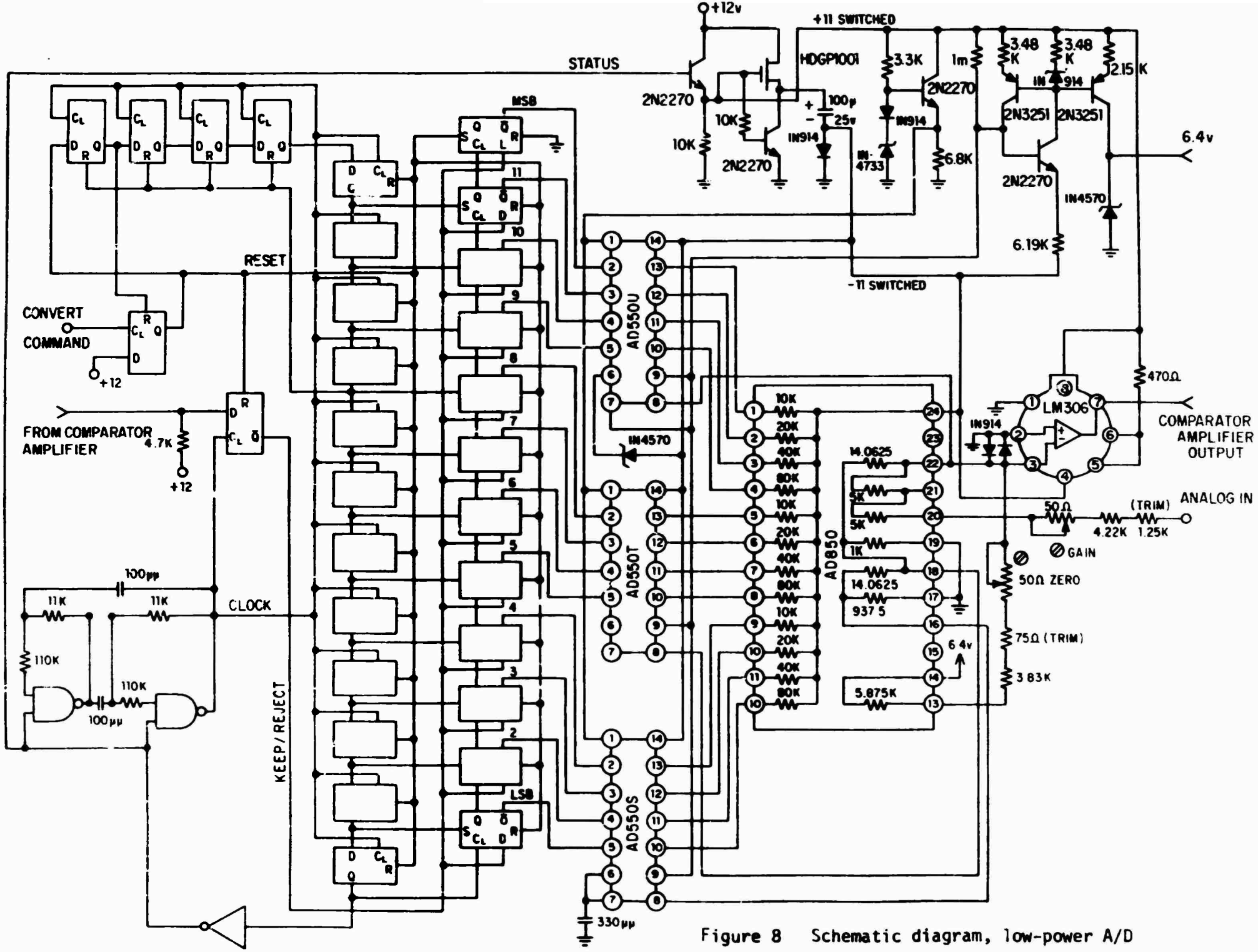

Figure 8 Schematic diagram, low-power A/D

MULTIPLEXER SPECIFICATIONS

Power:	200 μA @ +12v 180 μA @ -12v
Temperature Sensitivity:	< 10 ppm/°C
Crosstalk:	< 0.02%
Rate:	1 channel/sec.

MULTIPLEXER

11-30-70
SLW

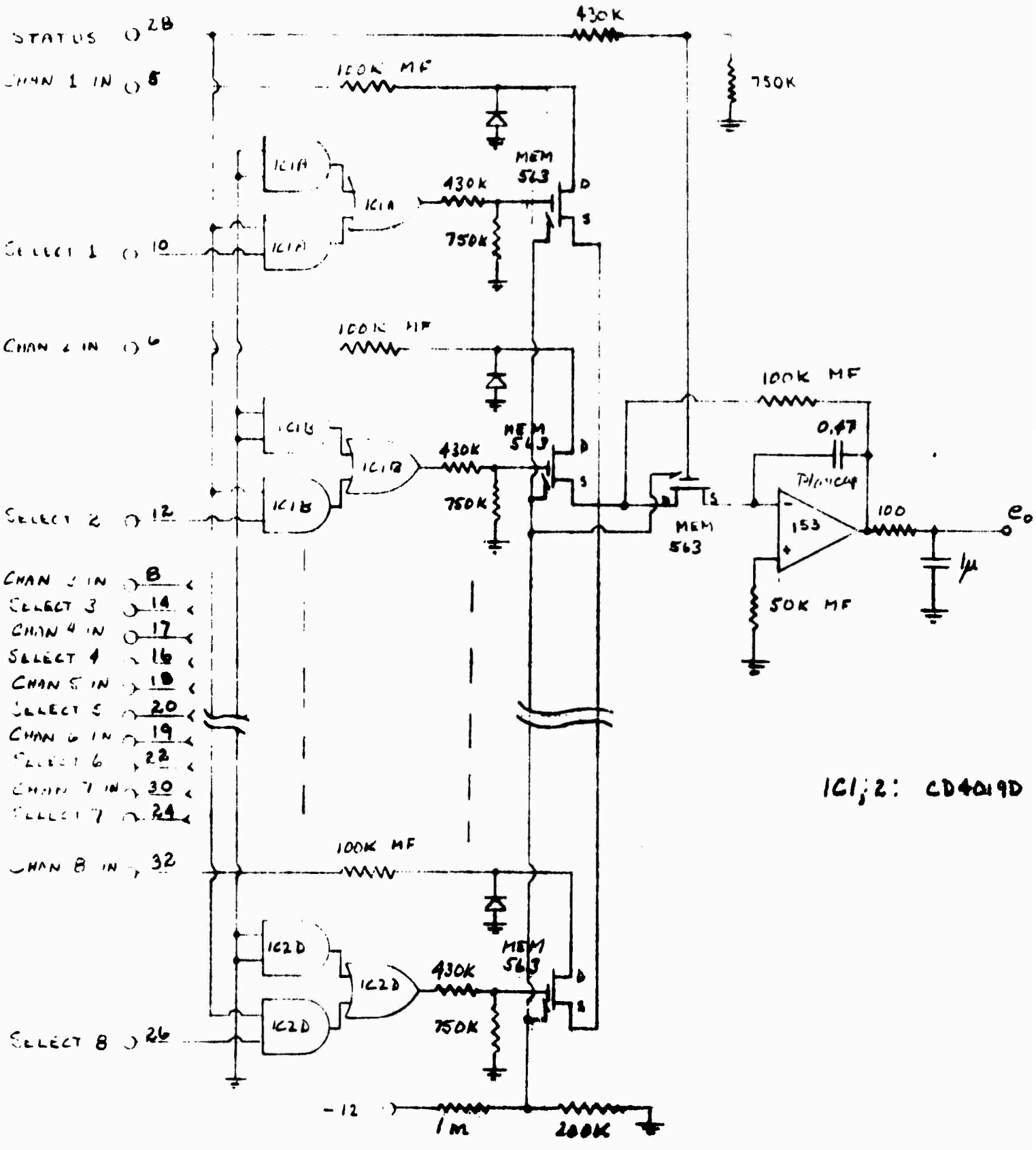

IC1,2: CD4019D

TAPE RECORDER POWER REQUIREMENTS

Power Supply:	Single 12v supply
Current Consumption:	0.52 amp-hr/100 ft of tape
	i.e. 12.8 amp-hr/2400 ft reel (independent of stepping rate)
Standby Current:	< 50μA

BLANK PAGE

Low Power Tape Recorder Electronics Functional Description

Refer to the timing logic schematic, Board No. 2. The design of the recorder is such that the major power consuming components, namely the record heads and the stepping motor are normally not powered. Power is applied to them only during a write cycle. When the recorder receives a write command the stepping motor and write heads are powered up in the appropriate sequence, a single character is written on the tape and these components are then shut down again. The function of the timing logic board is to produce the various pulses that control the internal operation sequence of the recorder during a write cycle. A write cycle is initiated by applying a positive going edge, COS/MOS compatible, to the step command input. This clocks FF1 setting the Q output true. This resets the 8 bit binary counter IC_2. The completion of the preceding write cycle has left this counter in the state 00010101, i.e. decimal 168. This is accomplished as follows: When the counter arrives at the binary state 00000101, both inputs to NAND gate G_1 go true. This results in the output of G_1 being driven low. This results in the output of following inverter I_1 going high or true. Thus one input of NAND gate G_2 goes true at this time. Thirty-two counts later output Q_4 of the binary counter goes true making both inputs to G_2 true and thus driving the output of G_2 low. The output of G_2 going low gates off the multi-vibrator consisting of G_3 and G_4. When running, this multi-vibrator produces a squarewave output with a nominal period of 100 microseconds. It will be noted that the multi-vibrator gates off with the output of

G_4 high. When the multi-vibrator is gated on, the output of G_4 makes a transition from high to low approximately 50 microseconds after the multi-vibrator is gated on. Thus, one of the inputs of G_5, a NOR gate is held positive continously between write cycles. Fifty microseconds after a step command is received, the output of G_4 goes low. Since the step command input drives the $\overline{Q}$ low, both inputs of G_5 are driven low 50 microseconds after the receipt of a step command. This results in the output of G_5 going high, resetting FF1. The Q output of FF1 is thus a positive pulse, 50 microseconds long which begins with the application of the step command. This pulse is referred to hereafter as clock (C_L). The $\overline{Q}$ output of FF1 is the logical negation of clock. It is referred to hereafter as not-clock and abbreviated $\overline{C_L}$. As was explained before, the output of NAND gate G_2 goes low at a count corresponding to decimal 168 and remains low between step commands. On the receipt of a step command the resetting of the counter drives the output of G_2 high where it remains until the count of decimal 168 is reached. The output of G_2 is called P_W and is used to control the application of power to the write heads. It will be seen that P_W is a positive going pulse with a length of approximately 16.8 milliseconds. The output of G_2 is passed through inverter I_2 produce the output $\overline{P_W}$ which is the logical negation of P_W. As was explained previously, 50 microseconds after the application of a step command the output of NOR gate G_5 goes positive resetting FF1. This output is also connected to the clock input of FF2. Thus at the same time that FF1 is reset, FF2 is clocked. This results in the Q output of FF2 going true and the $\overline{Q}$ output going false. These two outputs are denoted as P_S and $\overline{P_S}$ respectively. Flip flop 2 is reset

when the output of inverter 1, goes positive, i.e. at a count of decimal 160, thus P_S is a positive going pulse approximately 16 milliseconds long which begins at the end of clock and ends approximately .8 milliseconds before P_W ends.

Refer now to the schematic entitled Write Amplifier, final version, Boards No. 4, 5 and 6. This schematic shows the logic and interface amplifier used to drive one of the six data tracks. Boards 4, 5 and 6 each contain two of the amplifiers shown in the schematic. The data lines are assumed to swing between 0 and +12 volts compatible with the COS/MOS logic. The data line comes in at the point marked X on the schematic diagram. The 1K resistor and the diodes are to protect the gate input against excessive voltage swings on the data line. The inverter I_1 is used to generate the logical negation of the input X namely $\overline{X}$. The output of I_1 which will be logical 0 if X is logical 1, is applied as one of the inputs to gate 2. The other input to gate 2 is $\overline{C_L}$. $\overline{C_L}$ is normally positive and goes to 0 for approximately 50 microseconds at the beginning of a write cycle. If input X is a 1, the output of G_2 will go positive during the time that $\overline{C_L}$ is low. This will clock the flip flop. If input X is a 0, the flip flop will not be clocked at this time. Thus it is seen that $\overline{C_L}$ functions as a strobe defining the time at which data is taken from the data lines. The Q and $\overline{Q}$ outputs of the flip flop are coupled via gates G_3 and G_4 respectively, to the inputs of the head driver amplifier consisting of a pair of NPN transistors. The corresponding record head coil is connected between the points marked H_{X2} and H_{X1} on the schematic. Thus, the current

flow direction in the record coil will depend on the state of the flip flop. The output of whichever gate G_3 or G_4 is selected by the flip flop can go positive only during the time that the voltage applied to the point marked $\overline{P_W}$ is negative, i.e. during the 16.8 millisecond interval described in the preceding discussion. At all other times the outputs of the two gates must be low and thus no current flows through the 10K base resistors of the transistors. Furthermore the MOSFET transistor feeds supply current to the head drive amplifier only if $\overline{P_W}$ is low, again only during 16.8 milliseconds that P_W is true. The point marked monitor on the schematic diagram is brought out to the external interface connector and can be used to monitor the state of the head driving flip flop. It will be noted that power is never removed from the flip flop and thus it stores its preceding state to maintain the normal NRZ recording procedure. There are a total of 7 of these write amplifiers in the tape recorder, six of which drive the data tracks, the seventh of which drives the parity track. The six data track drivers are in three pairs on three boards. The seventh one is on board No. 8 along with the stepper logic, which is discussed below.

Refer now to the schematic diagram entitled Parity Generator Final, Board No. 7. This is simply a chain of NAND logic used to generate the parity recorded on the tape from the input data. The inputs marked 1, 2, 4, 8, a and b are obtained directly from the input data lines. The inputs marked $\overline{1}$, $\overline{2}$, $\overline{4}$, $\overline{8}$, $\overline{a}$ and $\overline{b}$ are obtained from the inverted data outputs generated by the write amplifier boards. The operation of this logic is completely conventional and will not be described further.

Refer now to the Schematic entitled Stepper Logic and Drive, Boards No. 8 and 9. The circuitry shown in this schematic is distributed over the two boards. Board No. 8 contains the logic portion, as mentioned above. Like the write heads, power is applied to the stepping motor only during a write cycle. Normally the power to the stepping motor is turned off. Stepper logic and drive consists of a flip flop which controls the direction in which current will flow in the stepper motor winding and the necessary gating to switch the power to the stepping motor on and off. The flip flop is clocked by the strobe C_L and changes state each time a write command is received. The Q and $\overline{Q}$ outputs of the flip flop are coupled to the stepping motor drive amplifier via gates G_1 and G_2 and inverters I_1 and I_2. G_1 and G_2 are NOR gates. The outputs G_1 and G_2 are held low except during the time when input $\overline{P_S}$ goes low. This occurs during the time interval discussed previously. During this time the output of whichever of G_1 or G_2 is receiving a low input from the flip flop will go high. Thus, during the time that $\overline{P_S}$ is zero, the output of one of inverter 1 or inverter 2 will be low, the other one being high. These outputs are used to control the stepper motor drive amplifiers consisting of MOSFETS Q_1 and Q_2 and NPN transistors Q_3 and Q_4. During the time that $\overline{P_S}$ is zero, the gate of either Q_1 or Q_2 will be held low, the other being held high. The MOSFET whose gate is low will be turned on hard, thus turning on the corresponding transistor. Thus a low resistance path will exist from either M_1 or M_2 to ground during the time that $\overline{P_S}$ is low. These points go to the two ends of the stepper motor drive winding, the center tap of which goes to +12 volts. Thus during the time the stepping motor is powered up, the current will flow

either from the center tap through M_1 or the center tap through M_2 depending on the state of the flip flop. Since the state of the flip flop reverses at each write command the stepping motor will step once for each write command. When $\overline{P_S}$ goes positive at the end of a write cycle, both Q_1 and Q_2 will be shut off by virtue of the fact that the outputs of both inverter 1 and inverter 2 go high at this time. It can be seen that if Q_1 and Q_2 are both shut off, that no current at all will flow in the stepper drive amplifier circuit.

Refer now to the schematic diagram entitled, One-half Reel Motor Driver, Board No. 10. Board No. 10 actually contains two of the circuits shown in the schematic, one for each reel drive motor. The points marked stop and start go to single pole, single throw normally open switches which are used to sense the state of the tape tension in a way that will be described later. The circuit operates as follows: If the switch connected between the start terminals is momentarily closed, the flip flop will be forced into its set condition, that is Q true. Under these conditions the gate of MOSFET Q_1 will be low, that of MOSFET Q_2 will be high. This turns on Q_1 and turns off Q_2. Q_1 going on, supplies base current to transistor Q_3 turning it on. The motor, connected between the terminals marked motor, thus begins to run. If now a momentary connection is made between the terminals marked stop, the flip flop will be reset turning off Q_1 and turning on Q_2. This results in Q_3 turning off and Q_2 shorting the reel drive motor. Q_2 provides dynamic breaking of the reel drive motor.

Refer now to the schematic entitled Record Gap Logic, Board No. 1. The purpose of this board is to enable standard IBM type record gaps to be generated and also to provide for erasing tape in 3/4 inch sections which is useful to provide an erased portion after the load point, etc. Upon receiving a record gap command, the logic inhibits the write strobe (C_L) so that the heads are held in whatever state they happen to be in at the time, advances the tape 4 character spaces, then resets the write heads, thus writing a longitudinal parity check character; and then advances the tape approximately 3/4 inch with the heads held in this reset condition. A record gap is commanded by applying a positive COS/MOS level to the input of gate G_2. Since both the external gap command input and erase inputs are normally low, the output of gate G_2 is normally high. The application of a positive level to the external gap command input thus will drive the output of G_2 low and if P_W is low at this time, this will result in a positive going transition being applied to the clock input of FF1. If P_W is high at the time the external gap command is applied, FF1 will not be clocked until the time at which P_W goes low. This insures that a record gap cannot be started in the middle of a write cycle. When FF1 is clocked, its Q output goes true resetting the 7-bit binary counter IC_3 and also FF2. FF2 and inverter I_2 are used to extend the counter capacity from 7 to 8 bits. The 8-bit binary counter consisting of a combination of IC_3 and FF2 has been left in the condition of 00000101 by the previous record gap cycle. When this count occurred the two inputs of G_4 went high, thus driving its output low and gating off the multi-vibrator consisting of G_5 and G_6. When IC_3 and FF2 are reset the STATUS line goes high starting the multi-vibrator

and resetting the flip flop FF1. This also results in a positive level appearing on the STATUS output. When the STATUS line goes high, the output of G_6 which had been clamped high immediately goes low and remains low for approximately half a clock period when it makes its first clock transition from low to high. The output of G_5 remains high for half a clock period and makes its first transition from high to low. The STATUS line is applied to the input of inverter 3 thus generating the term $\overline{\text{STATUS}}$. $\overline{\text{STATUS}}$ is normally high except during a record gap cycle when it is low. $\overline{\text{STATUS}}$ is applied along with the external step command signal to the input of G_8. As long as $\overline{\text{STATUS}}$ is high G_8 transmits the external step command, acting as an inverter. When $\overline{\text{STATUS}}$ goes low, the external step command pulses are prevented from getting through G_8 . When no record gap is being recorded the output of G_5 is clamped high. Thus, G_9 operates as an inverter and G_8 and G_9 transmit external step command pulses to the external step command out. When $\overline{\text{STATUS}}$ goes low the output of G_8 is clamped high, thus during this time the output of G_9 will be the inverse of the output of G_5 . The terminal marked "step command out" will be a negative level at the beginning of a record gap cycle, and will remain negative for one half clock period after the application of an external gap command pulse. The first transition is from negative to positive resulting in a step command to the timing logic. The binary counter IC_3 is clocked by the output of G_6 . IC_3 clocks on negative going transitions applied to its clock input. When STATUS goes positive the output of G_6 makes an immediate transition from high to low. This does not clock IC_3 however because at this time the Q output of FF1 is still positive holding the IC_3 in the reset condition. The first transition of the output of

G_5 occurs one-half clock period later and is from high to low. Because of the inversion of G_9 this produces a transition from low to high on the step command out. One-half clock period later, the output of G_6 makes a second transition from high to low which clocks IC_3. Thus the sequence of operations from startup is step, clock, step, clock. This continues until the fourth step takes place. On the next clock pulse the counter IC_3 is stepped to the count where Q_3 becomes true. This results in the output of G_1 going low and consequently the output of I_1 going high. The output of I_1 drives the reset input of all the head drive flip flops and consequently resets all 7 head drive flip flops. Thus the next step results in the recording of a longitudnal parity check character on the tape. The heads are held in a reset condition and the tape stepped until a count of decimal 160 is reached. That is a total of 156 steps after the writing of the longitudinal check character. Since each step represents a tape motion of 0.005 inch, the total tape motion after the parity check character is approximately 0.780 inches. This is well within IBM record gap tolerances. The function of G_1 is to prevent the write strobe from strobing data from the data lines into the record heads during the time that the record gap is being written. During the time a gap is being written the line $\overline{\text{STATUS}}$ is low holding the output of G_1 high, thus inhibiting the write strobe. Since the multi-vibrator that drives the stepping motor during the record gap cycle operates at approximately 40 cycles per second, the total time involved in writing the record gap is about 4 seconds. The erase input allows a record gap to be written without the longitudinal parity check character, that is the net result is to erase about 8/10 inch of tape. A positive transition applied to the erase input will start the record

gap cycle via G_2 and G_3 just as an external gap command. Simultaneously, via G_1 and I_1 it immediately resets all of the heads so the longitudinal parity check character doesn't appear on the tape.

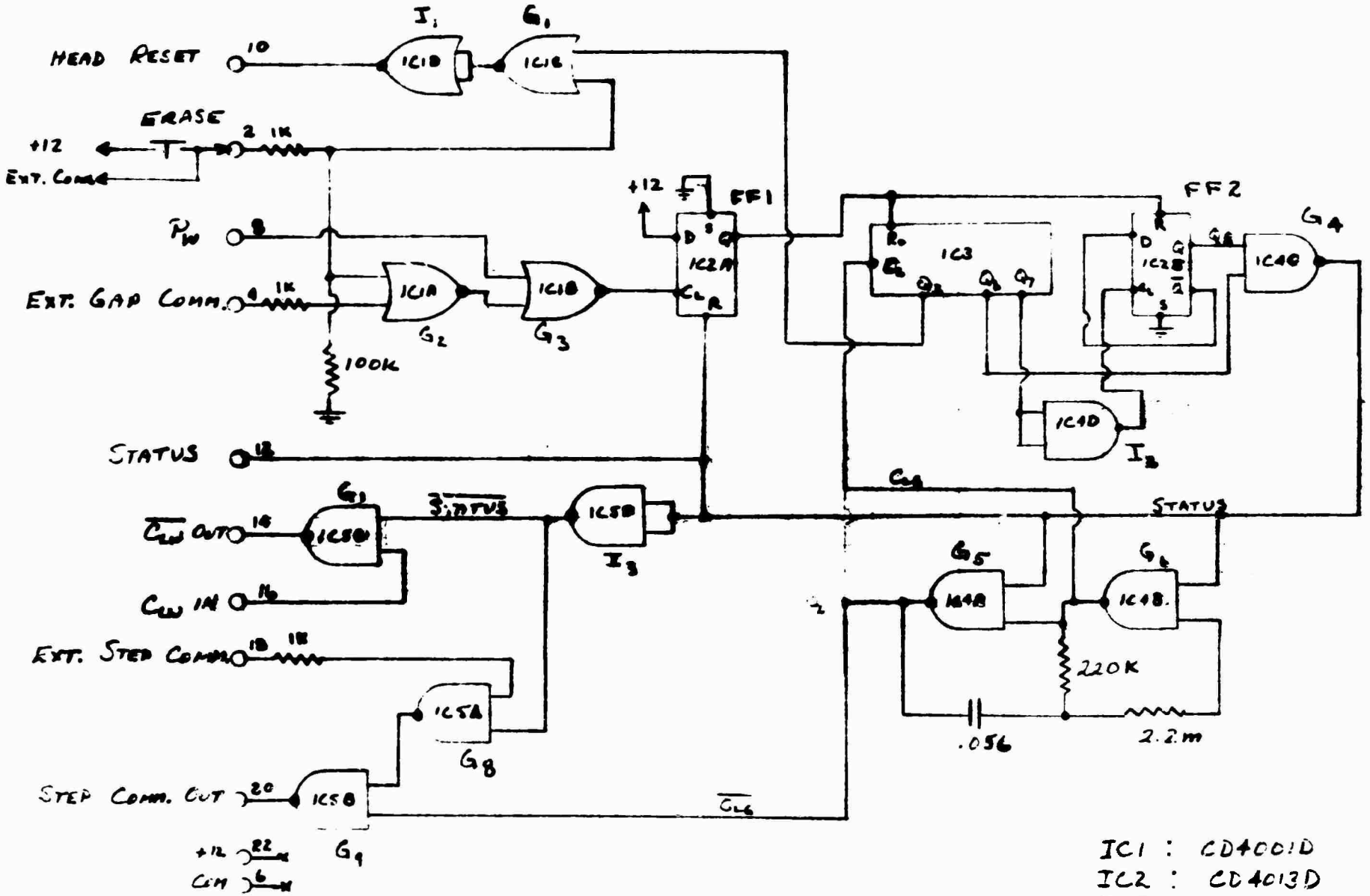

IC1 : CD4001D
IC2 : CD4013D
IC3 : CD4004T
IC4,5 : CD4011D

RECORD GAP LOGIC

10-19-70 SLW

BOARD # 1

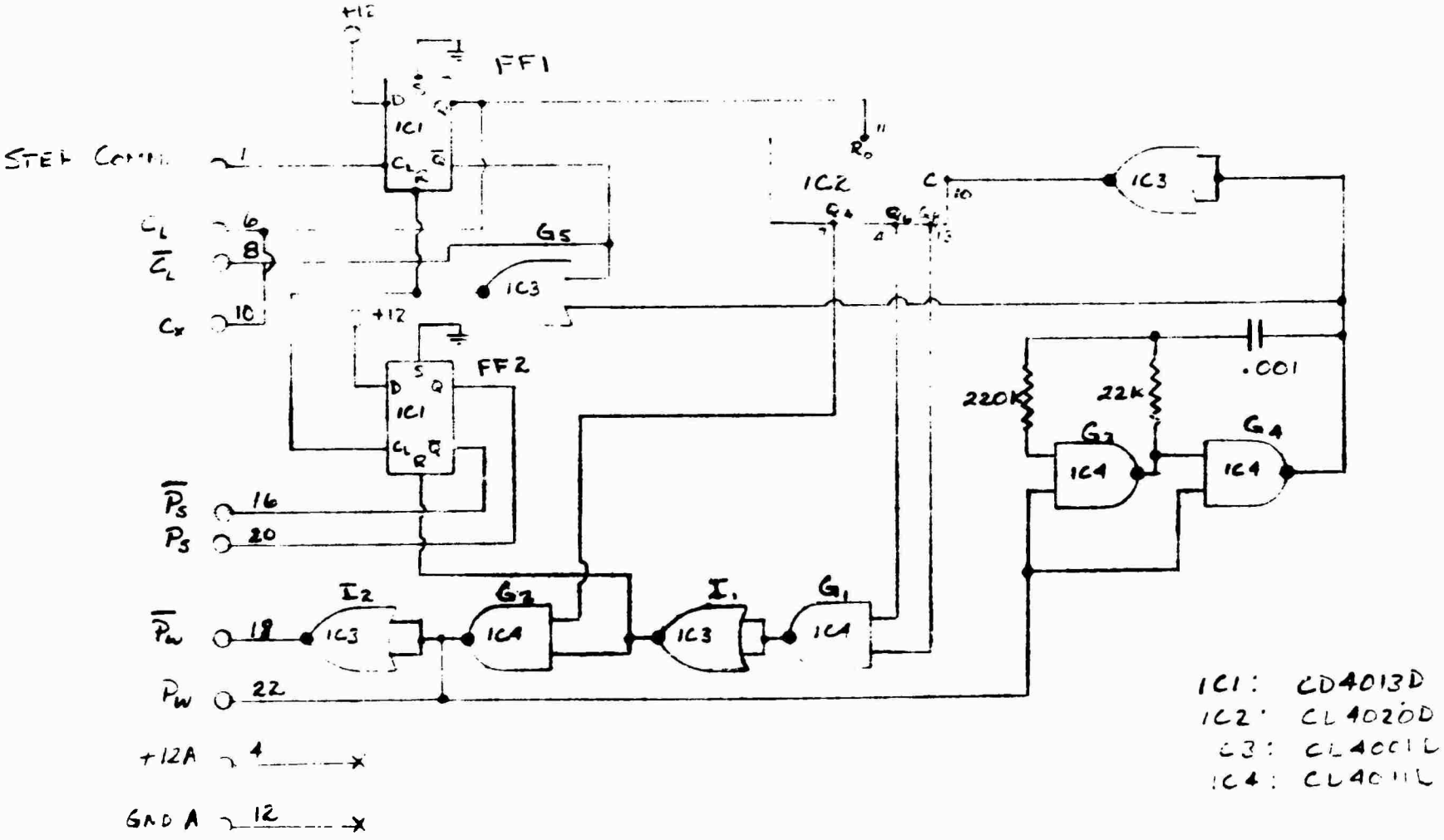

TIMING LOGIC

10-23-70 SLW

BOARD A 2

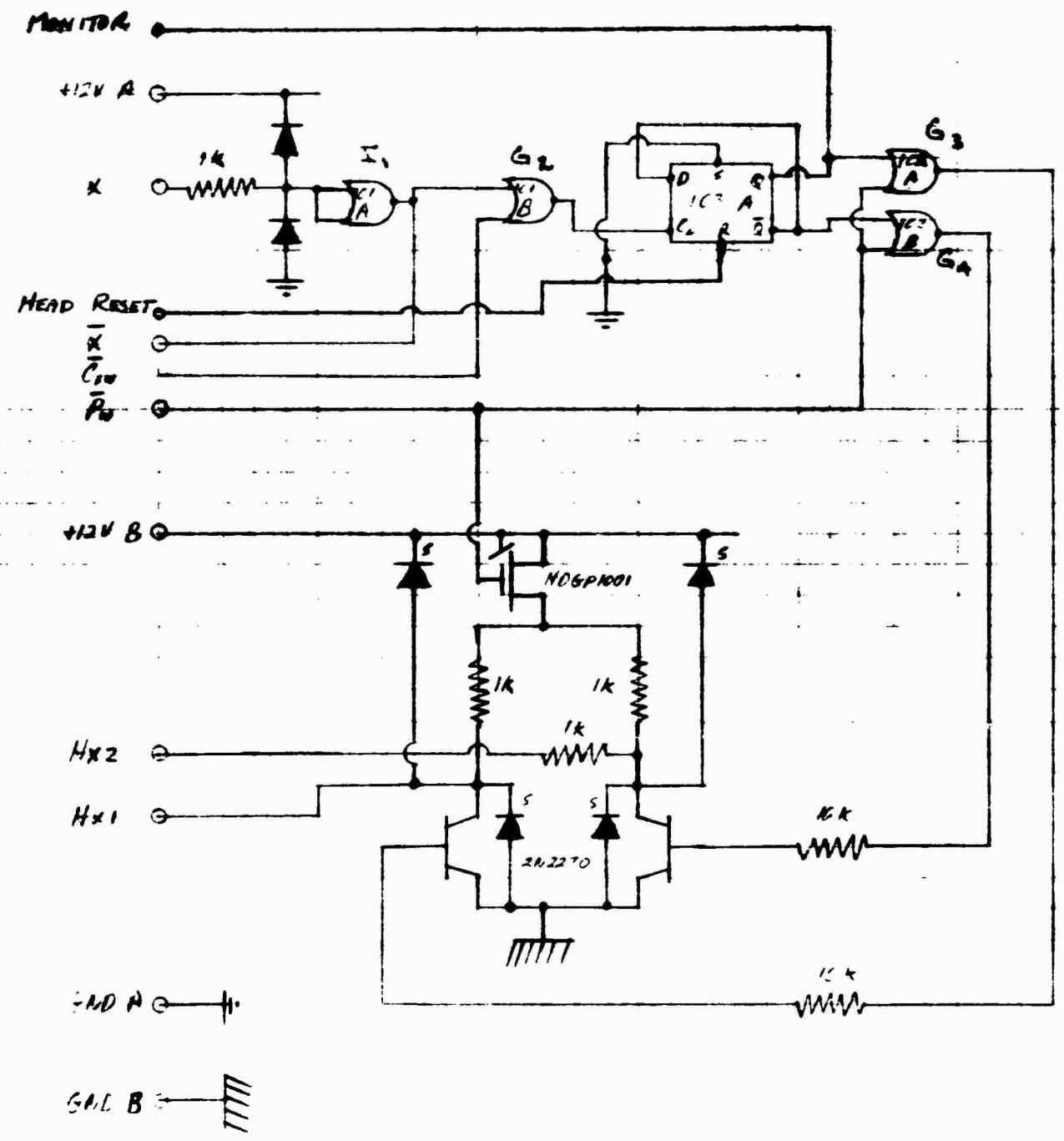

1 WRITE AMPLIFIER

FINAL VERSION

7/13/70 CBH

IC1, IC2 CD4021 D

IC3 CD4013 D

BOARDS # 4, 5, 6

TAPE RECORDER

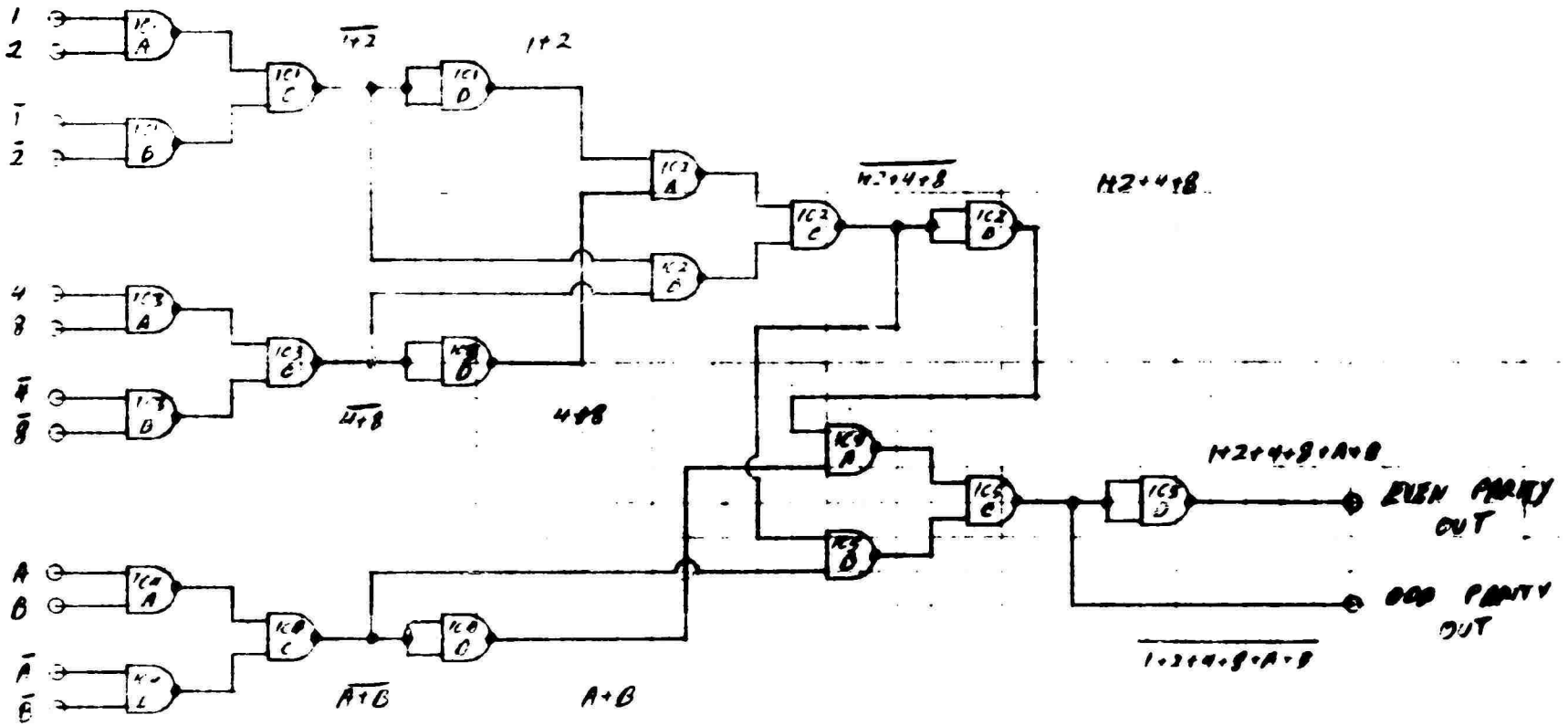

IC1 - 5 - COMMON

PARITY GENERATOR
FINAL

ROAD # 7

TAPE RECORDER

FINAL

STEPPER LOGIC

&

DRIVE

7/15/70

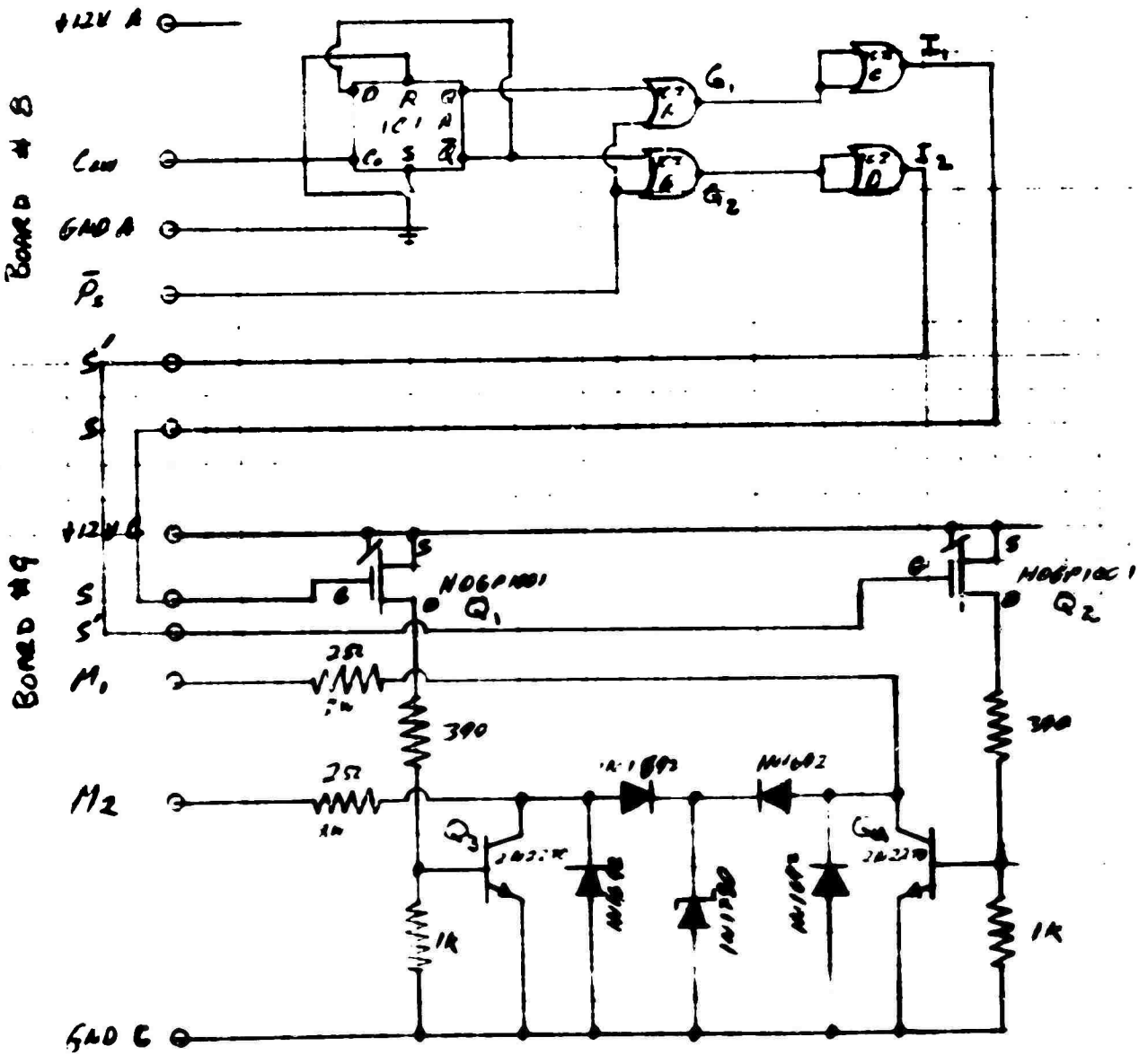

IC 1 - CD4013 D

IC 2 - CD4001 D

BOARDS # 8 & 9

TAPE RECORDER

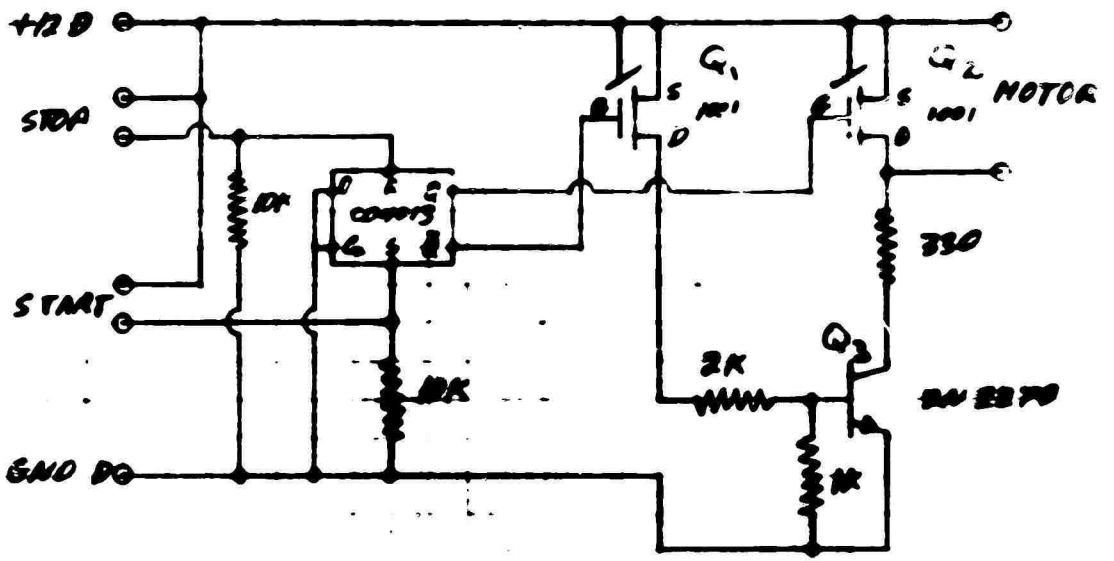

1/3 REEL MOTOR DRIVER

FINAL PIN

7414/10 CB14

Board # 10

Functional Description of Brake Motor Control Electronics

The function of this control circuit is twofold. In the "lock" function, it drives the motor in one direction until the motor current begins to rise above its normal value due to mechanical loading. When the motor current has reached a preset value, it shuts off the motor and also stops consuming power supply current on its own part. In the unlock operation, the motor is powered so as to run in the opposite direction and continues to run until a contact transfer takes place. Refer to the schematic diagram entitled Brake Motor Control.

To initiate a lock cycle, a negative going transition from +12 to 0 is applied to the lock input and thus directly to the one of the inputs of NOR gate G_1. If the other input, labeled B on the diagram, is low at this time, the output of the gate will make a positive going transition from ground to +12 thus clocking FF1. The gate input labeled B is connected to point B, namely the Q output of FF2. Thus in order for a lock cycle to be initiated, the Q output of FF2 must be low, that is the flip-flop must be in reset condition. If the lock command gets through the gate, FF1 will be driven into a set condition, that is, the $\bar{Q}$ will go low. The $\bar{Q}$ output going low turns on MOSFET transistor Q_1 thus essentially connecting the upper end of the 4.7 K resistor going to the drain of Q_1 to +12. This brings the upper end of Zener diode D_6, which is a 6.8 volt unit up to approximately 6.8 volts and thus the base of Q_2 goes to this voltage also. This pulls the emitter of Q_3 up to a voltage of approximately 6 volts and because of the 2 K resistor connected from the base of Q_3 to ground, a large base emitter

[illegible] This is sufficient to keep the transistor [illegible] current of 40 to 50 or 60 milliamps. This results [illegible] going to a potential of approximately +6 volts [illegible]. The current in the collector resistor of Q_2 [illegible] essentially equal to the motor current. Thus [illegible] simply be equal to R_s times the motor current in [illegible]. This voltage is applied via a low-pass filter to the base of Q_4. Q_4 is one side of a differential amplifier, the other side being Q_5. The [illegible] held about 4 volts below +12, that is, at a level of approximately [illegible] by the bias-string consisting of the 39 K and 82 K resistors. Current will flow through this bias-string only if transistor Q_6 is turned on and that will be seen to occur only when the base of Q_2 is high, that is, when Q_1 is on and the controller is in a lock cycle. As the motor begins to take an increasing mechanical load and approaches a stall condition, the motor current will increase and thus the drop across R_s will increase. When this drop reaches a value of approximately 4 volts, a sudden transfer of current from Q_5 to Q_4 takes place. This current amounts to about 1 milliamp and when the transfer to Q_4 is complete, the collector of Q_4 will rise from ground to approximately 8 volts. This is sufficient to swing NOR gate G_3 which is being used as an inverter through its transition level. Thus the output of G_3 will swing from +12 to 0. This is applied to a second inverter, G_2, whose output thus takes a transition from 0 to +12. This output is applied to the reset terminal of FF1 via an OR gate consisting of D_1 and D_2. When the output of G_2 goes positive, the result is to reset FF1, shutting off Q_1 and stopping the motor. It will be noted that when Q_1 is shut off, all current flow in

the upper portion of the circuit ceases. The OR gate, consisting of diodes D_1 and D_2 is used to insure that when power is applied to the circuit that FF1 will always come on in a reset condition. The other input to the OR gate is an RC network consisting of a one microfarad capacitor in series with a 100 K resistor. When the +12 is first applied, the capacitor will hold the anode of D_1 up to +12 thus resetting FF1. At the end of about 100 milliseconds, the capacitor will have charged sufficiently that the reset terminal of FF1 will be essentially at ground. Thus this arrangement plays a role in the operation of the circuit only at initial turn on and insures that the circuit will not come on with the motor running.

The unlock operation is somewhat simpler since the motor is stopped not when it has reached a preset current but when the thing it is driving has got to preassigned position and this position being detected by contact transfer of a microswitch. The microswitch is wired so that it is normally in the ground position. If an unlock command consisting of a negative going transition from +12 to 0 is applied to the unlock input, it will, if the other input of NOR gate G_4 is low, result in the output of G_4 making a positive going transition thus clocking FF2. The other input of G_4, marked A, is connected to the Q output of FF1. This is similar to the arrangement discussed previously. The purpose of this cross connection is to insure that the device will not accept an unlock command while it is running in the locked mode and vice versa. If this was allowed to happen, it could result in the destruction of Q_2, Q_3, Q_9, Q_{10} or just about any combination of them. Assuming the A input is low, FF2 will be clocked into the set condition. That is, the $\bar{Q}$ output will go low. A point to be noted is that FF2 is on the same chip as FF1 and thus, like FF1, is powered between +12 and ground. Therefore, the

... and ... the ... of FF2 are from 0 to +12. The transition of ... to ... causes the P-MOSFET transistor Q_7 being turned on. The drain ... goes essentially to +12 volts and pulls the junction of the ... and the anode of D_5 about 0.7 volts above ground at which ... is clamped by ... This turns on MOSFET Q_8. MOSFET Q_8 turning on ... current through Zener diode D_7 which again is a nominal 6.8 volt ... and this results in the base of Q_{10} being pulled about 6.8 volts below ground. This turns on transistor Q_9 and results in a current flow through the motor in the opposite direction to that during the lock cycle. Thus the motor runs in the opposite direction to that during the lock cycle. The motor will continue to run until the microswitch makes a transition from the ground to the +12 point. This applies +12 volts to the diode OR gate consisting of D_4 and D_3 and thus provides a positive level to the reset terminal of FF1, resetting FF2. As discussed previously the other input of the OR gate goes to an RC network and the purpose is exactly the same as discussed before, namely, to insure that when the circuit is first turned on, FF2 will come on in a reset condition.

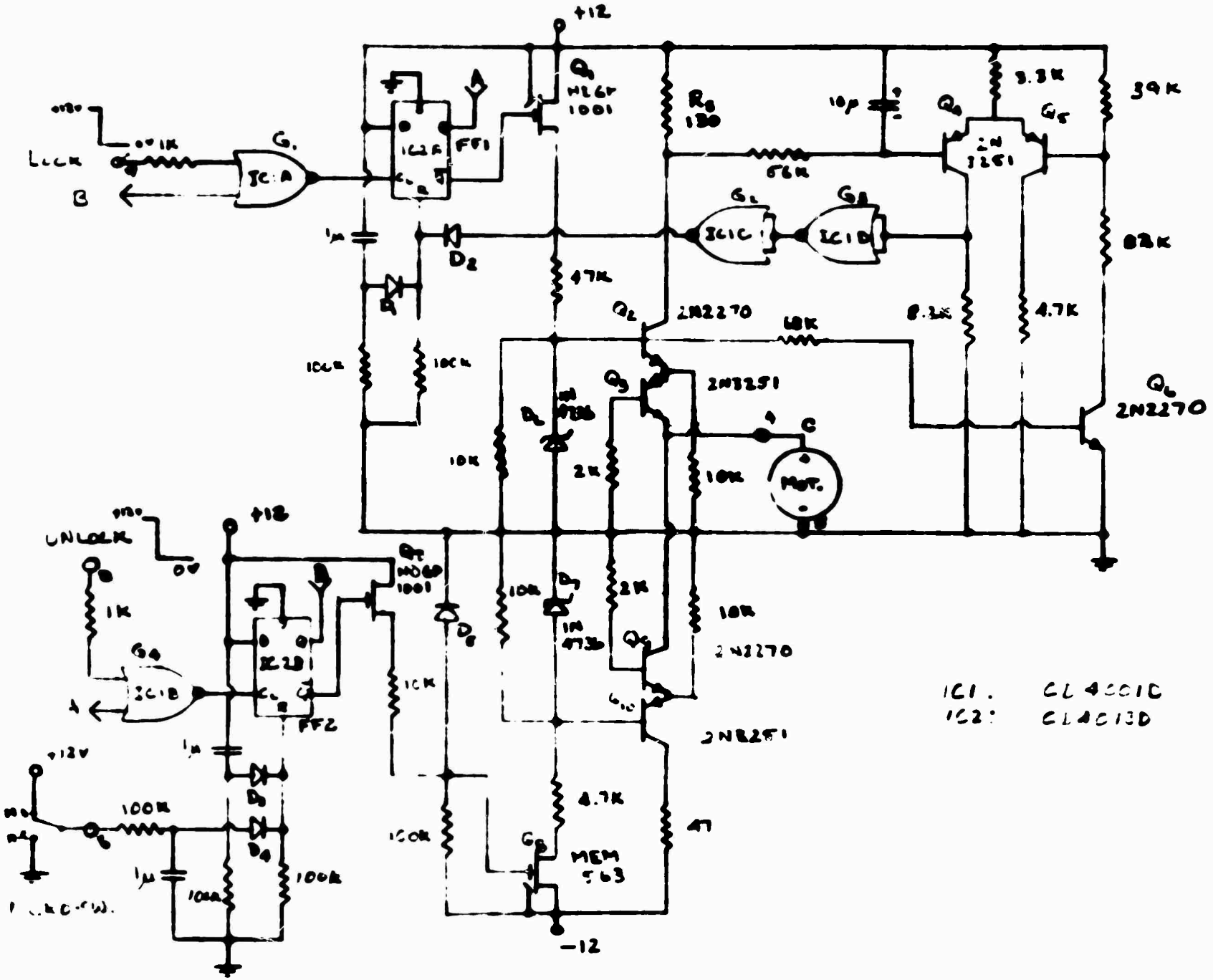

BRAKE MOTOR CONTROL

12-29-7[illegible] CLW

BLANK PAGE

Part III

OVERPRESSURES DUE TO EARTHQUAKES

Co-Principal Investigators

Dr. Hugh Bradner
Phone (714) 453-2000, Extension 1752

Prof. John D. Isaacs
Phone (714) 453-2000, Extension 1141

ADVANCED OCEAN ENGINEERING LABORATORY
Sponsored by
ADVANCED RESEARCH PROJECTS AGENCY
ADVANCED ENGINEERING DIVISION

ONR Contract N00014-69-A-0200-6012

Part III

Overpressures Due to Earthquakes

Table of Contents

List of Appendices

7 January, 1971

OVERPRESSURES DUE TO EARTHQUAKES

STATUS REPORT

A. Task

Work on subject contract is directed toward understanding the effects of undersea earthquakes, and in particular toward studying the increase in water pressure that would be experienced by submerged objects near an earthquake fault during an earthquake.

B. Theory

Dr. Paul Richards has solved the general problem of a source of finite extended with some quite general vertical acceleration function which is triggered by the passage of a wavefront. The triggering wavefront originates at an origin X = Y = 0 and moves in the horizontal X and Y directions with velocities which can be functions of the Y coordinate. Richards has made specific computations using Brune's model (step function upward velocity of 100 centimeters per second with one second duration) and finds that the additional pressure will be equivalent to approximately 600 feet of water depth. Brune feels that this 600 feet additional depth is an upper limit for his model except for possible increases due to reflection from the water surface.

Richard's theory is in close agreement with the more qualitative predictions that we made at the beginning of the project. Therefore we feel that preliminary estimates of hazard to submarines can now be made with adequate assurance although actual observation data of seaquakes are still of paramount importance.

C. Observational

Cdr. D. H. Walsh has brought to our attention one observation of a seaquake experienced by the USS RASHER SSR 269 in 1957. Cdr. W. Gibson Carter, who was Diving Officer writes-- "As we were hovering at a keel depth of 275 feet, the depth gauge suddenly went to approximately 310 feet, back to about 240 feet, and then settled down back near 275 feet. I estimate that this series of indicated depth changes occurred in a period of less than 4 seconds."

A. W. Adams, who was skipper of the submarine, remembers somewhat greater numbers but cautions that his memory may be faulty. He also says-- "To appreciate the trauma of this event you must realize that RASHER was a 'thin-skin' boat certified for 313 feet test depth." Copies of letters from W. Gibson Carter and A. W. Adams, Jr. are attached. Cdr. Walsh is trying to obtain the original records from the RASHER and from the other three submarines that were participating in the exercise south of the Alaskan peninsula. (It is probable that the actual pressures were greater than that indicated, as submarine depth gauges are somewhat damped.)

D. Experimental

1. We have assembled telemeter sonar buoy equipment for making observations of after-shocks from large seaquakes. This equipment has been described in previous Progress Reports.

2. Additional units are being assembled with self-contained tape recorders for use in areas where the telemeter signal is degraded.

3. Work on the modified oceanbottom seismometer has been continuing slowly because of the assembly effort on the other items. All components have been breadboarded, but assembly is not complete.

4. As a cooperative undertaking with the University of Hawaii and the Los Alamos Scientific Laboratory, a vibrating string accelerometer has been placed on the bottom at approximately 550 fathoms depth 17 miles west-southwest of Amchitka to monitor seaquakes in this active seismic region. It is now recording all accelerations greater than 10^{-4}G. Simultaneous records of pressure transducers are being made. The data is tape recorded on land and processed by Los Alamos personnel.

BLANK PAGE

GENERAL DYNAMICS
Electric Boat Division
Eastern Point Road, Groton, Connecticut 06340 • 203 446-3000

October 7, 1970

Mr. Jerry Fisher
Scripp's Institute of Oceanography
LaVolla, California 92037

Dear Jerry:

This letter is written in answer to your telephone call concerning the events surrounding an underwater pressure excursion experienced by the USS RASHER (SSR 269) while operating in waters south of the Alaskan chain during February-March of 1957.

I have searched my own personal files concerning the facts of this event and regret I possess no written records of my own. Therefore I must relate the events from my memory. Once again, as I did in our telephone conversation, you must weigh my statements to decide fact from fiction. This is necessary because after thirteen years of telling my "sea-story" I am not fully certain of what may have been added by me to make a better story.

Four snorkel submarines (CUSK, CARBONERO, RASHER and TUNNY) were participating in a TRANSIT EXERCISE south of the Alaskan peninsula while enroute to the Bering Sea for a regular missile exercise. On the final day of the exercise at about 2 a.m. and while proceeding eastward at about 200 feet depth, the Diving Officer (GIB CARTER and/or LOU FEAD) phoned me (the C.O.) to report we had just "hit a whale" and apparently changed depth from about 200 feet to 400 feet and back to 200 feet in less than four minutes. To appreciate the trauma of this event you must realize that RASHER was a "thin-skin" boat certified for 313 feet test depth. There were no reported leaks or damage that could be determined from within the submarine at that time, thus we continued submerged until about 9:00 a.m. when the exercise was completed. On surfacing we received weather reports which indicated a submerged volcano or earthquake had originated very close (10 miles) to the time and position of the alleged "whale collision."

The above paragraph relates the incident to the best of my knowledge at this time. Once again I caution you to analyze this event more thoroughly as I am quite capable of "improving" on a good sea-story.

Personnel associated with this incident or who may have some knowledge other than reported here include:

1. Lou M. Read - 1813 Hornblend, San Diego 92109 Phone 272-6376
2. Gib Carter - Active Duty Navy Commander/Captain
3. Capt. Dick Clark - COMSUBFLOT ONE - San Diego
4. C. Turner Joy - Lockheed MSC - Washington D. C. (XO RASHER)
5. Cdr Don Walsh - Office of Under Secretary of the Navy for R & D

Since your investigation into this incident for DR. BRADNER is under an ARPA Oceanographic project, I suggest that RADM W. W. BEIRENS, OCEANOGRAPHER of the Navy, might be able to assist in the review of the Ship's Logs of the ships previously mentioned. The others may have experienced the same incident. I might further suggest that the report of the TRANSIT EXERCISE as issued by COMSUBRON FIVE (also in San Diego) might give some light on the event.

I sincerely hope this letter might be of some assistance in your project. I am taking the liberty of sending copies to the above named individuals in the event they might assist you further.

Please extend my kindest personal regards to both Bill Nierenberg and Jeff Frantschy.

Sincerely,

A. W. Adams, Jr.
Chief of Technical Publications

AWAdams:ac
446-6823 (Area Code 203)

6 October 1970

Mr. G. H. Fisher
Faculty, Scripps Institution of Oceanography
Code 1 - 24
La Jolla, California 92037

Dear Mr. Fisher,

I have recorded, to the best of my memory, data observed during the earthquake in Alaska in March 1957.

Date: Approximately 20 March 1957. I know for certain the USS Razher SSK 269 arrived in port in Vancouver, B. C. on 29 March 1957 and I believe the earthquake occurred about 5 to 10 days prior.

Position: Approximately 200 miles south of the Unimak Pass in the Aleutian Islands. (Very south position)

Keel Depth: 275 feet. Water Depth: About 3,000 fathoms.

Ship status: Rigged for deep submergence and minimum electrical power load. Steering and diving planes in hand power. Ship trimmed for hovering. (No speed through the water)

About 0130 local time, shortly after having relieved the watch as diving officer, I experienced a sensation that had never been described to me nor had I read of such an experience in reports of other submarine operations. As we were hovering at a keel depth of 275 feet, the depth gauge suddenly went to approximately 310 feet, back to about 240 feet and then settled down back near 275 feet. I estimate that this series of indicated depth changes occurred in a period of less than 4 seconds. The sensation from my station (midships) was similar to that received when the ship suddenly applies a full backing bell with both propellers from a dead in the water condition. During this period there was never any noise through the hull or reported from sonar.

Most of the crew was asleep during this evolution and the majority of those sleeping were disturbed by the vibration. The ship movement was felt stronger toward the bow and stern compartments. The individuals on watch immediately asked one another what was going on in the other end of the ship. The Captain was not disturbed in his sleep and I reported by phone that I thought we had touched bottom or hit something while submerged, perhaps a whale.

Without the benefit of experience in casualties/exercises such as I had just experienced, my reaction was to immediately restore normal power to steering and the diving planes and add minimum power to the propellers to assist in depth control.

After the initial shock wave there was another shock wave within 15 to 20 minutes of lesser intensity and then a shock wave of very mild intensity about 30 minutes after the initial shock. No physical ship movement was noticed on either of these, only movement of the depth gauge needle. Obviously the ship only vibrated in response to the pressure wave and the depth gauge responded to changes in the water pressure as the shock wave passed.

There was no damage to the ship, instruments, or personnel as a result of this experience. Our only clue as to what had really happened came about three days later when we picked up a brief news report stating something about an earthquake in the Alaskian area.

Although the ship was on a highly classified mission, I consider the information revealed here as unclassified. I also feel that the ship's log book on this particular phase of the cruise is most likely downgraded to an unclassified level and know Don Walsh will do what he can to assist you in this research.

I hope my memory has served me correctly and that this may be of some value to you. Please let me know if you feel I may be of any furthur help.

Sincerely,

W. Gibson Carter

W. Gibson Carter
CDR USN
Faculty, U.S. Naval War College
Newport, R. I. 02840

P.S. My typing ability can be seen in emergency room.

Part IV

ADVANCED STUDIES IN NEARSHORE ENGINEERING

Co-Principal Investigators

Dr. Douglas L. Inman
Phone (714) 453-2000, Extension 1175

Dr. William J. Van Dorn
Phone (714) 453-2000, Extension 1179

ADVANCED OCEAN ENGINEERING LABORATORY

Sponsored by
ADVANCED RESEARCH PROJECTS AGENCY
ADVANCED ENGINEERING DIVISION

ONR Contract N00014-69-A-0200-6012

Part IV

Advanced Studies in Nearshore Engineering

Table of Contents

List of Figures

I. INTRODUCTION

This study was initiated as a concentrated research effort to define the transport and circulation mechanisms in nearshore waters as they apply to civil and military engineering. It was proposed that field and laboratory experiments would be conducted to resolve controlling factors in sediment transport phenomena, so that effective mechanisms could be designed such as:

1. Phase dependent roughness elements that produce preferential transport over the sediment bed.
2. Structures for control of nearshore circulation so that dispersion of water is enhanced and loss of sand from beaches is minimized.
3. Submarine dams that intercept the flow of sand into canyons so that the sand may be re-circulated on the beaches.

The shelf and nearshore zone is a complex region of intense interaction among waves, tides, currents, river run-off and the erosion products from the land. However, it is becoming increasingly clear that the closely interrelated driving forces, although masked by a high level of background noise, are essentially low frequency and regular in form. The background noise is random and largely associated with the processes of energy dissipation. However, recent measurements show that nearshore circulation is governed by a fundamentally simple incident-edge wave interaction and that shelf and canyon currents are probably related to the oscillating fields of set-up and set-down associated with waves and winds.

Most problems in nearshore engineering, whether the movement of sediment and its control, the design of temporary or permanent cargo

unloading and loading facilities, or the laying of cables, mines, or underwater obstacles, additionally presuppose a basic understanding of the dynamics of breaker action. Yet, the surf zone is particularly difficult environment in which to work.

II. RESEARCH PROGRAM FOR 1970

A. Research studies

Research effort during this contract year has been concentrated in two areas of investigation: (1) field and laboratory studies of the water-sediment interface near the breaker zone; and, (2) laboratory study of the velocity field in breaking waves. Much of the effort in this phase of our research has been directed toward developing suitable measurement techniques and in making measurements. Progress to date is summarized in this report and our previous reports for this year. Theoretical study of the nearshore region will continue in the coming year with the objective of gaining additional basic information to be applied in the design and development of other practical devices and systems such as the Crater-Sink Sand Transfer System described below.

The ARPA funded computer and analysis system, soon to be operational, will speed the translation of study results into a form useful to military planners.

1. Field Studies of Sediment-Water Interface. Much of the first quarter of the past contract year was spent in acquiring adequate personnel and equipment to study the problems presented in the proposal. Once the research staff was acquired, work progressed quite rapidly for the remainder of the year.

A series of measurements have been conducted of the water-sediment interface under wave action adjacent to the Scripps Institution Pier. The objectives of the measurements is to determine the thickness of the boundary layer under wave action and to ascertain the effects of irregularities of the sand bottom on the boundary layer. Preliminary measurements include photographing neutrally bouyant particles against a grid.

Sixteen millimeter underwater motion pictures of confetti injected into the sand-water interface under shallow water gravity waves have been analyzed. The work to date tends to substantiate earlier experimental work done in the laboratory (Inman and Bowen 1963), and theoretical predictions (Longuet-Higgins 1958). The recent measurements include local wind waves (T = 4-8 sec) and longer period southern swell (T = 10-15 sec).

The primary results of the study so far are threefold. First, wave periods, particle displacements and particle velocities can be measured near the bottom in the potential wave region. Second, a boundary layer phase lead predicted by Longuet-Higgins (1958) has been observed and characterized. Third, a variable boundary layer similar to that described by Inman and Bowen (1963) has been observed and studied.

Field investigation of the kinematics and the boundary layer in the water sediment-interface using 16 mm motion pictures, confetti, and dye are continuing.

Additional work this quarter include the development of new devices for measuring: (1) the kinematics of the water-sediment interface;

... the ... of the boundary layer; (3) the visual relation between the exterior potential flow of the waves, the motion in the boundary layer, and that of granular particles. The field application of hot film anemometer techniques now being developed in the laboratory study described below are expected to provide a principal field tool for study of the water dynamics in the boundary layer. Further, two additional methods are being developed, they include: (1) flow visualization using hydrogen bubbles as tracers; and, (2) velocity measurements using the strain gage flow meter.

The hydrogen bubble tracer method is simple both in concept and operation. A thin platinum wire is attached to the cathode of a lead-acid storage battery to reduce water and generate hydrogen bubbles on the wire surface. These bubbles form as monolayers and they are removed by the motion of water flowing past the wire. Surface tension and attractive forces overcome buoyancy and the bubbles become neutrally buoyant. Thus, at time zero a line of hydrogen bubbles is injected into the flow and subsequently trace the water movement.

We have progressed to the stage where only some smaller wire is required before testing it in the ocean. Figure 8a is a schematic of the system showing the power source, switch, copper anode, wire, and wire support. The switch permits the injection of fine lines of bubbles instead of the "curtain" of bubbles you would get from continuous flow.

The orientation of the wire to the waves, and therefore the flow, grid and photographic equipment are shown in Figures 8b and 8c. Note that a black background will be necessary in order for the small bubbles (2.5×10^{-3} cm) to be observed in the films.

The strain gage flowmeter is a system developed and used at the University of Cambridge by Dr. J. F. A. Sleath. It consists of a fine glass fiber (2.5×10^{-3} mm diameter) three inches long which is attached to a solid support at one end and to a cantilever strip on the other. Attached to the strip are strain gages. The glass fiber is oriented at right angles to fluid flow so that a force on it will cause it to deflect in the flow direction, thus causing the cantilever to bend inwards. The stress is inferred from strain on the cantilever. Sleath has used his meter to measure velocities of 1.8 - 21.6 cm/sec and with it he has verified for the first time the theoretical first-order solution as proposed by Lamb (1932, p 622) for the velocity distribution above a smooth horizontal bed due to waves.

Correspondence with Dr. Sleath has resulted in his sending us a copy of the blueprints of his probe. At the present we are studying the prints and modifying them to work under the velocities we expect (122 cm/sec). The modifications will consist of different fiber diameters and/or different cantilever thicknesses. This system has apparently performed well in similar flows, therefore we expect it to be useful for our work.

Additional field measurements are planned on a more extended scale to determine the effects of artificial roughness on the boundary layer. A laboratory phase of this work will begin in the wind wave channel as the channel becomes available following the Stable Floating Platform Study.

2. Laboratory Study of Velocity Field in Breaking Waves. Because of the difficulties of working in the surf zone, there have been very few significant measurements, and these have been principally confined to

[illegible] forces on various objects (Wiegel, [illegible], Savage, et al (1970) have determined [illegible] velocities near the breaking point in a conical laboratory channel, and have shown that none of the present [illegible] correctly predicts the observed velocities. This study was restricted to relatively small waves (7-9 cm), and there were no associated field measurements at large scale.

The present study was initiated with the threefold objectives of: (1) the measurement of the velocity fields in waves of greater height (50-60 cm) breaking on uniform slopes in the SIO 100-ft laboratory channel, and the corollary development of techniques for making similar measurements in natural breaker environments; (2) the extension of these experiments to measurements in natural surf; and, (3) the development of a more adequate theory for breaker dynamics, and application of these theoretical and experimental results to specific engineering problems. From the standpoint of application, a logical starting point appeared to be complementary to the field work on sediment movement and control methods reported above.

III. PRESENT STATUS

Except for preliminary review of possible measurement techniques reported for the first quarter of 1970, the instrumentation phase of the laboratory study did not get actively underway until adequate technical assistance became available. The second and third quarters were devoted to upgrading and equipping the wave channel with adjustable wave generating and beach-slope facilities and a circulating filter system, design and construction of dynamic calibration facilities for the velocity sensors, procurement and testing of pressure, velocity, and

photographic equipment for flow measurements, and the construction of a programmed instrument operating and recording console.

Much of the fourth quarter was expended in somewhat frustrating attempts to obtain reproducible flow calibrations to the 1% accuracy desired. We have now succeded in this, and because many other investigators contacted have experienced similar problems, our procedures are described in some detail below. Actual velocity field measurements were commenced in December 1970, and will be reported later.

IV. INSTRUMENTATION

Except for the photographic equipment which is standard, other instrumentation for velocity and pressure measurements was arrived at only after considerable review, selection, and testing. To function successfully in breaking waves, flow sensors must be capable of recording identifiable transitions from air to foam to water and out again without changing calibration, sustaining high impact forces without vibration, and have a dynamic range of about 200. In the sea, further complications are imposed by temperature fluctuations, and contaminating particles and debris, but our experience suggests that these difficulties can be resolved with minor modification of the present system.

A. System Components

Figure 1 is a schematic diagram of the 100 ft, glass-walled wave channel and accessory instrumentation for velocity-field measurements, comprising the following components:

a) A hinged-paddle harmonic wave generator capable of making periodic waves from 0-2 ft high with periods from 0-5 seconds.

b) A 3/8 inch thick plate glass beach slope assembly, fabricated in 2, 4, and 6-foot length increments. The glass sections are laid in

[illegible] supporting aluminum bars that are wedged [illegible] glass tank walls by spreader screws. The bars have [illegible] rubber [illegible] to grip the glass, and also rubber seals beneath the bar bottoms to prevent leakage past their edges. Uniform slopes from 1:4 to 1:20, as well as broken slopes, if desired, can be removed, installed, or altered within one or two hours.

c) A 10-hp water circulating pump with return flow beneath the channel is adapted for high-speed dynamic flow calibration. A separate filter pump keeps the water clear of particulate matter, and establishes uniform temperature conditions within the channel between wave experiments.

d) Measurement instrumentation consists of three independent, but compatible systems.

Two DISA, V-type, two element hot quartz-film probes are mounted on adjustable streamlined stainless steel fairings, and can be oriented at arbitrary angles within the plane of the flow field. While these probes were originally designed to measure quadrature components of flow, in an oscillating field, it is impossible to distinguish between their non-linear velocity and directional responses. In our study, they are oriented in different attitudes in repetitive experiments, and instants where the orthogonal elements give identical readings can then be interpreted unambiguously as flow velocities in the direction of probe orientation. This procedure is more laborious, but very accurate. The hot-film probes, and their accessory amplifiers and constant temperature circuitry have a dynamic range of about 200, can record velocities from 2-3 cm/sec to 2-3 m/sec, and have a 50 kHz response. Thus wave rise-times of about 1/100 sec are limited only by the response of the Brush Oscillograph.

Two independent pressure transducers are hydraulically connected to adjustable orifice plates set flush in the glass beach slope. One transducer reads differential pressure between two bottom orifices parallel to the flow axis, and the other monitors relative pressure between another orifice and ambient (atmospheric) pressure. Thus, both wave slope and wave elevation can be measured within the range where the hydrostatic approximation is valid, which includes about 95 percent of the wave history. These transducers can resolve pressure increments of about 1/100 mm, but their frequency response is limited to about 50 Hz by natural resonance of their mechanical and hydraulic compliances.

Flash photography of suspended, neutral-density, nitrile rubber discs is accomplished at single-exposure repetition rates up to 15 flashes/sec, by a synchronized Nikon camera, equipped with an adapter for 4 x 5 polaroid film. The camera has an 80-180 mm zoom lens, and is mounted 16 feet from the channel to minimize parallax, and shoots through a transparent 1-cm orthogonal grid taped to the tank wall.

All of the above instrumentation is controlled from a central console, which also includes the 6-channel recorder, and circuitry for initiating the wave generator, camera, flash unit, and recorder chart drive. Because the film probes have a relatively short life, power is supplied to them only during the brief recording cycle.

B. Calibration

Four separate calibration systems were devised to define the reproducable working range of the velocity probes and pressure transducers, and to provide dynamic spot calibrations between experiments:

a) The V-probes were dynamically calibrated over the range 3-300 cm/sec by converting the wave channel to a flow channel. A 20-ft long, 15-in high, parabolic [illegible] venturi section was installed in the [illegible] convergent section this velocity range of free-surface flow could be achieved at constant pump speed by moving the probes back and forth. This venturi, associated free-surface profile, and a V-probe and its recording console are shown in Figure 2.

b) Flow velocity as a function of position and pump speed was accomplished by independent standard hot-film probes, previously calibrated in the spinning tank described below.

c) Absolute calibration of the standard probes was conducted in a specially designed 24-in diameter spinning tank (Figure 3). The tank comprises an annular channel of 4 x 5 inch section equipped with 18 baffles to prevent establishment of variable flow and waves induced by probe drag. The tank is driven by a Graham variable-speed drive, and is capable of relative flow velocities of 0-180 cm/sec. Flow speed is determined by timing the revolution rate automatically on the same chart record on which the probe output appears.

d) During wave experiments, dynamic single-point calibration of the V-probes is accomplished before and after each test by slipping a flow-nozzle over the probe tips. The nozzle is tube-connected to a constant pressure source, referred to local still water level in the channel. The source comprises a vertical plastic cylinder maintained in a uniform head configuration between an overflow pipe and a supply pump that draws water from the channel. In this manner, it is not necessary to disturb the wave recording set-up during calibration, and the calibration is performed at channel temperature (Figure 4).

e) Pressure transducer calibration is also accomplished between runs by a water manometer integrated into the hydraulic measurement circuit.

C. Problem Areas and Solutions

Most of our problems have been associated with instabilities in the hot-film measurement circuits. These are worth recounting as an aid to other investigators, since they seem to be common among users of this equipment. Figure 5 shows a block diagram of the system; it comprises a 2 mm diameter quartz coated resistance element that is driven at constant temperature (resistance) by a feedback amplifier, whose output voltage, of the form $A + B(v)^n$, is exponential function of the fluid velocity v. This output is fed to a linearizing amplifier which supplies a convolution in which the exponent n can be varied to make the output approximately proportional to v. Since the probe resistance changes by only about 2 ohms from $0 < v < 200$ cm/sec in water at 15°C, the signal levels are in the microvolt range. Thus, the coupled system of three amplifiers (driver, linearizer, and recorder) was found to be extremely sensitive to balance, and often drifted erratically with transient stable intervals. Lastly, the hot-film probe tips tend to collect bubbles and minute particles in the water and were also extremely susceptible to overheating and burnout from power transients, poor gounding connections, or accidental, improper switching procedures. Instabilities were largely eliminated by removing the linearizer units, and performing the necessary corrections on the computer. Reduction of probe overheat ratios minimized the tendency to burnout and collection of debris, but increased temperature sensitivity. Temperature is now monitored separately, and computer-

[illegible] previous calibration. Lastly, thorough grounding [illegible] the channel and water within it and carefully [illegible] procedures have greatly extended probe life, make [illegible] calibrations practical, and have yielded reproducable results without constant readjustment of circuit controls.

Future Plans

Throughout the laboratory phase of this study, we have kept in mind application of the same instrumentation in the ocean. Concurrent with the present measurements we are conducting probe experiments in sea water, and working on methods for in-situ calibration. Ocean instrumentation is visualized as comprising one or more portable, combined wave staff-velocity probe assemblies, cable-connected to a shore-based record. Incoming waves will be monitored by bottom-mounted pressure sensors outside the breaker line. The installation will be designed for flexibility and mobility, using a suitable instrument van, such that varying wave environments can be studied.

V. APPLIED STUDIES

The major problem of harbor siltation was considered in a practical manner with the initial design of a "Crater-Sink Sand Transfer System" under partial ARPA support. A paper describing this system in detail has been forwarded to ARPA and the abstract is included in this report. The Crater-Sink Sand Transfer System has important bearing on any civil or military engineering problem involving the shoaling of harbor entrances due to littoral transport because it suggests an efficient method for maintaining proper channel depth. The design of this system was a major accomplishment of the past contract year and has generated considerable interest in the coastal engineering community.

The results of this study has been reported in a separate paper: "Crater-Sink Sand Transfer System" (Inman and Harris, a copy of which was included with submission of UCSD #3891 to ARPA) and which has been reviewed by CERC with plaudit. This paper describes a system for continuous maintenance of harbor openings, as abstracted below.

VI. CRATER-SINK SAND TRANSFER SYSTEM

A sand transfer system that requires no surface impounding area and that can be installed and operated at low cost is proposed. The system consists of a hydraulic jet assembly operating from the bottom of a sand crater. A jet pump and suction mouth are located at the lowest point of a crater-like depression dredged into the sea floor. The crater acts as a gravity-fed sink for sand and other cohesionless material, thus serving the dual purpose of a mechanism for collecting sand and a subsurface impounding area for the accumulation of sand.

In addition to the above study, various configurations of roughness elements, in the form of submerged, non-moving structures, to control and to direct sediment transport are currently being investigated. Testing of preliminary concepts is dependent upon availability of the 50 x 60 foot wave-sediment tank in the SIO Hydraulic Facility, but hopefully can be scheduled for late 1971.

We are also considering several applications of our results towards utilizing natural wave and current forces to control sediment transport. One possibility under study is that of constructing offshore cargo unloading facilities and artificial airfields and depots. It is well known that a longshore barrier at a critical distance offshore of a sandy beach will result in the creation of a tombolo, or sand spit, that builds out by natural wave action until it connects the barrier

with the shore. Thus, it is conceptually possible to introduce an artificial barrier, in the form, say, of an array of submersible caissons or a surplus aircraft carrier, which will connect itself to shore by a causeway, suitable for vehicular traffic, or a landing field. The caisson array could be designed to have a seaward depth sufficient for cargo vessels, and be equipped with suitable craneways, etc. for cargo handling. Figure 6 is a conceptual sketch of the sequential development of such a facility. Figure 7 shows an actual tombolo produced by an offshore breakwater near El Segundo, California.

The time-scale for development depends upon a number of factors, such as wave intensity and direction, sediment size and availability, and the barrier size deployment. Some of these are amenable to model study, but others depend, sensitively, upon a fundamental understanding of sediment transport mechanisms, which are not scalable, and to which our present studies are directed. We hope to undertake more detailed studies of such applications in the ensuing contract year. A tentative work schedule and a block diagram of the interaction of activities on this project are shown in Figures 9 and 10.

VII REFERENCES

Divoky, D., B. Le Mehaute, and A. Lin, 1970, "Breaking waves on gentle slopes", Jour. Geophys. Res., vol 75, no 9, p 1681-92.

Lamb, H., 1932, Hydrodynamics, 6th Edition, Cambridge, University Press.

Sleath, J. F. A., 1969, "A device for velocity measurement in oscillatory boundary layers in water", Jour. of Science Instruments, vol 2, series 2, p 446-448.

Wiegel, R. L., 1964, Oceanographical Engineering, Prentice-Hall, New York.

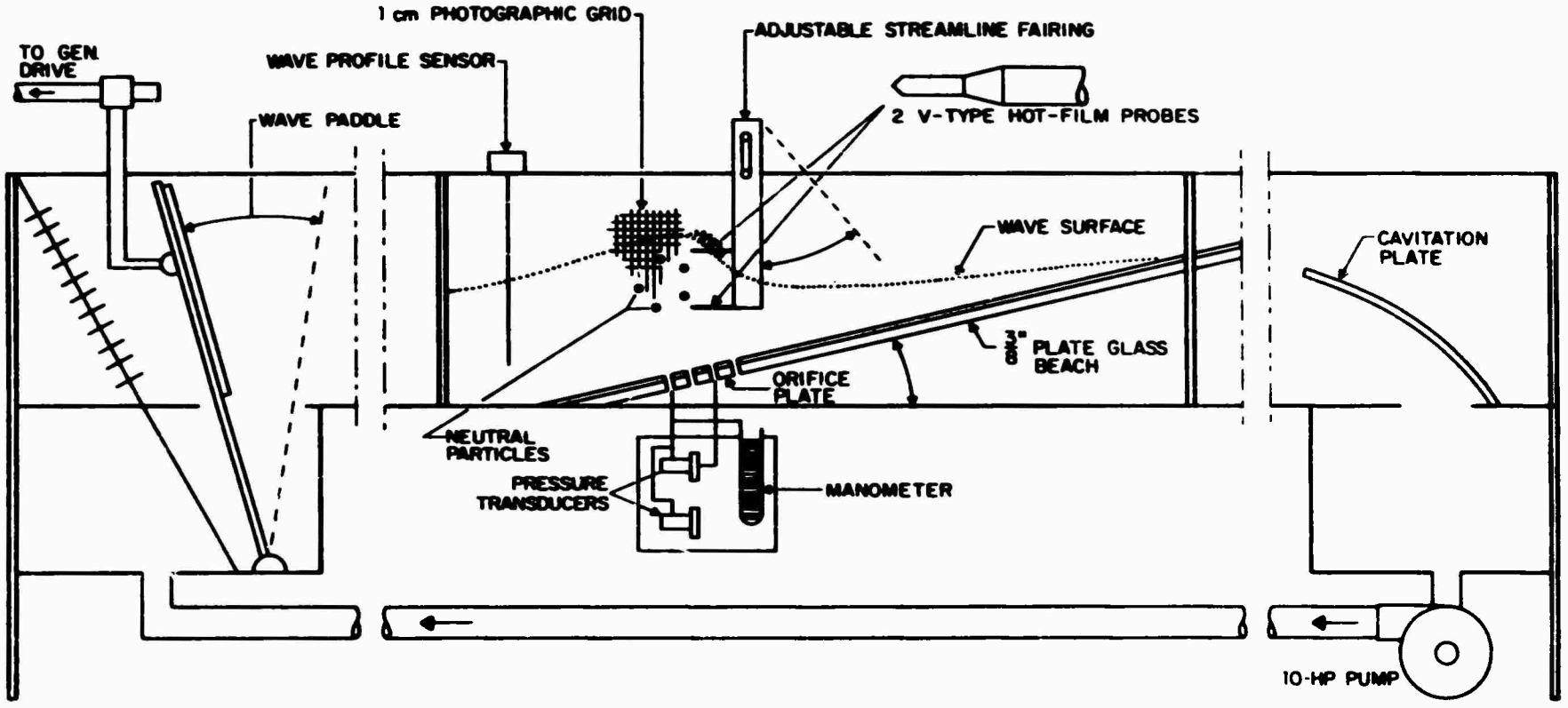

Figure 1. Schematic diagram of laboratory wave channel showing components used for velocity-field measurements.

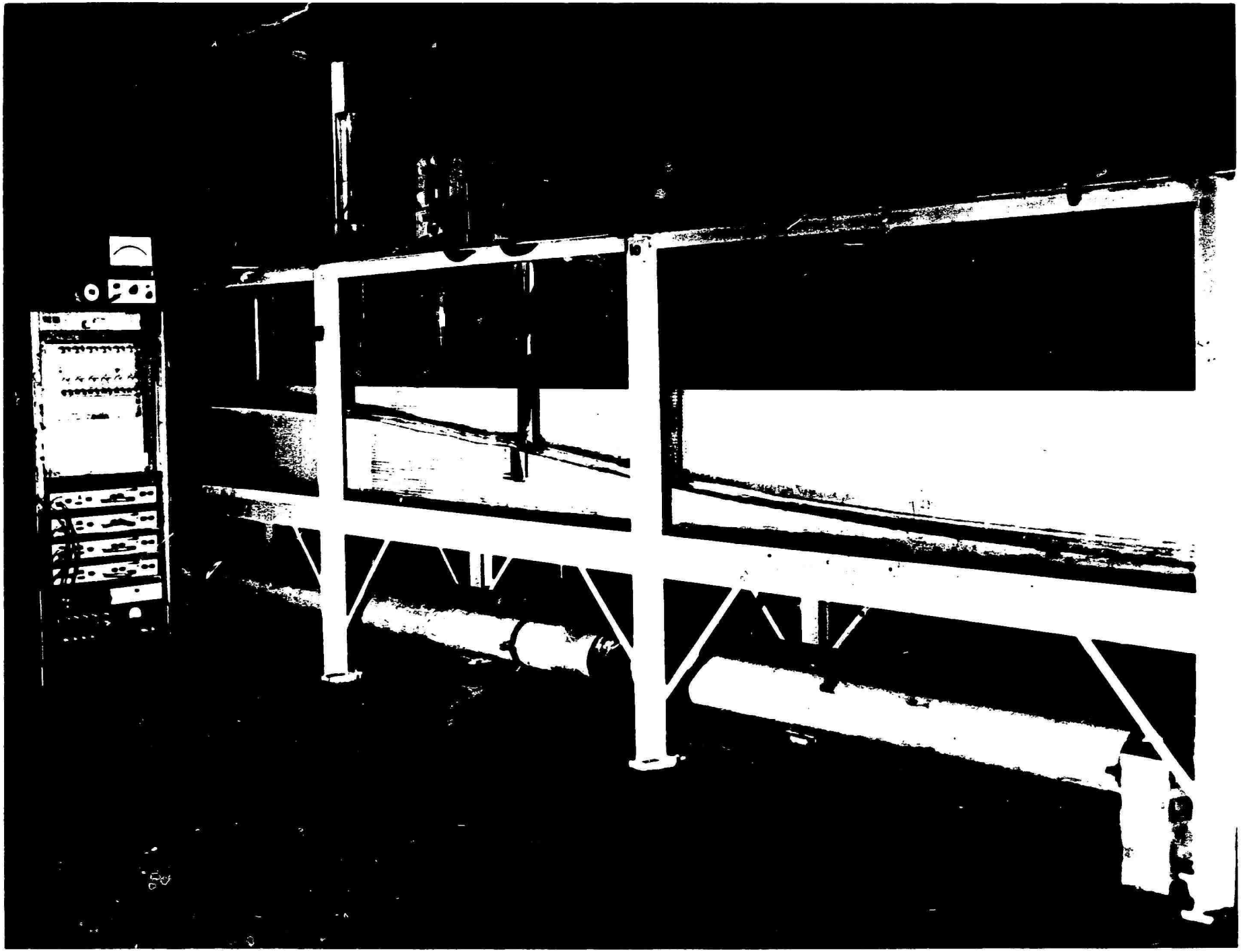

Figure 2. Dynamic flow calibration of V-probe in wave channel. Parabolic venturi section provides complete flow range from 12-270 cm/sec by moving probe. Instrument console is at left.

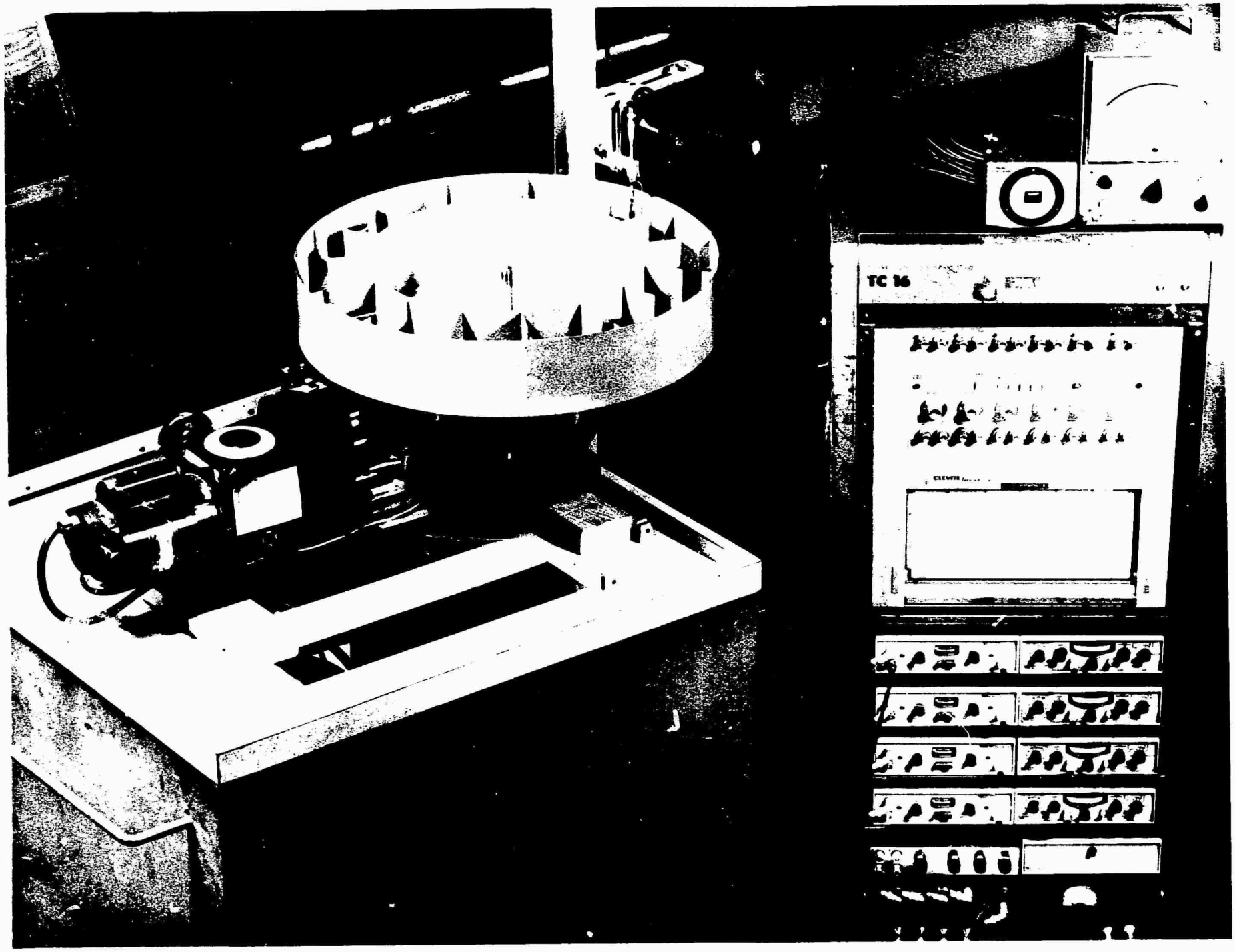

Figure 3. Spinning tank with standard probe in calibration position. Slotted baffles eliminate wave and flow from probe drag. Calibration range 0-180 cm/sec.

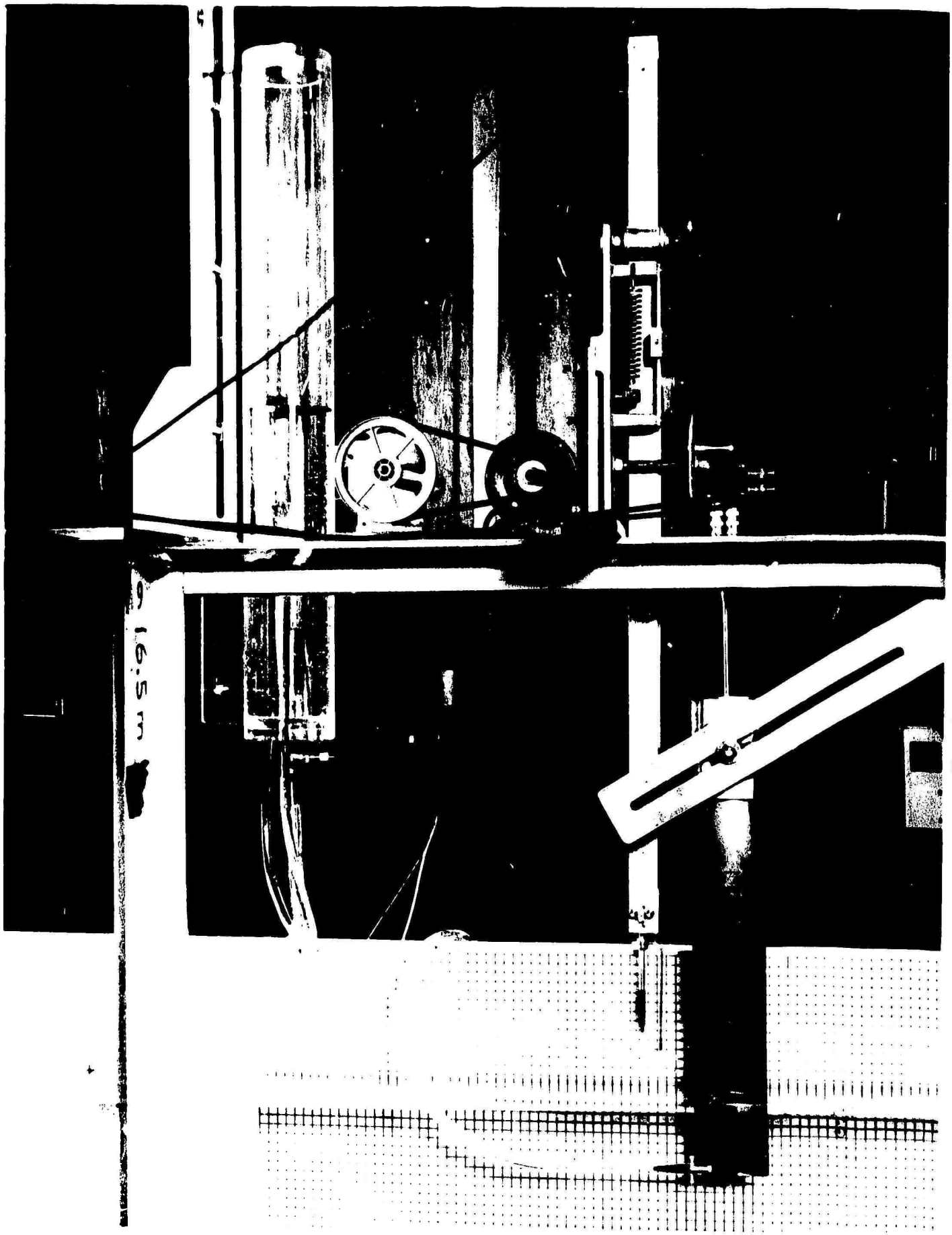

Figure 4. In-situ calibration of V-probe is accomplished by nozzle over probe. Plastic tube leads to bottom of vertical cylinder maintained at constant head above tank level by overflow tube and pump. Standard probe is to left of V-probe strut.

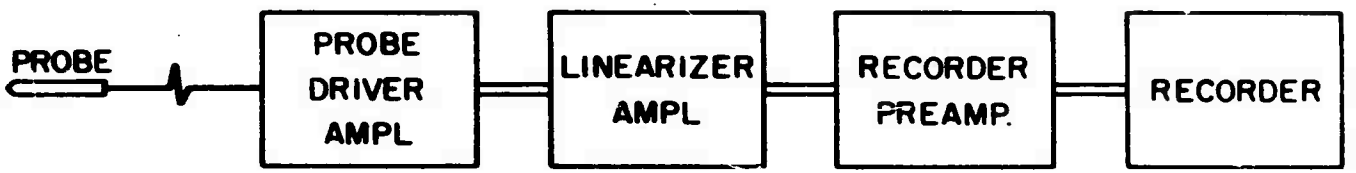

Figure 5. Block diagram of hot-film probe circuitry. Linearizer was later eliminated to improve stability.

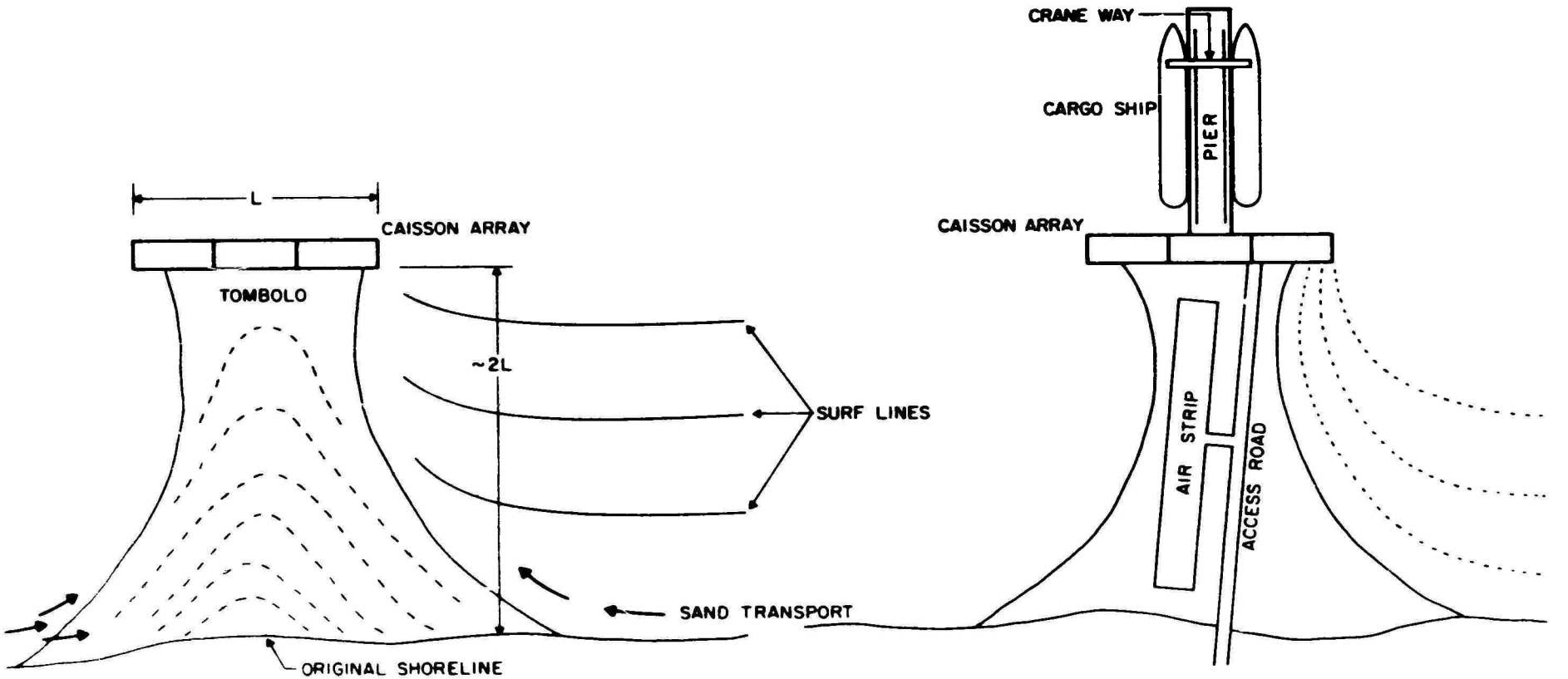

Figure 6. Conceptual construction of offshore port facility by introducing a caisson barrier, such that a tombolo grows out from shore under natural wave action.

Figure 7. Photograph of artificially induced tombolo (Santa Monica, California Beach).

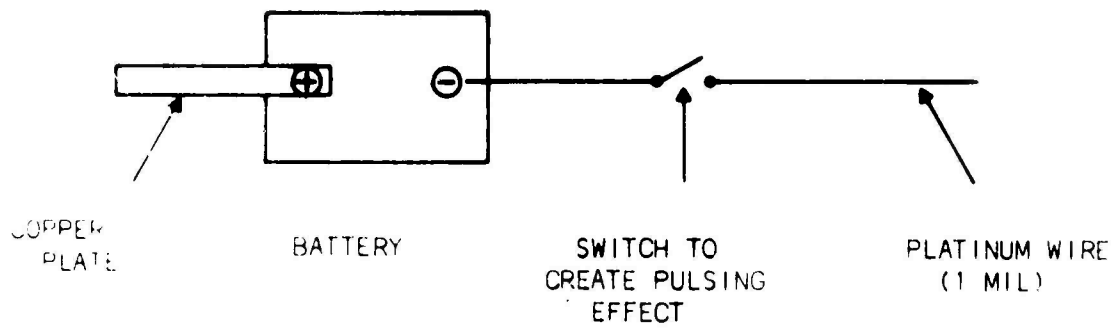

Figure 8a. Diagram of hydrogen bubble generator system.

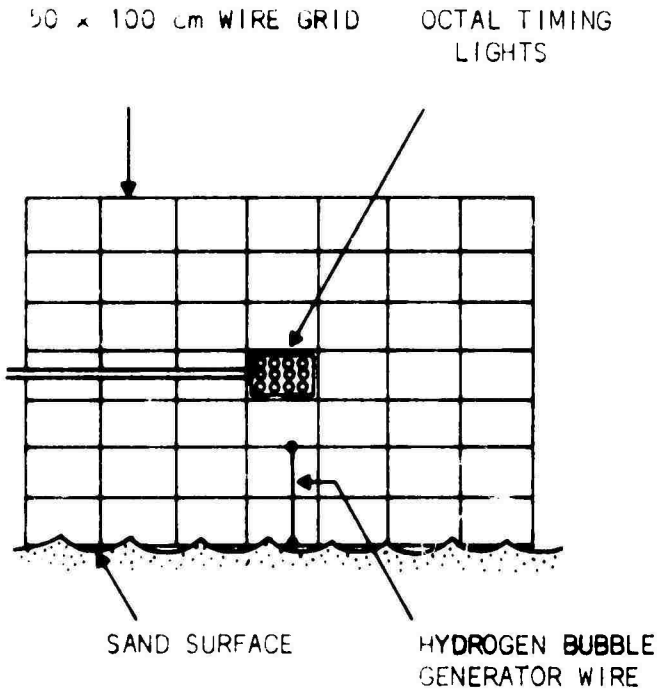

Figure 8b. View of hydrogen bubble generator as seen from camera station.

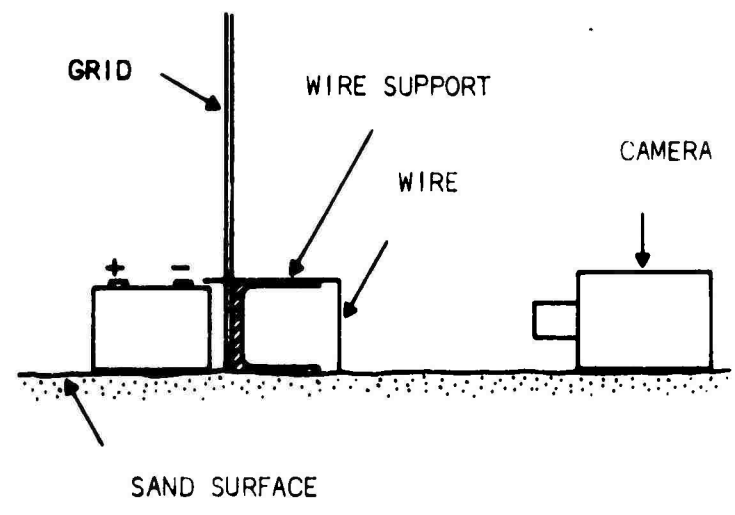

Figure 8c. View of hydrogen bubble generator looking onshore.

Figure 9. ADVANCED STUDIES IN NEARSHORE ENGINEERING PROPOSED WORK SCHEDULE 1971-72

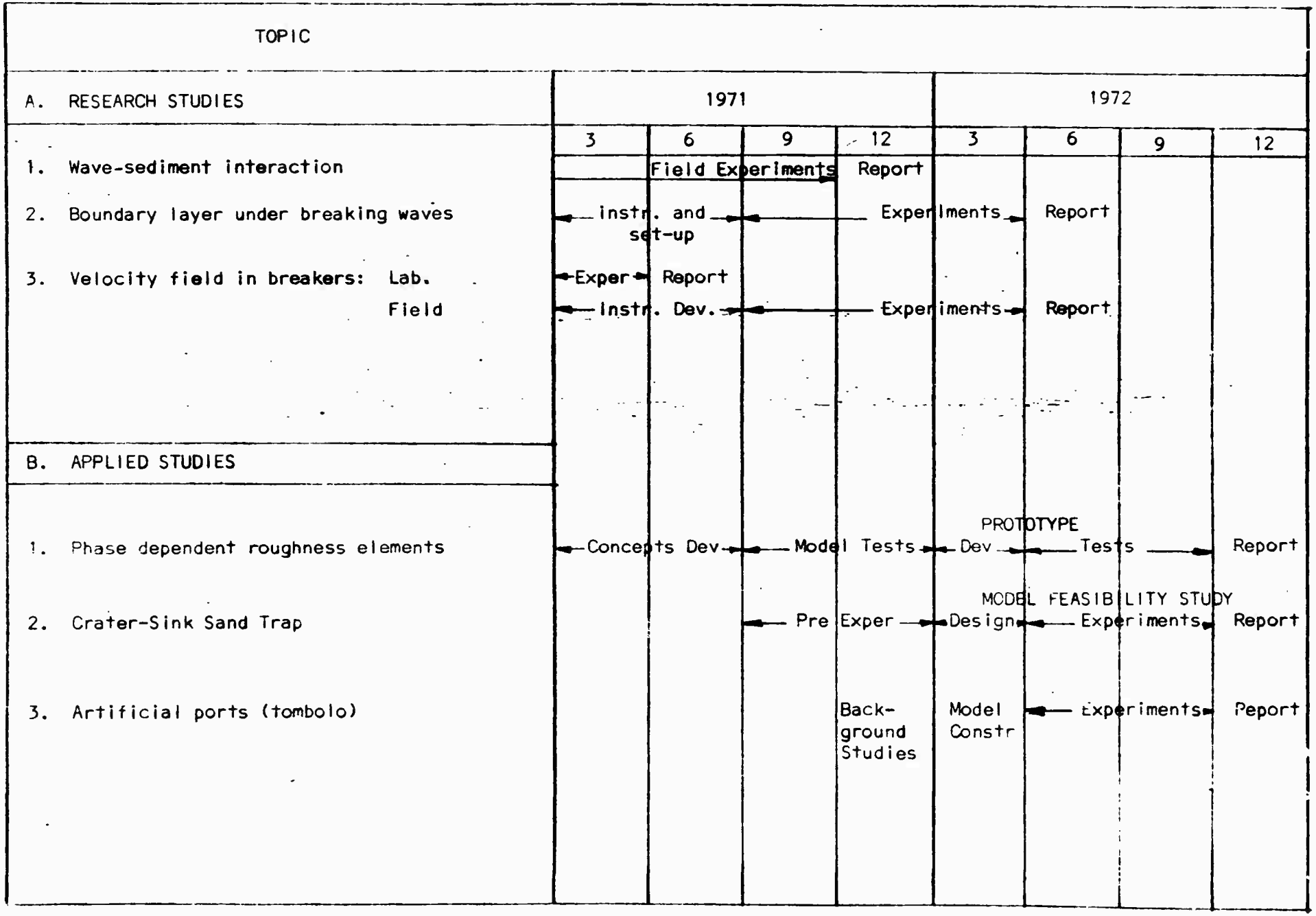

Figure 10. Interaction of Activities for Advanced Studies in Nearshore Engineering

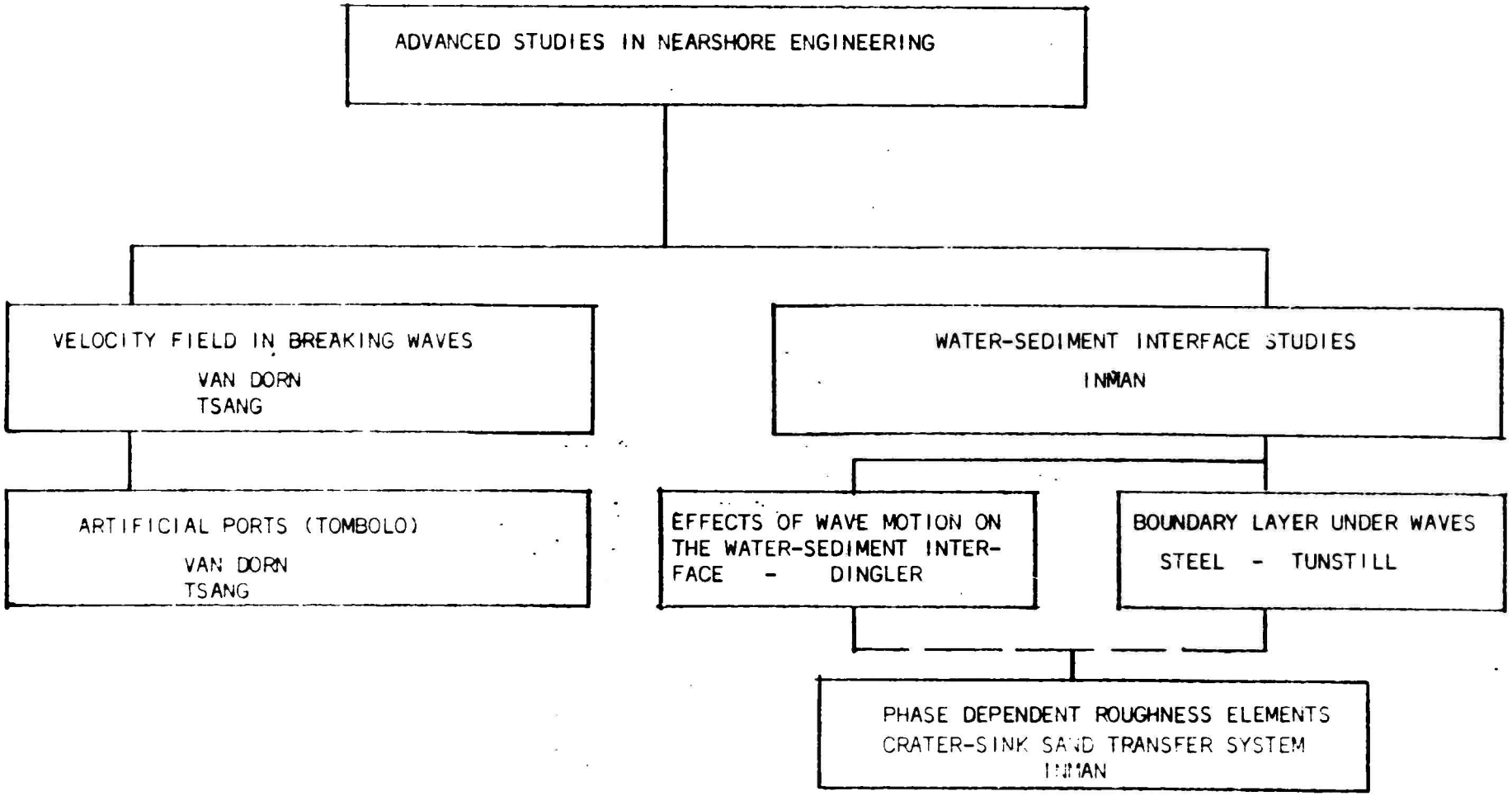

Part V

ELECTROMAGNETIC ROUGHNESS OF THE OCEAN SURFACE

Co-Principal Investigators

Dr. William A. Nierenberg
Phone (714) 453-2000, Extension 1101

Dr. Walter H. Munk
Phone (714) 453-2000, Extension 1741

ADVANCED OCEAN ENGINEERING LABORATORY

Sponsored by
ADVANCED RESEARCH PROJECTS AGENCY
ADVANCED ENGINEERING DIVISION

ONR Contract N00014-69-A-0200-6012

Part V

Electromagnetic Roughness of the Ocean Surface

Table of Contents

ELECTROMAGNETIC ROUGHNESS OF THE OCEAN SURFACE

I. INTRODUCTION

For several decades oceanographers have known that radio waves, scattered by ocean waves, could be used as an oceanographic tool. The technique requires measuring the radar cross-section of waves in a patch of ocean and relating this information to ocean wave properties. These properties could be the directional spectrum of ocean waves, the relation between their wavelength and frequency, or other properties associated with the random pattern of the ocean surface. Over the years considerable progress has been made in the development of this tool. Measurements, by various groups, of the radar cross-section indicated that the radar technique provides a sensitive and accurate measure of ocean waves.[1,2] Recent theories for the scattering of electromagnetic waves from slightly rough surfaces provide a framework for the proper interpretation of the wave data.[3] And, finally, the availability of multi-frequency pulsed-doppler radars has made possible systematic measurements of the ocean surface.

For the past year a group of electrical engineers from Stanford University and a group of oceanographers from Scripps Institution

ELECTROMAGNETIC ROUGHNESS OF THE OCEAN SURFACE

I. INTRODUCTION

For several decades oceanographers have known that radio waves, scattered by ocean waves, could be used as an oceanographic tool. The technique requires measuring the radar cross-section of waves in a patch of ocean and relating this information to ocean wave properties. These properties could be the directional spectrum of ocean waves, the relation between their wavelength and frequency, or other properties associated with the random pattern of the ocean surface. Over the years considerable progress has been made in the development of this tool. Measurements, by various groups, of the radar cross-section indicated that the radar technique provides a sensitive and accurate measure of ocean waves.[1,2] Recent theories for the scattering of electromagnetic waves from slightly rough surfaces provide a framework for the proper interpretation of the wave data.[3] And, finally, the availability of multi-frequency pulsed-doppler radars has made possible systematic measurements of the ocean surface.

For the past year a group of electrical engineers from Stanford University and a group of oceanographers from Scripps Institution

and range gating, it could select those radio signals scattered by waves along different parts of the circle, and could be used to measure the directional spectrum of a homogeneous ocean wave field. This method has one serious disadvantage. If we wish to measure typical ocean waves, those with periods around seven seconds, then we must use radio waves with a wavelength of 150m, and a sharply directional antenna (for example, one having a directional resolution of 10°) must be nearly 1/2km across. Such an antenna would be cumbersome to use and it would be advantageous to find a method which does not require it.

B. Bistatic Geometry

In 1969 Nierenberg and Munk showed that if the transmitter and receiver are separated (bistatic geometry), the large directional antenna could be replaced by a much smaller, less directional antenna. In this new geometry the radio wave is scattered by waves whose crests are tangent to an ellipse with the transmitter and receiver in the foci; and the frequency shift of the scattered wave will be a function of position on the ellipse, with four symmetric points on the ellipse having the same frequency shift. Radio signals scattered from these points can be selected by using range gating and frequency descrimination. A small, slightly directional antenna could then be used to select the signals from one of these four symmetric points.

C. Side-looking Radar

Somewhat later in 1969, Crombie, of the NOAA laboratory in Boulder, suggested that the technique of side-looking radar might also be used to select signals scattered from a particular patch of ocean. If we go back to the monostatic geometry and move the radar set at a constant velocity in a straight line (monodynamic geometry), everything remains as before except that the scattered radio waves will have an added frequency shift due to this motion, and it will be a function of position on the circle, with two points symmetric about the direction of motion having the same shift. As in the bistatic geometry, a slightly directional antenna can be used to select signals from one of the two points. In essence, this technique uses the motion of a small antenna to synthesize a much larger antenna, a technique long used in radio astronomy.

Following Crombie's suggestion, we have examined this technique in detail and found the conditions under which it would be useful. In particular, the radar set should have a velocity no greater than the phase velocity of the ocean waves it is to measure. At higher velocities, radio signals scattered from ocean waves travelling towards the rear of the radar will have the same frequency shift as those signals scattered from ocean waves travelling away from the front of the radar. This velocity, for our typical seven second ocean wave, is 11m/s (21 knots). Furthermore, the directional resolution is a function

only of the distance travelled. If the radar moves a distance of n/2 radio wavelengths at any velocity, the directional resolution of the synthesized antenna will be n^{-1} radians. This is identical to the optical resolution of a lens n/2 wavelengths in diameter. If only the transmitter or receiver moves, then it must traverse twice this distance for the same resolution. Again using a seven second ocean wave for illustration, if the radar moves 1500m at 10m/s (20 knots - this takes about three minutes) it could measure the directional spectrum of these ocean waves with a maximum resolution of 3°.

This technique is ideally suited for oceanographic work. Because it requires the radar to move at typical ship speeds for a few minutes, the radar could be mounted on a ship and taken to those ocean areas suitable for measuring the ocean wave directional spectrum. Alternatively, the receiver could be mounted on a truck and driven on small, suitably located oceanic islands.

D. Radar Equipment

So far we have described how ocean waves could be measured assuming we have suitable radar equipment. To measure the directional spectrum of 1.8 to 6.9 second ocean waves using the above techniques we would need a 2-30MHz, pulsed, doppler

radar; that is, a transmitter which transmits a train of coherent pulses and a receiver which remains synchronized to these pulses for a specified time. For a resolution in radio frequency of Δf Hz, the coherence time is Δf^{-1} s, or, for the above measurements, this is typically about 1000s or 15 minutes. Such a radar is complex and expensive; fortunately suitable radars of exactly this type have been used to study the earth's ionosphere and are available on loan.

III. EXPERIMENTAL WORK

Before assembling this radar equipment we decided to become familiar with the radar methods, and to test their practical usefulness by conducting experiments using radio signals from LORAN A stations. These stations, which are conveniently located along coasts, transmit a train of coherent pulses at a frequency of about 1.85MHz. The signals can be received by a simple radio receiver, provided it has an accurate time base (to keep it synchronized with the transmitter).

The Stanford group constructed a suitable LORAN receiver, using a Hewlett-Packard frequency synthesizer for the time base, and used it in several experiments to measure the signals scattered from ocean waves off the California coast. In one experiment, the receiver was placed on the coast at Sunset Beach 280km from the LORAN stations at Points Arena and Arguello, and the scattered radio waves were recorded as a function of range and

frequency shift (range-doppler map). The experiment showed 1) LORAN could be used to measure ocean waves up to several hundred kilometers from the receiver, and 2) the frequency shifts were those predicted by the Bragg theory applied to the bistatic geometry. Further details of this experiment were published in the 9 October 1970 issue of Science[4].

A second experiment, designed to measure the time variation in the strength of the scattered radio signals and to correlate this signal with a measured ocean wave directional spectrum, was performed at La Jolla. In this experiment, signals from the LORAN stations at Points San Mateo and Arguello were measured during a period when waves from tropical storm "Lorraine" were propagating into the area. At the same time the ocean wave directional spectrum was recorded at a point 100km offshore using a wave array on the FLIP.

In support of the experimental work, the Stanford group has calculated the normalization factor which must be applied to the received radio signal to calculate the radar cross-section of the ocean waves when the radar transmitter and receiver are in a bistatic geometry. To simplify the calculation they have assumed a rectangular radar pulse, but are proceeding to refine the calculation to properly account for non-rectangular pulses. The Scripps group has been writing programs to analyze LORAN data from any transmitter and to put this data into various useful forms.

A test of the monodynamic method, again using LORAN signals, is scheduled for early this year. In preparation for this experiment the Stanford group has been designing a simple LORAN receiver with a built in accurate time base suitable for field mobile use.

The experiment will be conducted on a one mile long straight piece of abandoned U.S. 101 parallel to the beach near the LORAN station at Point San Mateo.

IV. PLANNING OF FIELD EXPERIMENTS

Encouraged by this experimental work, the Scripps group has been planning two full scale field experiments to measure the directional spectrum of ocean waves in two idealized situations: 1) a fully developed sea generated by a stationary, homogeneous wind, and 2) a developing sea, downwind of a lee coast, generated by the same sort of wind. To date the planning of the field experiments has been concerned with 1) locating oceanic areas with constant winds; 2) determining from historical data how stationary and homogeneous these winds are; and 3) locating sites in these areas which may be suitable for shore based radar experiments.

A. Homogeneous Sea Experiment

Let us consider the first of these experiments. In order to have a fully developed sea, a wind, constant in both magnitude

and direction, must operate on a sufficiently large region for a time long enough for the waves to come to equilibrium with the wind. The most likely place to find such winds is in the trade wind or monsoon wind regions. Here the winds typically have speeds in the range of 5-10m/s and generate waves with periods of up to seven seconds. So a fully developed sea should require fetches of a few hundred kilometers and wind durations of 12-24 hours[5]. Such fetches are readily found, but sufficiently constant winds are not.

Some of the steadiest winds in the world should be found in the Pacific trade wind region in winter[6]. For example, in February at Kwajalein Island 85% of wind records indicate a wind from the NE octant and 72% indicate wind speeds in the band 5-10m/s. More detailed wind data, for example, that collected during the Line Islands experiment[7] indicate that the wind in this region can be constant within ·15% in speed and ·10% in direction during some 24 hour periods. These winds would be useful for the planned experiment, provided they were also homogeneous. Unfortunately very little is known about the homogeneity of the winds over areas 100km on a side. Nevertheless, the lack of variation in wind speed on the scale of a few hours[8], and the large size of the trade wind region imply the wind field should be homogeneous over a scale of a hundred kilometers.

For islands in the trade winds region to be useful for the shore based experiments, they should be small so they will not interfere with the measured wave field. Since the degree of interference will decrease with distance from the island, it will be a function of radar range, and since a good operating range for available multifrequency radars is about 40km, the islands should be less than 10km in diameter. It is difficult to find such an island in a suitable region. In the Pacific, Palmyra Island would be ideal, but it is inaccessible. Johnson, Wake, or Marcus Islands could probably be used, but are slightly north of the winter trade wind area.

B. Developing Sea Experiment

The second experiment requires a suitable wind blowing off a lee coast. Such winds could be produced by cold fronts or monsoon winds blowing off continental areas. The monsoon areas are remote and have not been considered. The winds behind cold fronts moving off the east coast of the U.S. have been used for wave growth experiments in the past, but useful fronts are rare. A more suitable area is the Texas gulf coast. This coast is straight and parallel to the cold fronts. The water slopes off smoothly to deep water. And data collected by Orton[9] indicates cold fronts with 10-15m/s winds extending several hundred kilometers offshore and lasting for 24 hours occur several times a month in January and February.

V. DESIGN OF EQUIPMENT

The field experiments will require several items of equipment not now available: 1) a pitch-and-roll buoy. This will be used to measure the ocean waves and some integrals of the directional wave spectra, and will be used for calibration and supplying wave data not measured by the radar techniques. 2) Three wind buoys. These will be used to measure the wind field in space and time and whatever other ocean variables, such as air-sea temperature difference, which may be needed in the field experiments.

Data from all buoys will be recorded in computer compatible digital format using versatile low power data recording systems. These systems will be unique in that they will use less than two watts of power, so they can be used for extended periods of time at sea, and will be small enough to fit into the wave measuring buoy.

A. Pitch-and-Roll Buoy

The pitch-and-roll buoy will measure the ocean surface height and slope at a single point, and will be similar to buoys built by the Hudson Laboratories of Columbia University[10,11] and the National Institute of Oceanography (England)[5], but will be completely self contained. This buoy will consist of 1) a flat disc shaped hull, about five feet in diameter, which should accurately follow the surface of the water up to

a cut-off frequency of around 0.5Hz, 2) an accelerometer mounted on the inner gimbal of a vertical gyro, and 3) a gyro compass. The output of the accelerometer is integrated to obtain the water surface height; resistance elements in the gyro give the attitude of the buoy with respect to the gyro's vertical reference, and thus the water surface slope. The slopes are then oriented with respect to the earth by the compass. These signals can then be used to calculate the first five Fourier coefficients of the angular distribution of ocean wave energy, and thus the one-dimensional wave spectrum and an integral of the directional spectrum[5].

B. Wind Buoys

The wind buoys will be catamaran buoys developed at Scripps by Isaacs' group, including some of their instrumentation, but with the data recorded in digital format.

This preliminary work has placed us in a position where we can conduct a number of comparative experiments designed to study the roughness of the ocean surface using the radio frequency band of 2-30MHz during the rest of this year.

VI. REFERENCES

1. Braude, S. Ya 1962 Radio oceanographic investigation of sea swells. Academy of Sciences of the Ukranian S.S.R. Kiev. Institute Radiofiziki i Elektroniki [Department of the Navy Translation No.2067, DDC#AD634242].

2. Crombie, D.D. and Watts, J.M. 1968 Observations of coherent backscatter of 2-10MHz radio surface waves from the sea. *Deep-Sea Research*, 15, 81-87.

3. Barrick, Donald E. 1970 Theory of ground-wave propagation across a rough sea at dekameter wavelengths. ARPA order no.1178, Battelle Memorial Institute, Columbus, Ohio.

4. Peterson, Allen M.; Teague, Calvin C.; and Tyler, G. Leonard 1970 Bistatic-radar observations of long-period, directional ocean-wave spectra with LORAN A. *Science*, 1970 , 153-161.

5. National Academy of Sciences 1963 *Ocean Wave Spectra*. New Jersey; Prentice-Hall.

6. United States Navy 1955-1959 *Marine Climatic Atlas of the World Vol. 1-5.*

7. Lipser, Edward J. and Taylor, Ronald C. 1969 A catalogue of meteorological data obtained during the Line Islands experiment February-April 1967. National Center for Atmospheric Research Tech. Note 35, Boulder, Colorado.

8. Zipser, Edward J. 1970 The Line Islands experiment, its place in tropical meteorology, and the rise of the fourth school of thought. *Bulletin of the American Meteorological Society*, 51, 1136-1146.

9. Orton, Robert R. 1964 *The Climate of Texas and Adjacent Gulf Waters*. Washington, D.C.: Superintendent of Documents, U.S. Government Printing Office.

10. Jordan, W. N. 1969 Mechanical design, construction, calibration, and field deployment of surface wave floats. Hudson Laboratories of Columbia University Tech. Report 171, Dobbs Ferry, New York.

11. Goldberg, Harold D. and Goldberg, Milton I. 1969 Transducer instrumentation for surface wave measurement. Hudson Laboratories of Columbia University Tech. Report 180, Dobbs Ferry, New York.